ION-MOLECULE REACTION STUDIES FOR THE
SCREENING OF POTENTIAL CARCINOGENS
BY TANDEM MASS SPECTROMETRY

By

JODY ANNE FREEMAN

A DISSERTATION PRESENTED TO THE GRADUATE SCHOOL
OF THE UNIVERSITY OF FLORIDA IN PARTIAL FULFILLMENT
OF THE REQUIREMENTS FOR THE DEGREE OF
DOCTOR OF PHILOSOPHY

UNIVERSITY OF FLORIDA

1991

TABLE OF CONTENTS

ION-MOLECULE REACTION STUDIES FOR THE
SCREENING OF POTENTIAL CARCINOGENS
BY TANDEM MASS SPECTROMETRY

By

Jody Anne Freeman

August 1991

Chairperson: Dr. Richard A. Yost
Major Department: Chemistry

This dissertation introduces a novel technique to screen for potential
carcinogens by gas-phase ion-molecule reactions between model nucleophiles
and potential carcinogens (introduced by gas chromatography) within the ion
source and collision cell of a triple quadrupole mass spectrometer. Potentially
mutagenic and carcinogenic chemicals are recognized to be electrophiles capable
of reacting with the many nucleophilic sites in the human body such as those
found in DNA. Reaction between the DNA base adenine and the suspected
carcinogen benzoyl chloride in the ion source is shown to produce the adduct
benzoyl adenine. The mass spectra obtained by ion-molecule reactions in the ion
source tend to be complicated. Furthermore, it is difficult to determine which ion

(e.g., $[M+H]^+$, $M^{+\cdot}$, or fragment ions) is reacting with which neutral species.

Mass-selected ion-molecule reactions between a nucleophile (e.g. pyridine) and electrophiles (e.g. allylic compounds) in the collision cell have been investigated where the ionized species is either the electrophile or the nucleophile. The mass spectra obtained by mass-selected reactions in the collision cell are less complicated and easier to interpret since only a single reactant ion is allowed to interact with the neutral species in the collision cell. The effects of various parameters (e.g. amount of reactant ion, neutral species pressure, and collision energy) on the product ions formed in the collision cell and competitive reactions is demonstrated. The degree of reactivity of various nucleophiles (e.g., pyridine, piperidine and aniline) with various potential carcinogens and non-carcinogens is investigated.

Low picogram limits of detection are obtained in the selected reaction monitoring mode for the collision cell reactions of allyl chloride and allyl iodide with pyridine. Thus, this technique could provide a rapid and sensitive method for screening complex environmental mixtures for potential carcinogens, as well as for estimating their relative electrophilic potential.

CHAPTER 1
INTRODUCTION

This dissertation evaluates the utility of ion-molecule reactions in a triple quadrupole mass spectrometer (a) to screen complex environmental samples for potential genotoxic carcinogens, and (b) to estimate the relative reactivity of these potential carcinogens. These gas-phase ion-molecule reactions, between electrophiles (carcinogens) and nucleophiles (DNA bases or model DNA bases), attempt to model what occurs in solution-phase reactions. This technique offers the distinct advantages of being very fast and permits testing of individual components of complex mixtures via on-line chromatographic separation.

The introductory chapter discusses a few of the current long-term and short-term techniques for detecting and quantitating potential mutagens and carcinogens. The types of gas-phase ion-molecule reactions involved in the on-line analysis of DNA adducts or model DNA adducts are also presented, along with the mass spectrometric instrumentation utilized in these analyses. The chapter concludes with an overview of the dissertation organization.

Methods For Identifying Potential Carcinogens

In 1962, the term carcinogen was defined as "an agent or process which significantly increases the yield of malignant neoplasms in a population" (Clayson, 1962). Since carcinogenesis is a multistep process, attempts to select adequate test systems for identifying carcinogens of all types and modes of action is extremely difficult. Four broad stages leading to carcinogenesis have been documented (ICPEMC, 1982): (a) transport from the site of application and possible metabolic activation; (b) interaction of the ultimate carcinogen with the critical target(s) (e.g. DNA); (c) DNA repair and replication processes leading to tumor initiation; (d) progressive development of tumor cells leading to clinical cancer. Due to this complexity of cancer processes, different techniques will assess certain steps of carcinogenesis, but few are capable of spanning the whole process in a single test.

Most carcinogens have been classified into two broad categories based on their mechanisms of action: genotoxic and epigenetic (Woo et al., 1985; ICPEMC, 1982; Barrett, 1987a; Boutwell, 1984). Genotoxic carcinogens are those chemicals which alter genetic information by interaction with nucleophilic targets, especially DNA. This category can be further subdivided into direct-acting carcinogens and pro-carcinogens. The direct-acting carcinogens are reactive electrophiles themselves, while pro-carcinogens require metabolic activation to produce ultimate electrophiles (Miller, 1970). In-depth studies have investigated the interactions of

these electrophilic centers with nucleophilic sites in the nucleic acids of DNA (e.g., N^7 and O^6 of guanine, N^3 and N^1 of adenine) (van Sittert, 1983; Montesano, 1981). Epigenetic (or non-genotoxic) carcinogens have been found to increase the incidence of tumors without reacting with DNA. These epigenetic carcinogens are incapable of initiating tumors by themselves and have been found to act by such mechanisms as cytotoxicity, immunosuppression, promoting effects and inhibition of intercellular communication (Williams, 1987). Table 1-1 contains examples of chemicals classified as genotoxic and epigenetic carcinogens. There are carcinogens called complete carcinogens (co-carcinogens) which span both classes, such as 2,3,7,8-tetrachlorodibenzodioxin (TCDD) and benzo(a)pyrene (Woo et al., 1985). These carcinogens can both initiate DNA damage and promote tumor growth.

These potential carcinogens and mutagens, however, represent only a small portion of the total number of contaminants in typical environmental samples. Accurate evaluation of these chemicals to provide data for human and ecosystem risk assessment depends upon analytical procedures to isolate, identify, and quantify each chemical and to provide a comparative measure of electrophilic reactivity. Much research has been done over the years and still continues to develop and perfect analytical techniques for studying potential carcinogens. Due to limitations apparent in each technique, many believe that a combination of techniques is more successful in determining potential risk of a chemical than a single method alone (Buzzi and Würgler, 1990; Ashby and Tennant, 1988).

Table 1-1: Classes of Carcinogens.

.

Genotoxic Carcinogens

       Direct-acting Alkylating and Acylating Agents
- epoxides
- nitrogen mustards
- methyl halides
- carbamates

       Pro-carcinogens
- polycyclic aromatic hydrocarbons
- N-nitrosamines
- vinyl chloride
- azodyes

Epigenetic Carcinogens

- saccharin
- *p*-dioxane
- acetamide
- thiourea

Animal Tests

Obviously, the most accurate tests of human carcinogenesis would be based upon data acquired from humans; however, this tends to be a long and inefficient process. Thus, many methods have been developed to perform carcinogen screening by using mammals (most commonly mice and rats). Long-term animal testing is dependent on many factors which affect the bioassay (Bannasch et al., 1986; Sontag, 1977). The number of dose groups and the dose for each animal group are critical considerations. Typically, two types of doses are administered: (a) the maximum tolerated dose (MTD) which is the highest dose that can be administered without causing a significant decrease in survival from effects other than carcinogenicity, and (b) a lower dosage, typically 1/2 the MTD. Due to latency of tumor production and the shorter life-span of animals compared to humans, higher doses must be applied to animals to estimate the effect of the chemical on humans. The dosage will also be dependent on the route of exposure such as ingestion, inhalation, and skin application. The type, age, strain and sex of the animals selected are important criteria. A major portion of the bioassays have been performed with mice or rats. Typically, the animals are exposed to the chemical at 6 to 8 weeks old and are treated for most of their expected life span. Approximately 250 animals are required for adequate statistical analysis. Two extrapolations are required to determine a chemical carcinogenic: one is from the incidence found at high dosages to an estimated incidence at low

dosages; the second is from the experimental animal to man. This extrapolation to low doses, based on a mathematical relationship between dose and effect, assumes there is no threshold below which normal repair and recuperative processes will prevent cancer (Lu, 1983). One advantage of animal bioassays is their ability to test for both initiators and promotors (Peraino et al., 1975; Solt and Farber, 1976; Pitot et al., 1978; Laurier et al., 1984; Solt et al., 1983). Unfortunately, animal bioassays of a chemical typically last 3 to 4 years, require a large staff and laboratory facilities, and cost approximately $500,000 (Zeiger, 1985).

In addition to long-term whole animal tests, short-term *in-vitro* mammalian tests have been developed and reviewed (Lambert et al., 1986; Barrett and Elmore, 1985). These *in-vitro* mammalian tests detect malignant cell transformations in rodent cells (usually embryos of mice, rats, and hamsters). *In-vitro* transformation assays utilize an endpoint which mimics *in-vivo* tumor processes in the conversion of normal cells to transformed cells. Thus these techniques are unique among short-term bioassays in their ability to screen for epigenetic carcinogens, especially promotors (Sivak, 1979; Mondal et al., 1976; Colburn et al., 1978). However, these mammalian cell tests are limited in their endogenous metabolic capabilities. Thus a limited number of pro-carcinogens have been detected in these systems. Development of external metabolic sources is ongoing. These tests have been plagued by irreproducibility among laboratories and limited availability of the assays. Although these *in-vitro* transformations tests are relatively quick (2 weeks) compared to whole animal tests, the assays are still

in the developmental stages and their utility in screening for potential carcinogens is still largely unknown.

<u>Bacteriological Tests</u>

One of the most extensively studied and controversial techniques is the Ames test, developed by Bruce Ames and co-workers in 1975 (Ames, et al., 1975; Ames, 1984). The Ames test is a bacteriological assay which detects chemicals capable of mutating or modifying DNA. This bacteriological assay uses *Salmonella typhimurium* which has been mutated so that the pathway for histidine production has been blocked. To this histidine-requiring bacterial mutant, the chemical to be tested is added; after incubation at 37 °C for 2 days, the number of bacterial revertant colonies is recorded. Thus, the chemical is identified as a mutagen if it is capable of modifying the defective histidine gene to a functional one. Since the majority of known mutagens require metabolic activation to become mutagens (electrophiles), development of an activation pathway was essential. The research of the Millers, Malling, and others has led to the conversion of chemicals into their active form by enzymes in liver or other tissues. Thus, mammalian liver tissue is added to the Ames test to provide an approximation of mammalian metabolism (Malling, 1971; Miller and Miller, 1977; Slater et al., 1971). Note that for a chemical to be a genotoxic carcinogen, it must be capable of mutating DNA; however, chemicals found to be mutagenic are not necessarily carcinogenic. For instance,

2-aminopurine mutates DNA in bacteriological assays, but has not been found to be carcinogenic in animals or humans (Barrett, 1987b). Conversely, benzene is non-mutagenic, but has been identified as a carcinogen in animals and humans. Various studies have reported that 50% to 90% of the chemicals identified as mutagens by the Ames test are carcinogenic (ICPEMC, 1982; McCann et al., 1975; Bartsch, 1976; Clayson, 1980). By combining short-term tests, Ashby and Tennant discovered a 90% correlation between chemical structure, mutagenicity in *Salmonella*, and rodent tumorigenicity (Ashby and Tennant, 1988). The Ames test typically requires a single technician, a maximum of 2 weeks (2 to 3 days/test), and $1,000 to $1,500 to adequately test a chemical for mutagenesis (Zeiger, 1985).

Bacteriological tests have been used for the detection of mutagens in complex mixtures, such as cooked food (Sugimura and Sato, 1983), cigarette smoke (Kier et al., 1974) and urine (Yamasaki and Ames, 1977); however they lack the necessary response (milliseconds) and often sensitivity (nanograms to picograms) to be used on-line with chromatography. Therefore, if a positive result is obtained from the complete mixture, off-line fractionation of the mixture components must be performed and the resulting fractions are tested for mutagenicity until the mutagenic component is identified.

Methods For Detecting and Quantifying DNA Adducts

Over the years, efforts to develop sensitive techniques for detecting and quantitating *in-vivo* and *in-vitro* DNA adducts have produced many different techniques, such as radioactive labelling, immunoassays, ^{32}P-postlabelling, liquid chromatography with ultraviolet and fluorescence detection, and tandem mass spectrometry (MS/MS). These techniques have been reviewed and compared (Lohman, 1988). Radioactively labelled carcinogens have been used to assess interactions of carcinogens with DNA; however, only a small fraction of all potentially mutagenic/carcinogenic chemicals are available in isotopically labelled form. One of the most promising *in-vivo* techniques to emerge is ^{32}P-postlabelling, which does not require radioactively labelling the test compounds themselves (Randerath et al., 1981; Gupta et al., 1982). There are four major steps in ^{32}P-postlabelling: (1) digestion of modified DNA to 3'-mononucleotides, (2) incorporation of the ^{32}P radionuclide into the 3'-mononucleotides, (3) removal of normal nucleotides by thin-layer chromatography (TLC) or reverse-phase high performance liquid chromatography (HPLC), and (4) detection of ^{32}P labelled adduct nucleotides by autoradiography (Swanstrom and Shank, 1978). Quantitation by scintillation counting (Reddy et al., 1981) enables detection of one adduct in 10^9 - 10^{10} DNA nucleotides (Randerath et al., 1988).

Reddy and co-workers evaluated the ^{32}P-postlabelling technique for 28 aromatic and methylating chemicals (Reddy er al., 1984). Of these 28 chemicals,

the 25 known carcinogens gave a positive result in this test, while 3 chemicals (anthracene, pyrene, and perylene) were negative in this technique and in animals tests. Everson and co-workers have shown the applicability of ^{32}P-postlabelling techniques for detecting DNA adducts in human placental tissues of smokers and nonsmokers (Everson et al., 1986). However, the ability of ^{32}P-postlabelling to detect DNA alterations of known and unknown sources is limited by the difficulty in characterizing the type of DNA alteration occurring (Randerath et al., 1988).

Mass spectrometry has been employed in various techniques for detecting and quantifying DNA adducts (McCloskey, 1986). On-line gas chromatography mass spectrometry (GC/MS) provides a sensitive method for the examination of the individual components of enzymatic hydrolysates of DNA. GC/MS of the trimethylsilyl (TMS) derivatives of the nucleic acid hydrolysates offers the advantage of considerable structural detail in their electron impact mass spectra (White et al., 1972; Lawson, et al., 1971). Full scan limits of detection for the modified nucleosides (TMS derivatives) of 100 to 500 picograms are generally attainable (Hattox and McCloskey, 1974). A sensitive assay (0.3 picomoles of methylated base in a DNA hydrolysate) for the detection of 5-methylcytosine in DNA has been developed based on stable isotope dilution GC/MS (Crain and McCloskey, 1983). The radiation-induced base products of calf thymus DNA have been characterized by GC/MS (Dizdaroglu, 1985). The DNA repair processes were assessed by GC/MS identification of the modified bases (TMS derivatives) removed from the DNA by base excision-repair enzymes.

Several examples of the applications of fast atom bombardment (FAB) (Schram, 1988; Tondeur et al., 1988; Crow et al., 1984), laser desorption (Hardin et al., 1984), and secondary ion mass spectrometry (Aberth et al., 1982) to the characterization of modified DNA products can be found in the literature. The applicability of these mass spectrometry techniques to polar compounds eliminates the need to derivatize the nucleic acid hydrolysates, and molecular weight information is achieved with these techniques since $[M+H]^+$, $[M+Na]^+$ or protonated base fragment ions are predominant in the mass spectra.

Alternatively, *in-vitro* chemical methods have been developed to estimate mutagenicity by determining the potential for covalent bonding of electrophiles to DNA or model DNA molecules, such as the nucleophiles 4-(4-nitrobenzyl)pyridine (Hermens et al., 1985), 4-nitrophenol (Agarwal et al., 1980; Chen and Carlson, 1981), or 3,4 dichlorobenzenethiol (Gothe et al., 1974). Although these methods are less time-consuming (1-2 hours), they are still limited to batch mode (i.e. not on-line with chromatographic separation). Also, off-line synthesis of DNA adducts by electrochemical oxidation and subsequent analysis by mass spectrometry has been reported (Rogan et al., 1988).

Modeling of Carcinogenic Potential by Structure Activity Relationships

The activity of a chemical towards living species will depend ultimately on the molecular structure of the chemical. In the last two decades, various attempts

have been made to relate biological activity to molecular structure with quantitative structure activity relationships (QSARs); these techniques have been reviewed in the recent literature (Turner et al., 1987; Lipnick, 1989; Klopman and Raychaudhury, 1988). These QSAR techniques use molecular structure and physical property data to make predictions about the biological activity of chemicals based on data from related compounds of known activity or reactivity.

QSARs are comprised of three components: chemical structure descriptors, the biological activity, and the technique used to establish the relationship. For example, Könemann and co-workers established a strong correlation ($r^2 = 0.988$) between the octanol-water partition coefficient (P_{ow}) and lethality to fish as determined by LC_{50} values (chemical concentration which kills 50% of the population within a particular timespan) (Könemann, 1981). Könemann used the Hansch linear regression technique which is based on the assumption that the biological response to a chemical is a function of its hydrophobic, electronic, and steric properties (Hansch and Fujita, 1964).

QSARs are used by regulatory agencies and industry to make rapid and cost-effective predictions about the toxicity and reactivity of industrial chemicals. According to a recent review of QSAR techniques, the toxicity, reactivity, and transport parameters needed to estimate environmental fate issues have been determined for approximately 1% of the 70,000 chemicals on the manufactured chemical inventory of the U.S. Environmental Protection Agency (EPA) (Borman, 1990). The EPA cost for determining these parameters for a single compound can

approach $100,000. Clearly, QSAR techniques are limited by the fact that the data required for determining the relationships are often not readily available. Furthermore, the correlations are typically applicable only within a narrow family of compounds. Also, great care must be exercised in the selection of the biological endpoint used.

One of the most useful tools for the efficient and rapid characterization of chemical contaminants in environmental samples is the computerized gas chromatography/mass spectrometry (GC/MS) system. Combining GC/MS with QSAR allows for chromatographic separation and identification of the mixture components by GC/MS, and prediction of the reactivities of the individual components with QSAR. The combination of QSAR and GC/MS is being used by the U.S. EPA in the premarket notification process for the registration of chemicals, and for the assessment of contaminants at hazardous waste sites. Disadvantages of GC/MS-QSAR are that, first, each contaminant must be identified correctly, and second, tremendous volumes of data can be rapidly produced by a GC/MS system, which can quickly overwhelm the data review and structural encoding processes required for QSAR.

Ion-Molecule Reactions For Screening of Environmental Mixtures

Ion-molecule reactions have been studied for many years in such instruments as drift tubes, flowing afterglows, ion traps, crossed-beams, ion

sources of mass spectrometers, and collision cells of tandem mass spectrometers. These instruments have yielded information and insights into characteristics of chemical reactions, such as energetics, cross-sections, gas-phase reactivity mechanisms, and kinetics.

Four common types of positive ion reactions with neutrals will be encountered in these studies: (a) charge exchange, (b) proton transfer, (c) collisionally activated decomposition (CAD), and (d) associative reactions (Harrison, 1983).

(a) $\quad A^{+\cdot} + B \longrightarrow A + B^{+\cdot}$

(b) $\quad A^{+\cdot} + B \longrightarrow [A+H]^+ + [B-H]^\cdot$

or $\quad A^{+\cdot} + B \longrightarrow [A-H]^\cdot + [B+H]^+$

(c) $\quad A^{+\cdot} + B \longrightarrow [A-X]^{+\cdot} + B + X$

(d) $\quad A^{+\cdot} + B \longrightarrow [A+B]^{+\cdot}$

or $\quad A^{+\cdot} + B \longrightarrow [A+(B-X)]^+ + X^\cdot$
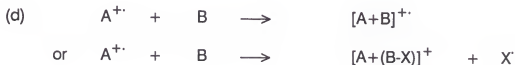
Reactions (a) and (b) form the basis of chemical ionization (CI) (Harrison, 1983), which is widely used in analytical mass spectrometry to produce ions indicative of the molecular weight of the compound (e.g., $[M+H]^+$ and $M^{+\cdot}$),

especially for compounds which fragment extensively under electron ionization (EI) conditions. Reaction (c) (CAD) is commonly employed in analytical tandem mass spectrometry (MS/MS) to fragment ions for mixture analysis or structure elucidation (McLafferty, 1981; Yost and Enke, 1979; Johnson and Yost, 1985). Reaction d (associative ion-molecule reactions), sometimes termed collisionally activated reactions (CAR), has been employed in a few studies to enhance the selectivity of analytical MS/MS methods (Fetterolf et al., 1984). Such associative ion-molecule reactions have also been studied in the gas-phase as an aid in understanding important solution-phase reactions as described below.

Initial studies reported here focus on ion-molecule reactions between DNA bases (or nucleosides) with potential carcinogens in the ion source of a triple quadrupole mass spectrometer. Davoli and co-workers have studied similar gas-phase reactions of pyridine and guanine with polynuclear aromatic hydrocarbons (PAH) in the ion source of a tandem mass spectrometer (Davoli et al., 1989). In addition, gas-phase synthesis of methylated nucleosides has been studied in the ion source of a mass spectrometer (Isern-Flecha, 1986). Burinsky and co-workers have investigated the similarity of ion source gas-phase reactions of primary amines and aldehydes to the analogous solution-phase reactions (Burinsky et al., 1984). They discovered that the gas-phase products corresponded in mass to the solution-phase products; confirmation was achieved by CAD of the product ions and the solution-phase synthesized standards. On the other hand, Burinsky and Campana found that the gas-phase site of electrophilic addition for reactions

between chlorinated alkyl ions with substituted benzenes differed considerably from that in solution-phase Friedel-Crafts alkylation (Burinsky and Campana, 1988). The differences were attributed to the accessibility of polar heteratoms in the gas-phase that are probably solvated in the solution-phase.

This dissertation reports the first evaluation of ion/molecule reactions in the ion source between potential carcinogens and nucleophiles as a screening technique, using on-line chromatographic separation. In these experiments, the electrophiles are introduced into the ion source via a gas-chromatographic (GC) column and reacted with the nucleophile introduced constantly into the ion source region via a solids probe or fine-metering valve, as illustrated in Figure 1-1. In addition to mass analysis of the product ions with the first quadrupole (Q1), CAD of the product ion mass-selected with Q1 can be performed in the second quadrupole (Q2, collision cell), followed by mass analysis of the resulting fragment ions with the third quadrupole (Q3). CAD of the product ion formed in the ion source can aid in structure elucidation of the product ion.

A serious limitation of ion-molecule reactions performed in the ion source is the lack of control over the reaction. In general, it is not known which species is ionized and which is neutral, as well as which ionic species is the most reactive and leads to the products observed. Although selection of the partial pressures of the reactants and of any reagent gas present may provide some control over the dominant ion-molecule reactions, rarely are the array of ions produced in the ion source simple enough to permit a clear understanding of the reactions which occur.
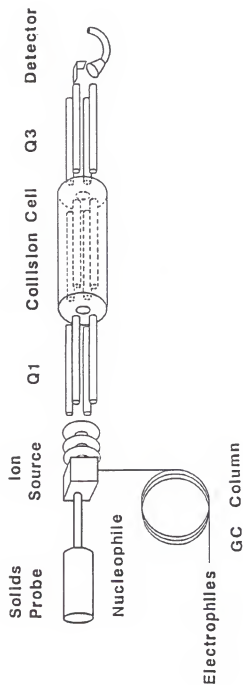
Figure 1-1: Instrumentation used for ion source ion-molecule reactions.

To further elucidate the types of reactions occurring in the ion source, mass-selected ion-molecule reactions have been performed in the collision cell of tandem mass spectrometers. For example, ion source reactions of iodopropane and benzene produce a $C_9H_{13}^+$ species. Miller and Gross have demonstrated that the $C_9H_{13}^+$ ion could be formed by reaction of $C_3H_7^+$ with neutral benzene in the collision cell as well as by reaction of $C_6H_6^{+\cdot}$ and neutral iodopropane (Miller and Gross, 1983). Collision cell reactions of mass-selected reactions of propane ions with neutral propane have aided in determining reaction mechanisms of this species and understanding the ions produced by ionization of propane in the ion source (Bone and Futrell, 1967).

Mass-selected reactions in the collision cell between vinylmethylether (VME) and propene aided in determining the mechanism of formation of the four-centered collision complex ($C_6H_{12}O^{+\cdot}$) (Fetterolf, 1983). The reaction of the mass-selected VME$^{+\cdot}$ ion with neutral propene in the collision cell generated a product ion at m/z 72 which is loss of C_2H_4 from the collision complex. In contrast, the equivalent product ion was not observed for the reaction of the mass-selected $C_3H_6^{+\cdot}$ with neutral VME in the collision cell.

In this dissertation, mass-selected reactions in the collision cell between potential carcinogens and nucleophiles are investigated both to study the types of product ions produced and to determine the utility of these reactions for potential carcinogen screening of complex environmental mixtures. In these experiments, two possible reaction pathways can be studied: nucleophile

ion/electrophile neutral and electrophile ion/nucleophile neutral reactions. Figure 1-2a depicts the instrumentation employed for studying nucleophile ion/electrophile neutral reactions in the collision cell. The nucleophile is constantly introduced into the ion source by a fine metering valve (for volatiles) or a solids probe (for nonvolatiles) and ionized. One mass-to-charge (m/z) ion is mass-selected with Q1, allowed to react with the neutral electrophiles entering the collision cell, and product ions are analyzed with the second mass analyzer (Q3). Based on technology developed by Hail in our laboratory, the electrophiles are introduced into the collision cell via a GC column (Hail et al., 1989) which allows for chromatographic separation of complex mixtures.

Figure 1-2b illustrates instrumentation employed for studying electrophile ion/nucleophile neutral reactions in the collision cell. The electrophiles are introduced in the ion source via a GC column and ionized. One m/z ion is mass-selected with Q1, allowed to react with the neutral nucleophile constantly introduced into the collision cell by a fine-metering valve, and product ions are analyzed with the second mass analyzer (Q3).

There are two general advantages to performing ion/molecule reactions in the collision cell as opposed to the ion source: (a) the reactant ion is clearly defined by mass-selection with Q1 and (b) the ability to vary the kinetic energy of the reactant ion. However, tandem mass spectrometric confirmation of the product ion by MS/MS is one advantage of reactions in the ion source; MS/MS of the product ions produced in the collision cell cannot be performed without the use of an instrument capable of MS/MS/MS.
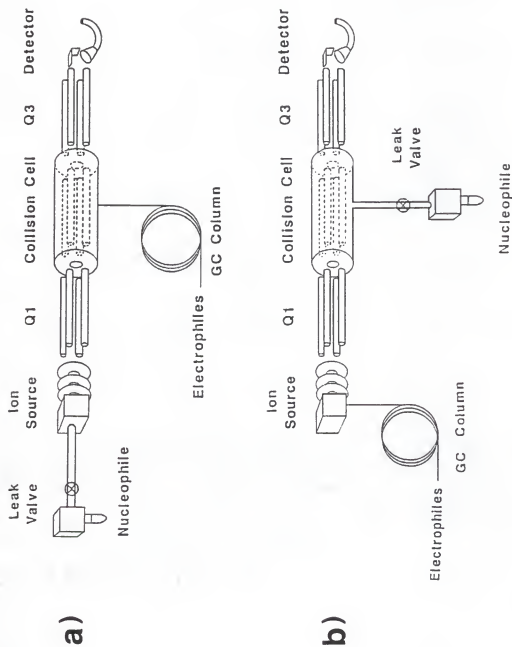
Figure 1-2: Schematic of instrumentation used for mass-selected a) nucleophile ion/electrophile neutral reactions and b) electrophile ion/nucleophile neutral reactions in the collision cell.

Scope of Dissertation

This dissertation comprises studies to characterize the use of tandem quadrupole mass spectrometry to perform electrophile/nucleophile ion-molecule reactions in an effort to develop a screening technique for potential carcinogens in complex environmental samples.

Chapter 1 introduces present methods for detecting potential carcinogens, such as animal tests, bacteriological tests, and mass spectrometric techniques. The concept and methodology of using ion-molecule reactions to screen for potential mutagens and carcinogens in an environmental mixture are introduced.

Chapter 2 describes ion-molecule reactions between adenine and benzoyl chloride performed in the ion source of a tandem quadrupole mass spectrometer under chemical ionization conditions. Confirmation of the product ion composition is achieved by CAD of the product ion produced in the ion source.

Chapter 3 evaluates the analytical characteristics of mass-selected reactions for nucleophile ion/electrophile neutral and electrophile ion/nucleophile neutral reactions between pyridine (a model nucleophile) and allylic compounds (known carcinogens). The reactivity of various electrophile and nucleophile ions (e.g., $M^{+\cdot}$, $[M+H]^+$, and $[M-H]^-$) as well as limits of detection are presented in this chapter.

Chapter 4 describes the effect of collision energy on the product ions obtained by nucleophile ion and electrophile ion reactions between allyl halides and pyridine in the collision cell. The effect of nucleophile pressure in the ion source (nucleophile ion/electrophile neutral reactions) or in the collision cell

(electrophile ion/nucleophile neutral reactions) on the product ions formed during reaction of several allyl halides with pyridine or piperidine is discussed. The types of competitive reactions occurring during these ion-molecule reactions in the collision cell are also presented.

In an effort to evaluate the utility of these ion-molecule reactions, Chapter 5 presents data obtained from a variety of electrophiles and different nucleophiles. The final chapter, Chapter 6, summarizes overall conclusions and presents ideas for future studies.

ION-MOLECULE REACTIONS IN THE ION SOURCE

Introduction

Since the introduction of chemical ionization (CI) (Munson and Field, 1966; Munson, 1971; Field, 1968), the study of ion-molecule reactions in the ion source of mass spectrometers has increased significantly. CI involves the reaction of the analyte species with the reagent ions produced from the high pressure of a reagent gas in the ion source to form typically a protonated molecule ($[M+H]^+$). These proton transfer reactions have been used extensively in mass spectrometers to determine gas-phase basicities of many species (Aue and Bowers, 1979).

In recent years, ion-molecule reactions in the ion source of mass spectrometers have been used to study more complex reactions. Gas-phase methylation of o-, m-, and p-dihyroxybenzene has been studied using methyl halides as CI reagent gases in the ion source (Isern-Flecha et al., 1984). The site of gas-phase methylation was investigated with the use of tandem mass spectrometry (MS/MS). Wood and co-workers have studied the ion source gas-phase methylation and ethylation sites of aniline, phenol, and thiophenol employing MS/MS for structure elucidation (Wood et al., 1983).

Ion molecule reactions have also played an important role in the identification of structural isomers. For example, ion source reactions of alkenes and cycloalkenes with CH_3NH_2, iso-C_4H_{10} or NO have been utilized for identification of structural isomers and for the determination of double bond positions (Budzikiewicz et al., 1985; Budzikiewicz and Busker, 1980).

The gas-phase reactions of metal ions have been investigated in ion sources of mass spectrometers. For example, the reaction of Fe(I) with alkynes and dienes to form $FeC_nH_{2n-2}^+$ in the ion source, followed by collisionally activated decomposition (CAD) of the adduct ion, provided structure elucidation and reaction mechanism information (Peake and Gross, 1986).

A recent application of these ion/molecule reactions is the exploration of gas-phase and solution-phase similarities of DNA adducts formed in the ion source of mass spectrometers. Utilizing MS/MS, the site and degree of gas-phase methylation of DNA nucleosides formed in the ion source have been characterized (Isern-Flecha, 1986). In the case of these simple methylating agents, the gas-phase reactions were found to parallel the solution-phase reactions with the nucleosides in DNA.

This chapter will present the extension of these ion-molecule reactions of DNA bases and nucleosides with potential carcinogens to the production of larger adduct species other than simple methylation or ethylation. The investigation of adenine and adenosine reactions with benzoyl chloride and methyl benzoate in the ion source of a triple quadrupole mass spectrometer will be presented. These

reactions are performed under methane CI conditions in order to increase the reaction time (and thus the probability of reaction) in the ion source. These compounds were chosen as examples of a reactive electrophile (benzoyl chloride) and a structurally similar, but less reactive compound (methyl benzoate). Benzoyl chloride is a strong lachrymator, and some authors have reported it to be carcinogenic to humans (Sakabe and Fukude, 1977; Sakabe et al., 1976). However, the IARC Monographs reviewed the reports and decided that there was insufficient evidence of human carcinogenesis for benzoyl chloride since the employees were exposed not only to benzoyl chloride, but also to production precursors, such as toluene, chlorine, benzotrichloride, and benzyl chloride (IARC, 1982). There is little evidence that benzoyl chloride is carcinogenic in animals, and it does not mutate bacteria (IARC, 1982). It has been suggested that the lack of mutation by benzoyl chloride in bacteriological assays could be due to the high susceptibility of benzoyl chloride to hydrolysis in the aqueous test system (Yasuo et al., 1978). There is no available literature on the carcinogenic or mutagenic potential of methyl benzoate; however, given the less favorable leaving group (CH_3O versus Cl), it is likely to be less reactive as an electrophile than benzoyl chloride.

MS/MS is utilized to further identify and characterize the product ions produced in the ion source. These gas-phase ion-molecule reactions between DNA bases or nucleoside and potential carcinogens could provide a sensitive technique to screen for potential carcinogens in complex mixtures, as well as provide further insights into solution-phase processes.

Experimental

The reactions of adenine and adenosine with benzoyl chloride and methyl benzoate (Figure 2-1) have been studied in the ion source of a Finnigan MAT (San Jose, CA) TSQ 45 triple quadrupole mass spectrometer. Adenine was introduced into the ion source continuously by a solids probe heated at a constant temperature of 140°C (adenosine at 230°C). Benzoyl chloride and methyl benzoate were introduced via a Finnigan MAT 9610 GC into the ion source by a J&W Scientific (Folsom, CA) 3m DB-1 (0.2 mm i.d., 0.25 μm film thickness) capillary column heated isothermally at 50°C. The injection port, transfer line, and interface were all held at 250°C. All species in the ion source were ionized by methane chemical ionization (CI), at a pressure of 0.40 torr indicated with a Granville Phillips (Boulder, CO) thermogauge. The instrument was mass-calibrated with perfluorotributylamine (FC43) under electron ionization (EI) conditions, followed by optimization of the FC43 ions under CI conditions.

Mass spectra were obtained at an electron energy of 100 eV, an emission current of 300 μA, and an ion source temperature of 190°C. Positive ion CI (PCI) and electron-capture negative ion CI (ECNCI) spectra were acquired with ±3 kV dynodes for pulsed positive ion-negative ion CI (PPINICI), an electron multiplier voltage of -800 V, and a preamplification gain of 10^8 V/A. The mass spectra were acquired by scanning the first mass analyzer (Q1) from 40 to 700 amu in 0.21 seconds (0.42 seconds for methyl benzoate reactions).
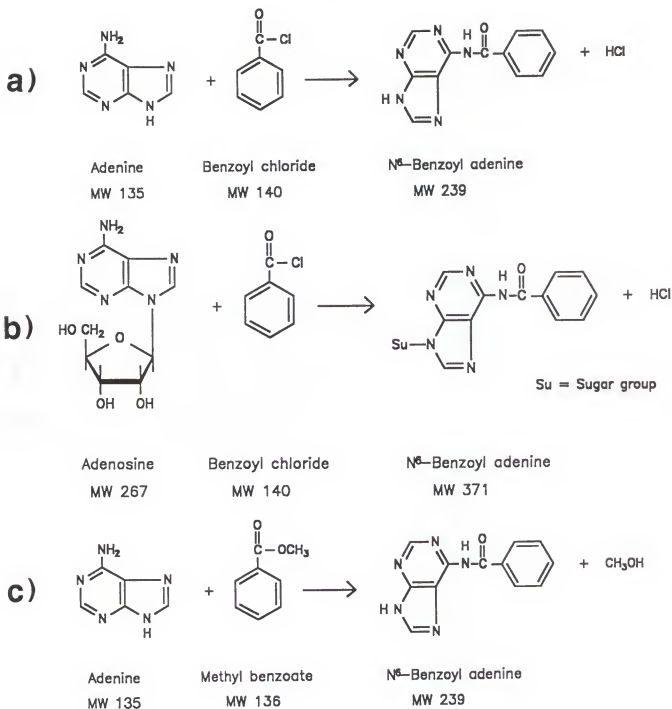
Figure 2-1: Reaction schemes for a) adenine and b) adenosine with benzoyl chloride, and c) adenine with methyl benzoate.

Daughter ion mass spectra were acquired at a collision energy of 28 eV and an indicated collision cell pressure of 1.0 mtorr Ar at an electron multiplier voltage of -1500 V. The collision cell pressure was measured with a Teledyne-Hastings-Raydist (Hampton, VA) DV-8 thermocouple gauge. The synthesized standard, N^6-benzoyl adenine, was introduced into the ion source by a solids probe which was heated from 90°C to 180°C at a rate of 60°C/min; daughter ion mass spectra were obtained under the above conditions.

One microliter splitless injections of 500 ng/μL solutions of either benzoyl chloride or methyl benzoate in methanol were made onto the GC column. Adenine, adenosine, and N^6-benzoyl adenine were obtained from Sigma Chemical Company (St. Louis, MO), benzoyl chloride from Eastman Kodak Company (Rochester, NY), and methyl benzoate from Chem Services (Media, PA).

<u>Positive and Negative Ion Mass Spectra</u>

<u>of Ion-Molecule Reactions</u>

The background-subtracted positive and negative ion CI mass spectra (Figure 2-2) obtained from the reaction of adenine (a DNA base) and benzoyl chloride in the ion source demonstrate the ability to produce DNA adducts in the ion source. The mass spectra are background-subtracted by subtracting 5 scans before the chromatographic peak from 5 scans centered around the peak maximum. In all the spectra shown, the nucleophile is labelled N, the electrophile,
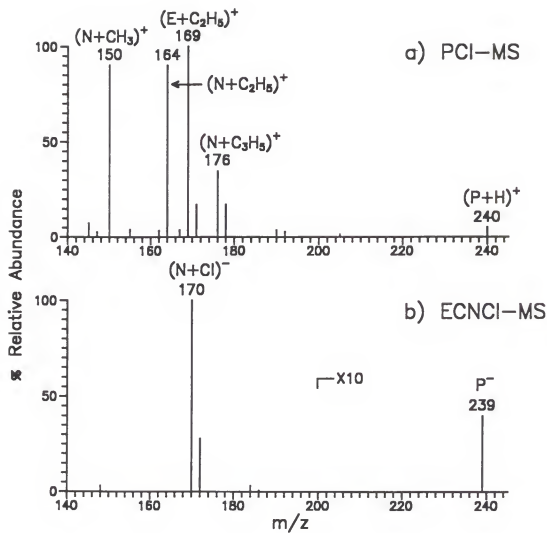
Figure 2-2: The background-subtracted a) PCI and b) ECNCI mass spectra of the adenine/benzoyl chloride reaction in the ion source.

E, and the DNA reaction product, P. The 240^+ ion in the PCI mass spectrum is the $(P+H)^+$ ion of the reaction product and the 239^- ion in the ECNCI mass spectrum is the P^- ion of the product. In addition, methane adduct ions (150^+, 164^+, 169^+, 176^+) of both reactants are observed in the positive mode, while chloride adduct ions (170^-, 172^-) of the nucleophile are observed in the negative mode.

The PCI mass spectrum of the adenine/benzoyl chloride reaction in Figure 2-3a illustrates an interesting phenomenon of ion-molecule reactions in the ion source under CI conditions. The mass spectrum is background-subtracted; thus the constant level of adenine-methane adduct ions (150^+, 164^+, and 176^+) should be subtracted from the mass spectrum. However, these ions are still prominent in the mass spectrum after background subtraction, indicating that the adenine-methane adduct ion intensities increase as benzoyl chloride elutes into the ion source. This increase in adenine adduct ions above the baseline is observed in the mass chromatograms shown in Figure 2-3b. Ions which are a function of the electrophile (169^+ and 240^+) are easily recognized by chromatographic peaks beginning at zero or nearly zero baseline.

Two mechanisms have been reported in the literature which can explain this increase in adenine-methane adduct ions as benzoyl chloride elutes into the ion source. Studies have shown that in a PCI mass spectrum the total ion current is increased by the addition into the ion source of species with large electron-capture cross sections (Rudewicz et al., 1984; Foltz, 1983; Johnson and Yost, 1986).

Figure 2-3: a) PCI background subtracted mass spectrum and b) mass chromatograms of the adenine/benzoyl chloride reaction illustrating the effect of benzoyl chloride elution on the adenine-methane adduct ions.

Major ion losses in the ion source are attributed to diffusion of all ions to the source walls and ion/ion or ion/electron recombination processes (Siegel and Fite, 1976). The increase in positive ion intensities can be explained by longer residence times in the ion source due to a decrease in the ambipolar diffusion rate of the combined charged species. The ambipolar diffusion constant of a positive ion-negative ion-dominated population is less than that for a positive ion-electron-dominated population; thus, an increase in the positive ion abundance would be expected with an increase in negative ions in the ion source.

In addition, since the recombination rates of the positive and negative ions are slower than those of positive ions and electrons, then replacing electrons with negative ions from electron-capture agents will decrease the loss of positive ions and increase the total positive ion current.

For comparison, Figure 2-4 displays the mass spectrum and mass chromatograms for the adenine/methyl benzoate reaction. The background-subtracted mass spectrum in Figure 2-4a is simpler than that for the adenine/benzoyl chloride reaction due to the absence of the adenine-methane adduct ions. The product ion, $[P+H]^+$, is observed at m/z 240. Comparing the relative intensities for the product ions (240^+) of the adenine/benzoyl chloride and adenine/methyl benzoate reactions, 6.1% and 0.5 % respectively, the benzoyl chloride is approximately 12 times more reactive than methyl benzoate. The mass chromatograms in Figure 2-4b confirm that there is no increase in the adenine-methane adduct ion intensities when methyl benzoate elutes into the ion source, since it is not an efficient electron-capturing agent.
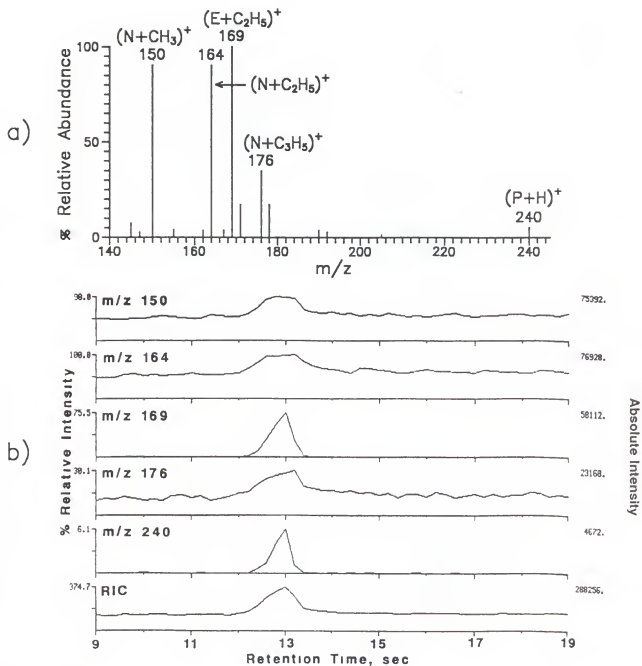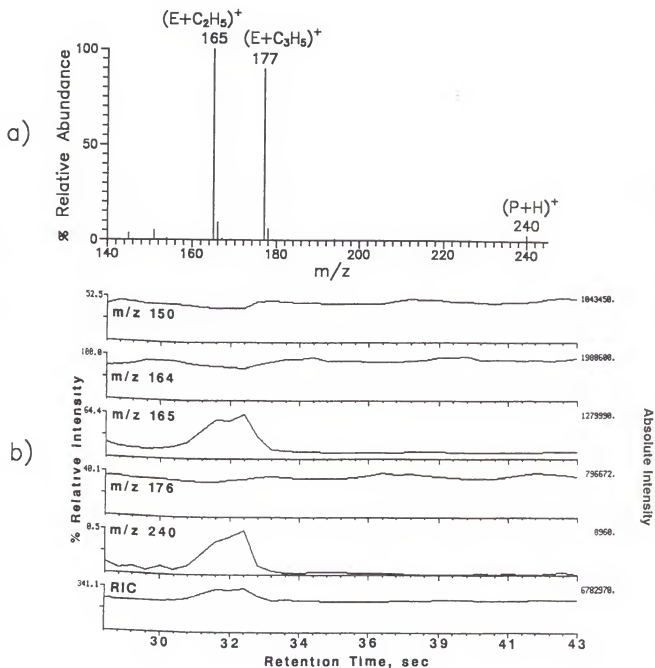
Figure 2-4: a) PCI background-subtracted mass spectrum and b) mass chromatograms of the adenine/methyl benzoate reaction illustrating the lack of enhancement of the adenine-methane adducts.

The background-subtracted PCI and ECNCI mass spectra in Figure 2-5 demonstrate the ability to produce DNA adducts between adenosine (a DNA nucleoside) and benzoyl chloride in the ion source. The 372^+ ion in the PCI mass spectrum of Figure 2-5a is the $[P+H]^+$ ion; the 268^+ ion is the protonated adenosine molecule ($[N+H]^+$). As in the reaction with adenine, there is a 240^+ ion in the reaction with adenosine; this ion could be formed from two different reaction pathways. Adenosine readily fragments to produce the adenine ion which could react with benzoyl chloride to produce the 240^+ ion; alternatively the 372^+ product ion of the adenosine/benzoyl chloride reaction could unimolecularly decompose to produce the 240^+ ion by loss of the neutral sugar moiety. The ions below m/z 200 have the same identity as those in the adenine/benzoyl chloride reaction in Figure 2-2.

The ECNCI mass spectrum obtained from the adenosine/benzoyl chloride reaction (Figure 2-5b) contains the 371^- ion which is the P^- ion; the 302^- and 304^- ions are the $[N+^{35}Cl]^-$ and $[N+^{37}Cl]^-$ ions, respectively. The 239^- ion (benzoyl adenine) and the 170^- and 172^- ions (chlorine adducts of the adenine fragment) could arise from the same two possible mechanisms, as described for the 240^+ ion in the reaction of adenosine and benzoyl chloride.

These data illustrate the complexity of the mass spectra produced from these ion-molecule reactions in the ion source. This complexity is a considerable disadvantage in using these ion-molecule reactions as a screening tool for complex environmental mixtures of unknown composition. Identifying the product
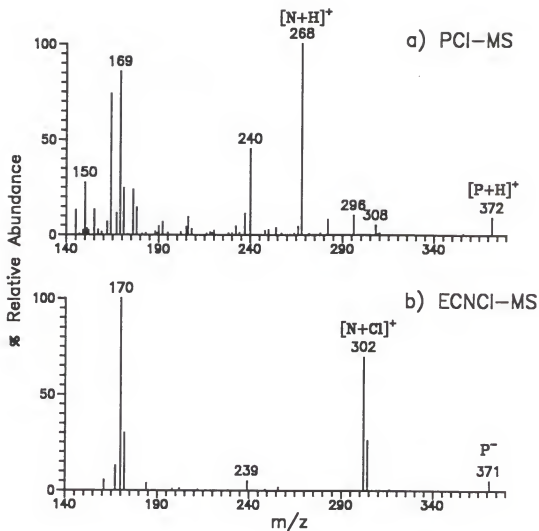
Figure 2-5: The a) PCI and b) ECNCI background-subtracted mass spectra of the adenosine/benzoyl chloride reaction in the ion source.

ion of interest in every chromatographic peak from an unknown mixture would quickly overwhelm the analyst.

MS/MS of Ion-Molecule Product Ions

Table 2-1 lists the ions in the daughter ion mass spectra of the $(P+H)^+$ and P^- adduct ions (240^+ and 239^-, respectively) produced by reaction of adenine and benzoyl chloride in the ion source. These daughter ions provide further information for identification of the gas-phase reaction product. It is interesting to observe that the positive and negative daughter ions complement one another; the 240^+ ion fragments to the benzoyl ion, whereas the 239^+ ion fragments to the adenine ion.

Further confirmation is possible by comparison of the daughter ion spectra obtained from the product ions ($[P+H]^+$ and P^-) of the ion-molecule reaction and the $[M+H]^+$ and M^- ions of the synthesized standard. CAD of the reaction product ion and the synthesized standard produce similar daughter ion mass spectra, confirming that the 240^+ and 239^- ions produced in the ion source are benzoyl adenine adduct ions. The differences observed, especially in the ratios of the daughter ion abundances to that of the parent ion remaining after collisionally activated decomposition (CAD) may arise from differences in internal energy of the parent ions. These differences could also indicate that the gas-phase reaction product is a mixture of structures. The benzoyl species could

Table 2-1: Comparison of daughter spectra for the $[P+H]^+$ and P^- product ions resulting from adenine/benzoyl chloride reactions in the ion source and for the $[M+H]^+$ and M^- ions of the corresponding synthesized standard N^6-benzoyl adenine.

		% Relative Abundance	
m/z	Structure	Ion-Molecule Reaction[*]	Synthesized Standard[*]
Daughter spectra of 240^+			
240	$[P+H]^+$	27	54
105	$C_6H_5CO^+$	100	100
77	$C_6H_5^+$	9	8
Daughter spectra of 239^-			
239	P^-	6	72
134	$[N-H]^-$	100	100
133	$[N-2H]^-$	-	32

[*]All daughter ions >4% are reported.

attach to positions other than the N^6-position of adenine to form the 240^+ product ion.

The stability of the ion-molecule reaction product can be estimated by examining the MS/MS parent and daughter ions as a function of collision energy. As the collision energy is increased, more energy is deposited into the parent ion causing greater fragmentation. The collision energy breakdown curves for the $[P+H]^+$ (m/z 240) produced by the reaction of adenine and benzoyl chloride in the ion source are shown in Figure 2-6a. The intensities of the benzoyl and phenyl daughter ions (105^+ and 77^+, respectively) increase with increasing collision energy, while the parent ion intensity (240^+) decreases with increasing collision energy. The parent and daughter ion traces cross each other at 8 eV. For comparison, the collision energy breakdown curves for the N^6-benzoyl adenine synthesized standard are illustrated in Figure 2-6b. In this case, the parent ion (m/z 240) and daughter ions (m/z 105 and 77) reach a crossover point at 22 eV. These data suggest that the protonated product ion of the adenine/benzoyl chloride reaction is not as stable as the synthesized standard. As previously mentioned, this effect may be due in part to the product ion being a combination of structures or having higher internal energy than the $[M+H]^+$ ion of the synthesized standard.
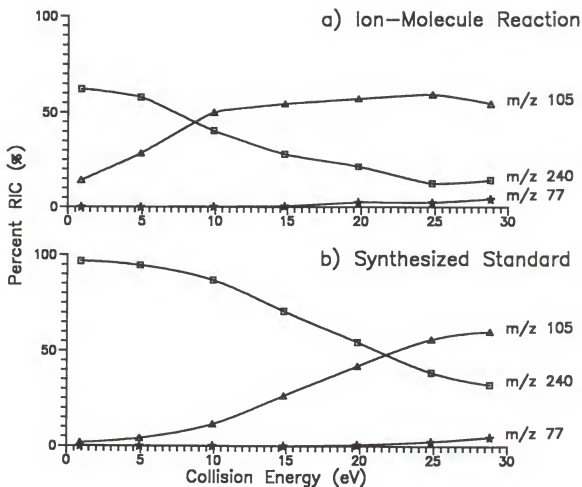
Figure 2-6: Collision energy breakdown curves for the a) adenine/benzoyl chloride reaction in the ion source and b) synthesized standard, N[6]-benzoyl adenine.

Conclusions

The ability to produce and detect products of ion-molecule reactions between DNA bases or nucleosides and benzoyl chloride or methyl benzoate has been demonstrated in the ion source of a triple quadrupole mass spectrometer. Other studies, employing various DNA bases (e.g., cytosine and thymine) and electrophiles (e.g., benzoyl chloride, methyl benzoate, and phenylacetonitrile) yield similar results.

In terms of a screening technique, ion source reactions use typical mass spectrometric configurations (no instrumental modifications); however, each GC eluent gives rise to a chromatographic peak in which the product ions must be identified. As demonstrated, the ion source ion-molecule reactions result in complicated mass spectra. The complicated nature of these mass spectra will make it difficult to identify product ions in unknown complex mixtures. Furthermore, reaction pathways are difficult to ascertain because all species are ionized in the ion source. Thus, it is difficult to determine which form of which species is reacting (e.g. $[M+H]^+$, M^+, fragment ions, or neutrals).

Ion source reactions do offer the advantage of performing MS/MS on the product ions of interest. MS/MS of the adduct ion produced by the adenine/benzoyl chloride reaction aided in confirming the identity of the reaction product. Tandem mass spectrometry also allows for structure elucidation, reaction mechanism and bonding site studies of these ion-molecule reactions.

EVALUATION OF NUCLEOPHILE/ELECTROPHILE REACTIONS
AS AN ENVIRONMENTAL SCREENING TECHNIQUE

Introduction

Potentially mutagenic and carcinogenic chemical contaminants are recognized to be reactive electrophiles (or metabolically activated to electrophiles) capable of modifying biological macromolecules such as DNA (Miller, 1970). These compounds, however, represent only a small portion of the total number of contaminants in the typical environmental sample. Accurate evaluation of these chemicals to provide data for human and ecosystem risk assessment depends upon analytical procedures to isolate, identify, and quantify each chemical and to provide a comparative measure of electrophilic reactivity.

This chapter evaluates the analytical utility of mass-selected ion-molecule reactions between pyridine (a volatile model DNA base) and allyl compounds (electrophiles) in the collision cell of a triple quadrupole mass spectrometer. These ion-molecule reactions can provide a rapid and sensitive technique, not only to screen complex environmental samples for potential carcinogens, but also to estimate the relative mutagenic (i.e., possibly carcinogenic) potential of each. The chapter investigates two types of reactions: those between nucleophile ions and

electrophile neutrals and those between electrophile ions and nucleophile neutrals. Comparisons to reactions in the ion source, the choice of mass-selected ion, and limits of detection will be presented; the gas-phase results will also be compared to solution-phase data for a series of allyl compounds, for which Ames test mutagenicities have been established (Eder et al., 1982).

<div align="center">

Nucleophile Ion/Electrophile Neutral Mass-Selected Reactions in the Collision Cell

</div>

This section of Chapter 3 deals with reactions in the collision cell between mass-selected ions of pyridine (a model DNA base) and neutral electrophiles eluting into the collision cell via GC (Figure 1-2b). The general scheme for the reaction of various mutagenic allylic compounds with pyridine ions is demonstrated in Figure 3-1. In this case, the radical molecular ion of the nucleophile pyridine ($N^{+\cdot}$) is mass-selected to react in the collision cell with the neutral electrophiles (E) of the general form C_3H_5X, where X can be Cl, Br, I or NCS. The product ion depicted (e.g. N-allyl pyridine) is formed by nucleophilic substitution of the allyl compound and loss of a neutral X radical.

Experimental

All experiments were performed on a Finnigan MAT TSQ 70 triple quadrupole mass spectrometer equipped with a Varian 3400 gas chromatograph.
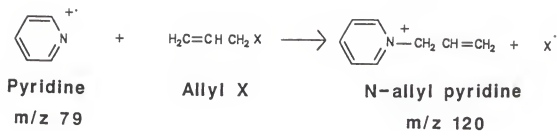
Figure 3-1: Collision cell reactions of the mass-selected $N^{+ \cdot}$ of pyridine with neutral allyl compounds of the general form C_2H_5X, where X is NCS, Cl, Br or I.

Pyridine was constantly introduced into the ion source with a Granville Phillips fine-metering valve (Boulder, CO) and ionized under electron ionization (EI) or chemical ionization (CI) conditions. All experiments were performed at an emission current of 200 μA, electron energies of 70 eV (EI) or 100 eV (CI), a manifold temperature of 100°C, and ion source temperatures of 170°C for EI or 150°C for CI.

The pyridine ion of interest was mass-selected by Q1 and reacted in the collision cell with the neutral electrophiles introduced into the collision cell via a GC column. The product ions were mass analyzed with Q3 and detected with an electron multiplier (EM) (conversion dynodes: $\pm$5 kV).

The GC transfer line for introduction into the collision cell, designed by Hail and co-works (Hail et al., 1989), consists of a capillary column passed through a 1 m long stainless steel (s.s.) tubing (1/16 inch o.d.) which is heated resistively by applying an AC voltage provided by a variable transformer (Variac) and step-down transformer across the s.s. tubing. The temperature of the transfer line was adjusted by varying the voltage applied to the tubing; $\approx$7 to 8 volts were needed to heat the transfer line to 200°C. The original transfer line extended about an inch into the vacuum chamber and was heated to the very end of the s.s tubing (by grounding the tip to the inside wall of the vacuum chamber). This resulted in temperatures inside the vacuum chamber high enough to char the capillary column, since the rate of thermal loss is significantly lower at 10^{-6} torr than at atmosphere. The transfer line was modified so that ground is established at the point where it enters the manifold through a feedthrough; the s.s. tubing extends

about 1/8 of an inch into the vacuum chamber. Thus, the last 6 or 7 cm of the capillary column, between the point where it enters the vacuum chamber and is inserted into the collision cell, is heated only by the manifold heater (held at 100°C).

The mass spectrometer was mass-calibrated with perfluorotributylamine (FC43), then tuned for ion-molecule reactions in the collision cell. Allyl chloride was constantly introduced into the collision cell with a Negretti fine-metering valve (Hampshire, England) via the collision gas inlet. The collision energy, collision cell rf potential, and the potentials on the lenses immediately before and following the collision cell were optimized for maximum transmission of the reactant ion (N^+) and the product ion (120^+). Typically, the collision energy maximized at 2 or 3 eV (see Chapter 4 for further details).

Note that initial experiments were performed with the original TSQ 70 quadrupole collision cell; however, the calibration and gas-phase versus solution-phase studies were performed with a new TSQ 700 octapole collision cell. No noticeable effects on the product ions were detected for the compounds studied.

Samples and reagents. Propyl bromide, propyl chloride, and benzyl chloride were purchased from Eastman Kodak (Rochester, NY), allyl chloride, allyl iodide, allyl isothiocyanate, allyl bromide, and 2,3-dichloropropene from Aldrich Chemical Company (Milwaukee, WI), and pyridine from Fisher Scientific (Fair Lawn, NJ). The solvents, HPLC grade pentane, and Spectro grade heptane, were purchased from Fisher Scientific and Eastman Kodak, respectively.

Ion source reactions. Gas chromatography was carried out on a J & W Scientific (Folsom, CA) DB-5 (6 m long, 0.178 mm i.d., 0.4 μm film thickness) capillary column in the split mode (split ratio (SR) = 30:1) with helium carrier gas at an inlet pressure of 5 psig. The GC oven was temperature programmed from 25°C to 150°C at 40°C/min after an initial hold period of 1 min. One-microliter injections were made at an injection port temperature of 250°C and transfer line temperature of 200°C (TSQ 70 transfer line). The test mixture was prepared in heptane containing 6 μg/μL each of allyl chloride, allyl bromide, and allyl isothiocyanate.

The positive ion chemical ionization (PCI) mass spectra obtained by reaction of pyridine with the GC eluates were acquired with a CI ion volume at an ion source pressure of 1.6 torr CH_4 indicated with a Granville Phillips convectron gauge, an EM voltage of -900 V, and a Q1 scan function of 55 to 350 amu in 0.3 seconds. The high vacuum pressure in the analyzer region was 1.2 x 10^{-5} torr as measured by a Varian Bayard-Alpert ionization gauge (Palo Alto, CA).

Reactivity of nucleophile ions. Gas chromatography was carried out on a J & W Scientific DB-5 (6 m long, 0.178 mm i.d., 0.4 μm film thickness) capillary column in the split mode (SR=30:1) with helium carrier gas at an inlet pressure of 5 psig. The GC oven was temperature programmed from 25°C to 150°C at 20°C/min after an initial hold time of 1 min. One-microliter injections were made in triplicate at an injection port temperature of 250°C and a collision cell transfer line temperature of 200°C. One-microliter injections of two test mixtures (6 μg/μL

per component) were made: allyl chloride, allyl bromide, and allyl isothiocyanate in heptane and allyl iodide in pentane. Due to the limited resolution of the short column (6 m), two mixtures were needed because allyl iodide co-elutes with heptane and allyl chloride with pentane.

The EI mass spectra (EI ion volume) were obtained by alternately mass-selecting between the $N^{+\cdot}$ ion of pyridine and the $CH_4^{+\cdot}$ ion of methane to react with the electrophiles eluting into the collision cell. The positive and electron capture negative CI mass spectra were obtained by alternately mass-selecting between the $[N+H]^+$, $[N+C_2H_5]^+$, $[N+C_3H_5]^+$ or $[N-H]^-$ ions of pyridine and the $CH_5^{+\cdot}$ ion of methane to react with the electrophiles eluting into the collision cell. The mass spectra obtained by reaction of the various pyridine ions were acquired at an ion source pressure of 1.6 torr CH_4, an EM voltage of -1000 V; Q3 was scanned from 30 to 300 amu in 0.25 seconds. The analyzer high vacuum pressure was 1.2×10^{-5} torr.

Calibration studies. Gas chromatography was carried out on a J & W Scientific DB-5 (20 m long, 0.178 mm i.d., 0.4 μm film thickness) capillary column in the split mode (SR=100:1) with helium carrier gas at an inlet pressure of 5 psig. The GC oven was temperature programmed from 50°C to 100°C at 20°C/min. One-microliter injections were made in triplicate at an injection port temperature of 200°C and transfer line temperature of 200°C. Allyl chloride and allyl iodide mixtures were prepared in pentane in the following manner: the 5 and 10 μg/μL were prepared from a stock solution of 30 μg/μL ; 75, 100, and 500 ng/μL

solutions from the 5 $\mu g/\mu L$ solution; 10, 25, and 50 ng/μL solutions from the 500 ng/μL solution; 1 and 2.5 ng/μL solutions from the 100 ng/μL solution. Triplicate 1 μL injections of the blank (pentane) were made under the same conditions.

Pyridine was introduced into the ion source at a constant pressure of 2 x 10^{-4} torr as measured by a Varian Bayard-Alpert ionization gauge mounted on the ion source vacuum manifold. Pyridine was ionized under EI conditions (EI ion volume) and the radical molecular ion ($N^{+\cdot}$) was mass-selected by Q1. Selected reaction monitoring (SRM) of the product ion was performed by scanning Q3 from 119.5 to 120.5 amu in 0.25 seconds. Product ions were detected at an EM voltage of -1600 V.

Gas-phase reactivity studies. Gas chromatography was carried out on a J & W Scientific DB-5 (20 m long, 0.178 mm i.d., 0.4 μm film thickness) capillary column in the split mode (SR=100:1) with helium carrier gas at an inlet pressure of 5 psig. The GC oven was temperature programmed from 50°C to 200°C at 10°C/min after an initial hold time of 1 min, with an injection port temperature of 200°C and transfer line temperature of 200°C. Triplicate 1μL injections (SR=100:1) were made of an equimolar (29.8 nmol/μL) solution containing allyl chloride, allyl bromide, allyl iodide, allyl isothiocyanate, benzyl chloride, 2,3-dichloropropene, propyl bromide, and propyl chloride in pentane.

The $N^{+\cdot}$ ion of pyridine and $CH_4^{+\cdot}$ ion methane (1.2 torr) were alternately mass-selected to react with the electrophiles eluting into the collision cell. Q3 was scanned from 30 to 300 amu in 0.25 seconds and product ions were detected at

an EM voltage of -1200 V. The pyridine ion source pressure without methane present was 2.0 x 10^{-4} torr as measured by the ionization gauge mounted on the ion source vacuum manifold.

Comparison to Ion Source Reactions

Due to the complexity of ion source reactions (Chapter 2), mass-selected reactions in the collision cell were investigated. The PCI mass spectrum of the pyridine/allyl chloride reaction in the ion source (Figure 3-2a) is compared to one obtained from the pyridine ion/allyl chloride reaction in the collision cell (Figure 3-2b). In the mass spectrum obtained by ion source reactions, the 120^+ ion can correspond to the $[N+C_3H_5]^+$ methane CI adduct ion of pyridine and/or the reaction product of pyridine and allyl chloride. Many lower mass ions are observed in the mass spectrum obtained from reaction in the ion source which are due to reactions of the electrophile or nucleophile with methane as well as fragment ions. The collision cell mass spectrum, however, is simpler and less ambiguous since only one ion, pyridine $N^{+\cdot}$ (produced under CI conditions), is mass-selected with Q1 to react in the collision cell with the neutral analytes eluting from the GC. The collision cell mass spectrum contains the mass-selected $79^{+\cdot}$ ion of pyridine ($N^{+\cdot}$) and the 120^+ ion which can only be the product ion since no methane ions or neutrals are present in the collision cell to form the $[N+C_3H_5]^+$ ion.
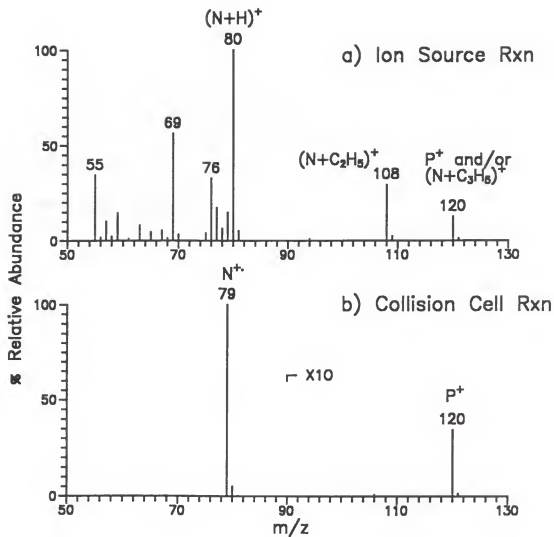
Figure 3-2: Comparison of a) the reaction of pyridine with allyl chloride in the ion source and b) the reaction of the mass-selected $N^{+\cdot}$ ion of pyridine with allyl chloride in the collision cell.

Performing mass-selected reactions in the collision cell has advantages over ion source reactions other than simpler mass spectra. Because only one ion is mass-selected with Q1 to react with the neutral electrophiles in the collision, the mechanisms for product ion formation can be more readily studied. Also, only those GC eluates which react with the nucleophile will produce a chromatographic peak, thus the number of chromatographic peaks which require further investigation will be significantly reduced. In the ion source reactions of Chapter 2, all the species eluting into the ion source will produce chromatographic peaks regardless of whether the species react with the nucleophile.

The reaction schemes in Figure 3-3 demonstrate an experiment which illustrates one of the advantages of mass-selected reactions in the collision cell. Under methane CI conditions in the ion source, one can alternately mass-select between $79^{+ \cdot}$ of pyridine ($N^{+ \cdot}$) and 17^{+} of methane (CH_5^{+}) to react with the neutral electrophiles eluting from the GC into the collision cell. Allyl compounds (C_3H_5X) are known mutagens which react with DNA to form adducts, whereas the analogous propyl compounds (C_3H_7X) are non-mutagenic and therefore do not react with DNA (Eder et al., 1982). Based on these solution-phase results, the allyl halides are expected to react with the $N^{+ \cdot}$ ion of pyridine in the gas-phase, whereas the propyl halides should not (Figure 3-3a). Mass-selection of the CH_5^{+} of methane in the next scan (Figure 3-3b) allows for identification of all compounds eluting into the collision cell by proton transfer between CH_5^{+} and the analyte; the resultant mass spectra would be expected to be similar to those produced under normal methane PCI conditions.

a) Reactions with Pyridine:

$H_2C=CH\ CH_2\ X$ **Allyl halides** $\longrightarrow$ [pyridinium]$^+$ $N-CH_2\ CH=CH_2$ + X$\cdot$

[pyridine]$^{+\cdot}$ +
m/z 79

$H_3C\ CH_2\ CH_2\ X$ **Propyl halides** $\xrightarrow{\ \ X\ \ }$
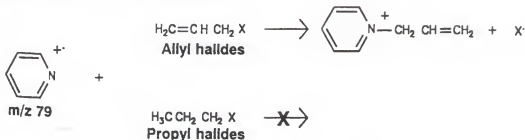
b) Reactions with Methane:

$H_2C=CH\ CH_2\ X$ **Allyl halides** $\longrightarrow$ $\left[H_2C=CH\ CH_2\ X\ +\ H\right]^+$ + CH_4

CH_5^+ +
m/z 17

$H_3C\ CH_2\ CH_2\ X$ **Propyl halides** $\longrightarrow$ $\left[H_3C\ CH_2\ CH_2\ X\ +\ H\right]^+$ + CH_4
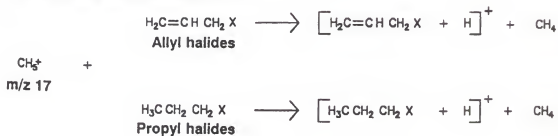
Figure 3-3: Schemes for the reactions of the alternately mass-selected a) $N^{+\cdot}$ ion pyridine and b) CH_5^+ ion of methane with allyl halides and propyl halides.

Figure 3-4 illustrates the mass chromatograms obtained by alternately mass-selecting the $79^{+\cdot}$ ion of pyridine ($N^{+\cdot}$) and the 17^+ ion of methane (CH_5^+) with Q1 to react with the components of the test mixtures eluting from the GC into the collision cell. The results of alternating between $79^{+\cdot}$ ion of pyridine and 17^+ ion of methane, shown in Figure 3-4, are compared for equivalent amounts of the two classes of compounds. The allyl halide chromatograms (a) and (b) demonstrate the gas-phase reactivity of the carcinogenic allyl compounds with the $79^{+\cdot}$ ion and proton transfer with CH_5^+. The propyl halide chromatograms (c) and (d), in contrast, illustrate that no significant reaction with the $79^{+\cdot}$ ion of pyridine is observed for these non-carcinogenic compounds. The chromatographic peak observed in chromatograms (b) and (d) before the elution of allyl chloride has been identified by its EI mass spectrum to be a cyclopentane impurity in the pentane solvent. Note that no reactivity with the $N^{+\cdot}$ ion of pyridine is observed for the cyclopentane impurity in chromatograms (a) and (c). Thus, mass chromatograms can be obtained that either depict only reactive compounds (reaction with pyridine $N^{+\cdot}$) or depict all the compounds in the mixture (protonation by CH_5^+). Note in Figure 3-4 that the reactivity with CH_5^+ of methane is approximately the same for the equivalent concentrations of the allyl and propyl compounds. Therefore, monitoring reactions of the $79^{+\cdot}$ ion of pyridine relative to the 17^+ ion of methane may aid in estimating the degree of reactivity of electrophiles of varying concentrations in complex mixtures.
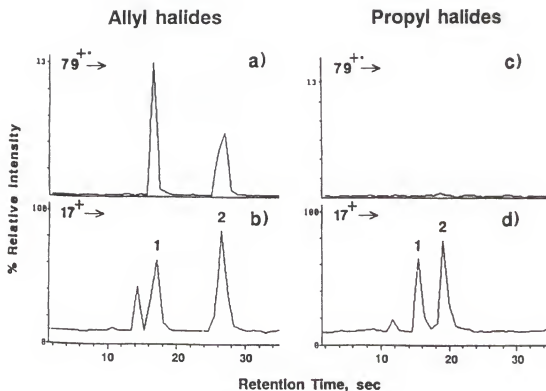
Figure 3-4: Mass chromatograms comparing collision cell reactions of mutagenic allyl compounds (a and b) and nonmutagenic propyl halides (c and d). Mass chromatograms (a) and (c) are a result of mass-selecting the $79^{+\cdot}$ ion of pyridine to react with the GC eluates in the collision cell; (b) and (d) are a result of mass-selecting the 17^{+} ion of methane to react with the eluates. The GC eluates are (1) allyl chloride, (2) allyl bromide, (3) propyl chloride, and (4) propyl bromide. The earlier peak in (b) and (d) is a cyclopentane impurity in the pentane solvent.

GC/MS is the most widely used technique for detecting potential carcinogens in complex environmental mixtures; however, the large volumes of data obtained quickly overwhelm the analyst. Each analyte produces a chromatographic peak which must be correctly identified and its mutagenicity and/or carcinogenicity determined. The nucleophile ion gas-phase reactions are capable of reducing the number of chromatographic peaks the analyst must evaluate since analytes which do not react with the model nucleophile will not produce a chromatographic peak. Note that some competing reactions such as charge exchange can produce ions and hence a chromatographic peak for non-electrophiles. This is discussed in greater detail in Chapters 4 and 5.

Reactivity of Various Nucleophile Ions

The reactivity of the variety of nucleophile ions which are produced in the ion source under EI and CI conditions is of fundamental interest in these ion-molecule reactions. The reactivity of the mass-selected pyridine $N^{+\cdot}$ ion produced under EI conditions and the $[N+H]^+$, $[N+C_2H_5]^+$, $[N+C_3H_5]^+$, and $[N-H]^-$ ions produced under CI conditions was studied for allyl isothiocyanate, allyl chloride, allyl bromide, and allyl iodide. In the case of these four allylic compounds, only the $N^{+\cdot}$ ion of pyridine demonstrated any product ion formation with the neutral eluates. The fact that the $[M+H]^+$ and methane adduct ions of pyridine do not react suggests that the site of reactivity in pyridine is blocked by the addition of the proton or alkyl groups.

The reactivity experiments for the $N^{+\cdot}$ ion of pyridine were performed by alternately mass-selecting the $N^{+\cdot}$ ion of pyridine (under EI conditions) and the $CH_4^{+\cdot}$ ion of methane. Since the $N^{+\cdot}$ ion of pyridine is produced under EI conditions, the $CH_4^{+\cdot}$ ion of methane (rather than the CH_5^+ ion) is used to detect all the GC eluates. The $CH_4^{+\cdot}$ ion of methane is capable of charge exchanging with most organic compounds, since its ionization energy (IE) is relatively high (12.51 eV).

The background-subtracted mass spectra obtained by reaction of the $N^{+\cdot}$ ion of pyridine with the allyl chloride, allyl bromide, and allyl iodide are shown in Figure 3-5. The product ion, 120^+, is the base peak in all the mass spectra; comparison of the base peak intensities indicates that the order of reactivity with pyridine is allyl chloride < allyl bromide < allyl iodide. The carbon-halide bond strength decreases in the order Cl > Br > I; this explains the lack of a 41^+ ion $(C_3H_5^+)$ in the allyl chloride mass spectrum and the large 41^+ ion in the allyl iodide mass spectrum. The allyl bromide mass spectrum demonstrates an $[N+^{79}Br]^+$ ion at m/z 158 (and $[N+^{81}Br]^+$ at m/z 160) which undergo further reaction with neutral pyridine present in the collision cell to form the $[N_2+Br]^+$ ions at m/z 237 and 239. Allyl iodide is observed to undergo analogous reactions to give m/z 206 and 285, $[N+I]^+$ and $[N_2+I]^+$, respectively, while allyl chloride does not. Due to similar ionization energies, charge exchange can occur between allyl iodide (IE = 9.298 eV) and pyridine (IE = 9.25 eV) to produce the radical molecular ion of allyl iodide $(E^{+\cdot})$ at m/z 168. Allyl chloride (IE = 9.9 eV) and allyl

Figure 3-5:   Background-subtracted mass spectra obtained from the reaction of N$^{+\cdot}$ ion of pyridine with a) allyl chloride, b) allyl bromide, and c) allyl iodide.

bromide (IE = 10.06 eV) do not undergo charge exchange with pyridine since their ionization energies are above that of pyridine.

The mass spectra obtained by mass-selecting the $CH_4^{+\cdot}$ ion of methane were investigated as a method for identifying all the compounds eluting into the collision cell. The background-subtracted mass spectra obtained by reaction of the $CH_4^{+\cdot}$ ion of methane with allyl chloride, allyl bromide, and allyl iodide are shown in Figure 3-6. All the mass spectra contain many ions which were observed in the mass spectra obtained by mass-selecting the $79^{+\cdot}$ ion of pyridine. Since the methane and pyridine ions are mass-selected in the same experiment, both species are present as neutrals in the ion source (and therefore in the collision cell), thus the $CH_4^{+\cdot}$ ion not only reacts with the electrophile (equation a), but also with pyridine (equation b), to produce radical molecular ions of pyridine by charge exchange.

(a) $CH_4^{+\cdot}$ + E $\longrightarrow$ $E^{+\cdot}$ + CH_4

(b) $CH_4^{+\cdot}$ + N $\longrightarrow$ $N^{+\cdot}$ + CH_4

Therefore, there are two possible pathways to produce the 120^+ product ion (allyl pyridine) when mass-selecting the $CH_4^{+\cdot}$ ion: (equation c) reaction of the electrophile radical molecular ion with the neutral pyridine and (equation d) reaction of the nucleophile radical molecular ion with the neutral electrophile. The reaction of equation (d) has been shown in this section to occur with pyridine as

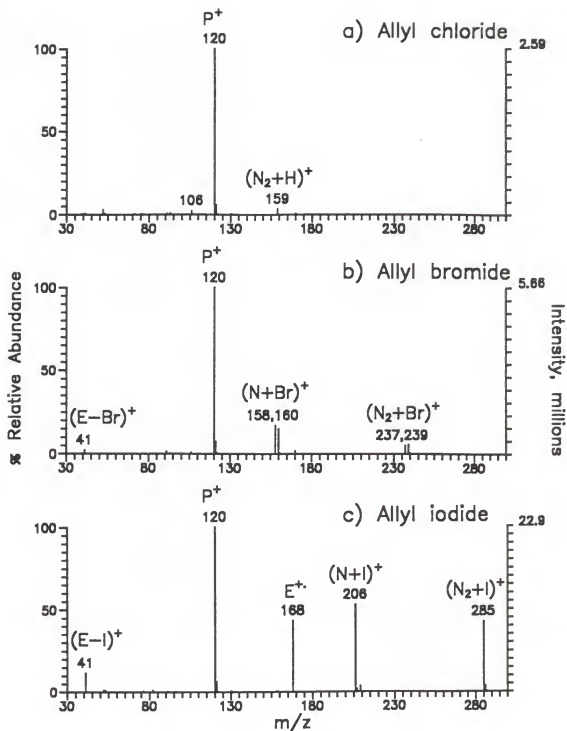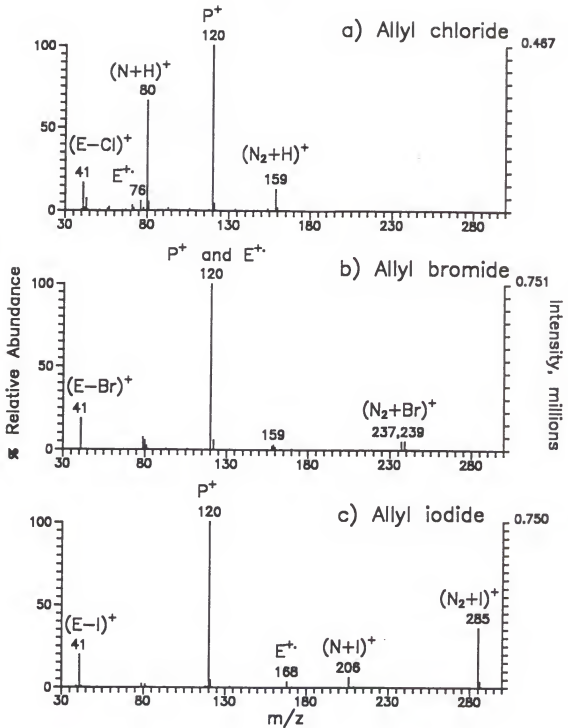Figure 3-6: Background-subtracted mass spectra obtained by the reaction of $CH_4^{+\cdot}$ ion of methane with a) allyl chloride, b) allyl bromide, and c) allyl iodide.

the nucleophile; a later section will demonstrate that equation (c) also occurs readily with neutral pyridine. These reactions are discussed in further detail in Chapter 4.

It is clear from these mass spectra obtained by mass-selecting $CH_4^{+\cdot}$ of methane that identifying the eluting electrophile from these mass spectra would be

(c) $\quad E^{+\cdot} \quad + \quad N \quad \longrightarrow \quad P^+$

(d) $\quad N^{+\cdot} \quad + \quad E \quad \longrightarrow \quad P^+$

extremely difficult. Given the large difference between the IE of the allyl species and the recombination energy (RE) of the $CH_4^{+\cdot}$ ion, the $E^{+\cdot}$ ions of the allyl species fragment extensively and are of much lower abundance than the $[E-X]^+$ fragment ion at m/z 41. More importantly, the ions resulting from the pyridine neutrals which have diffused into the collision cell from the ion source are more abundant than the electrophile ions. Decreasing the pyridine pressure in the ion source (and therefore in the collision cell) does increase the abundance of the ions representative of the electrophile relative to those which include the nucleophile; nevertheless, the product ions are still present in the mass spectra. Naturally, decreasing the amount of pyridine in the source also reduces the absolute intensity of the product ions observed in the alternate scan in which $79^{+\cdot}$ ion of pyridine is mass-selected. However, since all the ions present in the mass spectra are a function of the electrophile, the mass chromatograms produced by mass-selection of the $CH_4^{+\cdot}$ ion of methane can be used to normalize the product ion reactivity to the amount of electrophile in the sample.

Calibration Studies of Allyl Halides

Figure 3-7 depicts the log-log calibration curves obtained for the reaction of allyl chloride and allyl iodide with the radical molecular ion of pyridine in the selected reaction monitoring (SRM) mode (Q3 scanned over one amu). The calibration curves for the reaction of both allyl halides are linear over approximately 3 decades (slope (m) = 0.87 and 0.91 for allyl chloride and allyl iodide, respectively). At quantities above 5 ng ($\approx$100 pmol) the curves level off due to saturation of the data system summation algorithms as indicated by flat-topped chromatographic peaks. The average area count (in millions) for the blanks is 0.009 for both allyl chloride and allyl iodide. The reproducibility, calculated as the average relative standard deviation (RSD), of the allyl chloride and allyl iodide reaction product ions (m/z 120) is 6.0% for both compounds over the linear portion of the calibration curves. The offset in the calibration curves between the product ion areas of the allyl iodide and allyl chloride is indicative of the difference in the gas-phase reactivity of the two allyl halides.

Low picogram ($\approx$100 femtomoles) limits of detection (LOD) were observed for the product ions of these two allyl halides. Studying the mass chromatograms produced at low concentrations introduced an interesting phenomenon of nucleophile ion/electrophile neutral reactions. Figure 3-8 illustrates the SRM mass chromatogram obtained for the reaction of the allyl halides with the pyridine ion at 25 picograms. The peaks labelled allyl chloride and allyl iodide are the m/z 120
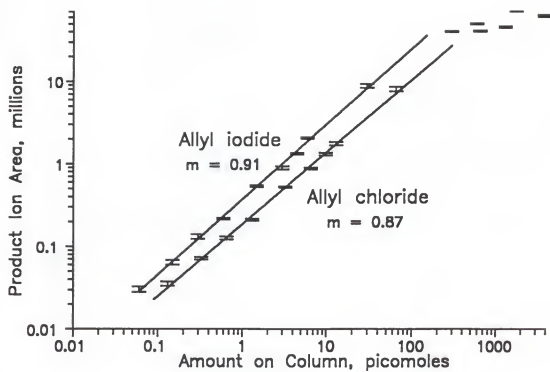
Figure 3-7: SRM calibration curves obtained for the reaction of the $N^{+\cdot}$ ion of pyridine with allyl iodide and allyl chloride.
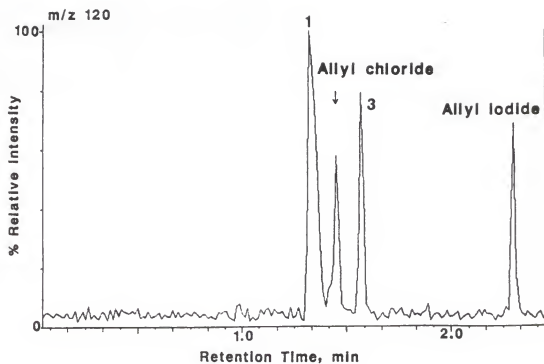
Figure 3-8: SRM mass chromatogram obtained by the reaction of the $N^{+\cdot}$ ion of pyridine with 25 picograms of allyl iodide and allyl chloride. The peaks labelled (1) and (3) are due to the elution of pentane (solvent) and cyclopentane (impurity) into the collision cell.

ions (P^+) due to the reaction of these allyl halides with the pyridine radical molecular ion $(N^{+\cdot})$. The peaks for the reaction of allyl chloride and allyl iodide have nearly equal intensities because there are approximately twice the number of moles of the less reactive allyl chloride in the 25 pg mixture. These allyl halide peaks demonstrate a signal-to-noise (S/N) ratio of approximately 10, calculated as the analyte peak height divided by the peak-to-peak noise of the baseline. The peaks labelled 1 and 3 occur at the retention times expected for pentane (solvent) and cyclopentane (solvent impurity), respectively. Neither pentane or cyclopentane gives rise to a mass spectral peak at m/z 120 in full scan modes, thus it was surprising to discover peaks for pentane and cyclopentane when scanning Q3 over one amu (119.5 to 120.5 amu). The centroid mass spectrum of the pentane peak produced by scanning Q3 over a slightly wider scan range (117 to 124 amu) is shown in Figure 3-9a; essentially a centroid peak is observed at every mass. This suggests that a large quantity of a species entering the collision cell causes increased noise levels which are most likely due to neutrals striking the dynodes or detector. Acquiring the pentane mass spectrum in profile mode rather than centroid mode produces the mass spectrum shown in Figure 3-9b. Rather than profile peaks at each mass, an elevated baseline is observed, which when centroided gives a peak at each mass. In wide scan ranges, the noise is spread over a large number of masses, whereas in SRM scan modes, all the noise is placed into one mass producing a deceiving "chromatographic" peak for m/z 120. Thus as the large amounts of pentane and cyclopentane present in
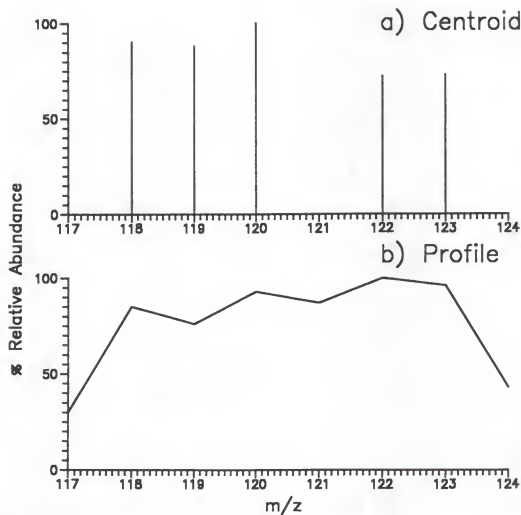
Figure 3-9: a) centroid mass spectrum and b) profile mass spectrum of the chromatographic peak produced when pentane (solvent) elutes into the collision cell while scanning Q3 from 117 to 124 amu.

solution elute into the collision cell, the noise produced gives rise to peaks (in Figure 3-8) which are not indicative of any reaction to give a product ion at m/z 120.

Gas-Phase vs Solution-Phase Reactivity

Not only is this method capable of detecting electrophile/nucleophile gas-phase adducts, but the extent of reactivity can be determined and compared to established methods for detecting potential carcinogens. Eder and co-workers have extensively studied the mutagenicity and alkylating activity of a series of allyl compounds (Eder et al., 1982a; Eder et al., 1982b). Mutagenicity is predicted by the Ames test, as described in Chapter 1. Alkylating activity is determined by the reaction of the allyl species with 4-(p-nitrobenzyl)-pyridine (NBP) to produce a colored product which can be quantified by absorbance measurement. The authors reported a nearly quantitative correlation between mutagenicity and alkylating activity for allyl compounds. Table 3-1 compares the gas-phase reactivity with the pyridine $N^{+ \cdot}$ ion (average of 3 injections) of an equimolar set of allyl compounds and two propyl compounds to their solution-phase reactivity determined by the NBP alkylating test and the Ames bacteriological test. The gas-phase reactivity is defined as the area of the product ion (m/z in parenthesis). The compounds which show mutagenic or alkylating effects are also reactive in the gas-phase with pyridine. The propyl halides, which do not demonstrate mutagenic

Table 3-1: Comparison of the gas-phase $N^{+\cdot}$ ion reactivity, Ames mutagenicity test and NBP alkylating test.

	Gas-Phase Reactivity[a]	Mutagenicity[b]	Alkylating Activity[b,e]
Propyl chloride	0.02 (RIC)[c]	0	0
Propyl bromide	0.03 (RIC)	ND[f]	ND
Allyl isothiocyanate	1.0 (120)[d]	1	1
Allyl chloride	2.3 (120)	9	10
2,3-dichloropropene	2.0 (154,156)	26	8
Benzyl chloride	0.5 (170)	560	98
Allyl bromide	3.1 (120)	700	1800
Allyl iodide	5.3 (120)	2000	5467

[a] product ion areas for equimolar solutions normalized to allyl isothiocyanate reactivity = 1.0.

[b] ref: Eder et al., 1982a; Mutagenicity in rev/μmole without metabolic activation; alkylating activity defined as the extinction coefficient at 560 nm.

[c] no detectable chromatographic peak, so baseline noise of the RIC is measured.

[d] m/z of product ion measured.

[e] reported values normalized to allyl isothiocyanate.

[f] not determined.

or alkylating effects, are not reactive in the gas-phase with pyridine. The reactivity of benzyl chloride with the $N^{+\cdot}$ ion of pyridine is notably low compared to the solution-phase results. The mass spectrum obtained by the reaction of benzyl chloride and pyridine is illustrated in Figure 3-10. The base peak is the $126^{+\cdot}$ ion which is the $E^{+\cdot}$ (^{35}Cl isotope) of benzyl chloride (IE=9.14 eV) produced by charge exchange with pyridine (IE=9.25 eV). Therefore, this abundant charge exchange reaction competes with the product ion formation (as discussed in more detail in Chapter 4). The 2,3-dichloropropene is less reactive in the gas phase than allyl chloride (note that the reactivity of 2,3-dichloropropene includes m/z 154 and 156 due to the product ion containing a chlorine atom), whereas it is more mutagenic in the Ames test. In contrast, the alkylating activity of 2,3-dichloropropene is lower than allyl chloride. The authors attribute the difference in alkylating activity and mutagenicity for 2,3-dichloropropene to probable activation during incubation in the Ames test. The mutagenicity of this compound was found by Eder and co-workers to significantly increase upon metabolic activation with rat liver, thus activation (without S-9 mix) may occur either by bacterial enzymes or by other components of the bacterial suspension. Eder and co-workers also noted that allyl iodide demonstrated stronger alkylating activity than mutagenicity due to allyl iodide forming iodine during incubation in the Ames test which is extremely toxic to the bacteria. Therefore the mutagenicity of allyl iodide as determined in the Ames test may be too low due to the decomposition of the bacteria.
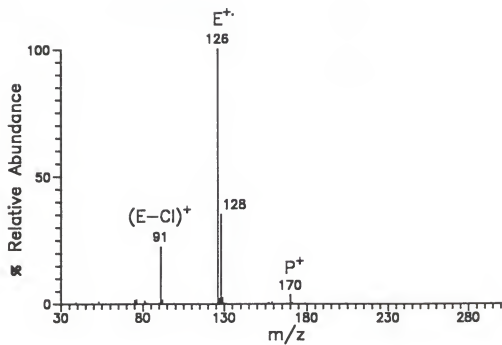
Figure 3-10: Mass spectrum obtained from the reaction of benzyl chloride with the N$^{+\cdot}$ ion of pyridine.

Note that the range of gas-phase reactivities is not nearly as great as the magnitude of the mutagenicity or alkylating activities; therefore, species with close mutagenicities may begin to merge together on the gas-phase reactivity scale. There does not appear to be a simple mathematical correlation between the gas-phase reactivity of the $N^{+\cdot}$ ion of pyridine and the Ames mutagenicity test or NBP alkylating test for these allyl compounds.

<u>Electrophile Ion/Nucleophile Neutral Mass-Selected Reactions in the Collision Cell</u>

This section of Chapter 3 deals with reactions in the collision cell between electrophile (E) ions (GC introduction of E into the ion source) and neutral pyridine (N) constantly introduced into the collision cell (see Figure 1-2b). The most extensively studied reactions, those of electrophile ions with neutral pyridine, are demonstrated in Figure 3-11. In reaction (a) of Figure 3-11, the radical molecular ion of the electrophile ($E^{+\cdot}$) is mass-selected to react with neutral pyridine to produce the product ion (m/z 120) by nucleophilic substitution with loss of a neutral X radical. Nucleophilic addition of pyridine to the allyl ion (m/z 41) in reaction (b) of Figure 3-11 is achieved by mass-selection of the allyl ion to react with the neutral pyridine in the collision cell. Note that none of the mass spectra obtained by electrophile ion reactions will be background-subtracted because the only time an ion enters the collision cell is when the analyte elutes via GC into the ion source. Thus, there is no elevated background, unlike the nucleophile ion

a)

$$H_2C=CH\,CH_2\,X^{+\cdot} \;+\; \text{(pyridine ring)} \xrightarrow{\quad} \text{(N-allyl pyridine ring)}^+ - CH_2\,CH=CH_2 \;+\; X^\cdot$$

Allyl X ion   **Pyridine**   **N-allyl pyridine**

             MW 79   **m/z 120**

b)

$$H_2C=CH\,CH_2^{+} \;+\; \text{(pyridine ring)} \xrightarrow{\quad} \text{(N-allyl pyridine ring)}^+ - CH_2\,CH=CH_2$$

Allyl ion   **Pyridine**   **N-allyl pyridine**

          MW 79   **m/z 120**
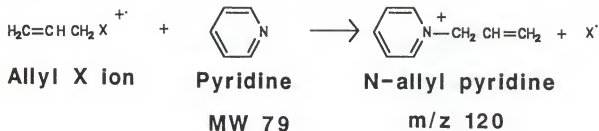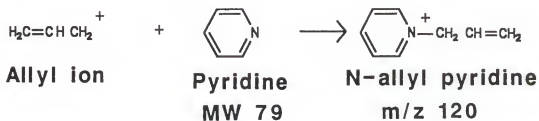
Figure 3-11: Reactions of a) the $E^{+\cdot}$ ion and b) the $[E-X]^{+}$ ion of allyl compounds of the general form C_3H_5X, where X is NCS, Cl, Br or I, with neutral pyridine in the collision cell.

reactions where there is a constant background due to the mass-selected pyridine ions.

Experimental

All experiments were performed on a Finnigan MAT TSQ 70 equipped with a Varian 3400 gas chromatograph. The electrophiles were introduced into the ion source via a GC column and ionized under electron ionization (EI) or chemical ionization (CI) conditions. All experiments were performed at an emission current of $200\mu A$, electron energies of 70 eV (EI) or 100 eV (CI), a manifold temperature of 100°C, and ion source temperatures of 170°C for EI or 150°C for CI.

The electrophile ion of interest was mass-selected by Q1 and reacted in the collision cell with neutral pyridine introduced into the collision cell via a Granville Phillips fine-metering valve (Boulder, CO). Typical pyridine pressures in the collision cell were 1.0 to 1.5 mtorr (high vacuum of 8×10^{-6} torr) as measured by a Granville Phillips convectron gauge. The product ions were mass analyzed with Q3 and detected with an electron multiplier (EM) (conversion dynodes: ± 5 kV).

The mass spectrometer was mass-calibrated with FC43 then tuned for ion-molecule reactions in the collision cell. Allyl chloride was constantly introduced into the ion source with a Negretti fine-metering valve (Hampshire, England). The collision energy, collision cell rf potential, and potentials on the lenses immediately before and following the collision cell were optimized for maximum transmission

of the reactant ion (E^+·) and the product ion (120^+). Note that all experiments in this section were performed with a quadrupole collision cell.

Samples and reagents.   Propyl bromide and benzyl chloride were purchased from Eastman Kodak (Rochester, NY), allyl chloride, allyl iodide, allyl isothiocyanate, allyl bromide, benzo[a]pyrene, and benzo[e]pyrene from Aldrich Chemical Company (Milwaukee, WI), and pyridine from Fisher Scientific (Fair Lawn, NJ).   The solvents, HPLC grade pentane and Spectro grade heptane were purchased from Fisher Scientific and Eastman Kodak, respectively.

Reactivity of electrophile ions. Gas chromatography was carried out on a Perkin-Elmer (Norwalk, CT) bonded methyl silicone (15 m long, 0.32 mm i.d., 1.0 μm film thickness) capillary column in the split mode (SR=20:1) with helium carrier gas at an inlet pressure of 5 psig. The GC oven was temperature programmed from 30°C to 200°C at 15°C/min, with an injection port and transfer line temperature of 200°C. One-microliter injections were made in triplicate of a 6 μg/μL test mixture containing allyl isothiocyanate, allyl chloride, and allyl bromide in heptane; 6 μg/μL allyl iodide in pentane.

The EI and CI (1.6 torr CH_4) mass spectra were obtained by alternating between a Q1MS scan and mass-selection of the various electrophile ions with Q1 as a function of the retention time of the eluting allyl compound. For the Q1MS scan, Q1 was scanned from 35 to 280 amu in 0.15 seconds at an EM voltage of -800 V. Q3 was scanned from 30 to 280 amu in 0.3 seconds and product ions were detected at an EM voltage of -1000 V.

Calibration studies. Gas chromatography was carried out on a Perkin-Elmer bonded methyl silicone (15 m long, 0.32 mm i.d., 1.0 μm film thickness) capillary column in the split mode (SR=20:1) with helium carrier gas at an inlet pressure of 5 psig. The GC oven was temperature programmed from 25°C to 70°C at 20°C/min. One-microliter injections were made in triplicate at injection port and transfer line temperatures of 200°C. The allyl chloride and allyl iodide mixtures were prepared in pentane in the following manner: the 100 ng/μL and 2 μg/μL solutions were prepared from a stock solution of 6 μg/μL; the 1, 2, 5, 7, 15, and 20 ng/μL solutions from the 100 ng/μL solution; the 500 pg/μL solution from the 1 ng/μL solution. Triplicate 1 μL injections of the blank (pentane) were made under the same conditions.

The electrophiles were ionized in the ion source under EI conditions and the radical molecular ion ($E^{+\cdot}$) was mass-selected by Q1. Q3 was scanned from 119.5 to 120.5 amu in 0.25 seconds in the selected reaction monitoring mode (SRM) and from 30 to 280 in 0.25 seconds for full scan detection limits. Product ions were detected at an EM voltage of -1600 V.

Gas-phase reactivity studies. Gas chromatography was carried out on a J & W Scientific DB-5 (20 m long, 0.178 mm i.d., 0.4 μm film thickness) capillary column in the split mode (SR=100:1) with helium carrier gas at an inlet pressure of 5 psig. The GC oven was temperature programmed from 25°C to 200°C at 10°C/min with an injection port and transfer line temperature of 200°C. One-microliter injections were made in triplicate of an equimolar (29.8 nmol/μL) mixture

containing allyl isothiocyanate, allyl chloride, allyl bromide, allyl iodide, propyl chloride, propyl bromide, and benzyl chloride in pentane.

The electrophiles were ionized in the ion source under EI conditions. Data were obtained by alternating between a Q1MS scan and mass-selection of the $E^{+\cdot}$ ions of the eluting compounds. For the Q1MS scan, Q1 was scanned from 30 to 300 in 0.20 seconds at an EM voltage of -800 V. During Q1 mass-selection of the $E^{+\cdot}$ ion, Q3 was scanned from 30 to 300 amu in 0.20 seconds and product ions were detected at an EM voltage of -1400 V.

For the benzo[a]pyrene and benzo[e]pyrene studies, the GC oven was held isothermally at 250°C with injection port and transfer line temperatures of 275°C. One-microliter injections (SR=20:1) were made of separate 6μg/μL solutions of benzo[a]pyrene and benzo[e]pyrene in methylene chloride. The $E^{+\cdot}$ ion (252$^{+\cdot}$) of each species was mass-selected by Q1. Q3 was scanned from 30 to 450 amu in 0.25 seconds and product ions detected at an EM voltage of -1200 V.

Comparison to Ion Source Reactions

The reaction of allyl chloride and pyridine in the ion source is compared in Figure 3-12 to the mass-selected reaction of the $E^{+\cdot}$ ion of allyl chloride with neutral pyridine in the collision cell. The reaction of allyl chloride and pyridine in the ion source produces the complicated mass spectrum depicted in Figure 3-12a. For example, the 120^{+} ion in this mass spectrum can correspond to the
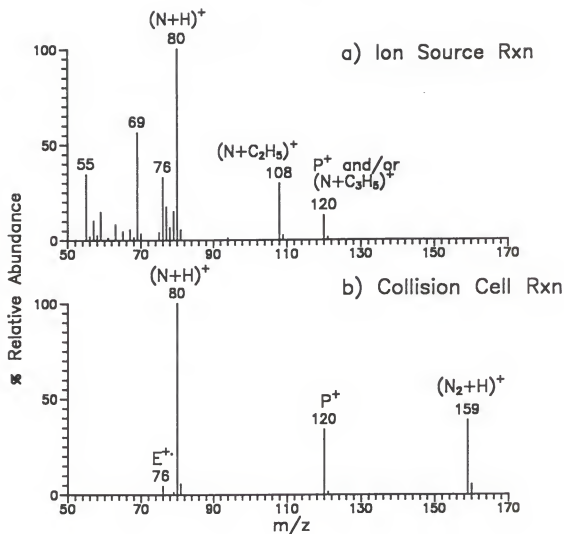
Figure 3-12: Comparison of mass spectra obtained by reaction of a) pyridine and allyl chloride in the ion source and b) the $E^{+\cdot}$ ion of allyl chloride and neutral pyridine in the collision cell.

$[N+C_3H_5]^+$ methane CI adduct ion of pyridine and/or the reaction product of pyridine and allyl chloride. The reaction in the collision cell between the mass-selected $E^{+\cdot}$ ion of allyl chloride ($76^{+\cdot}$) and neutral pyridine, shown in Figure 3-12b, is less complicated; the 120^+ can only be due to reaction between allyl chloride and pyridine. The base peak in the mass spectrum of the collision cell reactions is the $[N+H]^+$ of pyridine formed by abstraction of a proton from the allyl chloride ion. The formation of the $[N+H]^+$ ion is not surprising since the proton affinity of an amine is greater than most other species (i.e., a stronger base). The $[N+H]^+$ then undergoes further reaction in the collision cell to produce the hydrogen bound dimer of pyridine, $[N_2+H]^+$.

In contrast to nucleophile ion reactions where the reactant ion intensity is constant, in electrophile ion reactions, the electrophile is introduced by GC into the ion source; thus the reactant ion is not constant so a chromatographic peak is produced for each GC eluate. Even if no reaction occurs, the mass-selected $E^{+\cdot}$ ion will give rise to a chromatographic peak. Furthermore, in order to mass-select the electrophile ions, not only must the sample components be known, but also the retention times of each component. Q1 is set to pass the $E^{+\cdot}$ ion of each analyte into the collision cell as a function of its retention time. As the number of sample components increases, so does the complexity of the mass spectrometer scan function, limiting the practical use of electrophile ion reactions. However, these electrophile ion reactions are of fundamental use in studying these gas-phase electrophile/nucleophile reactions.

A similar experiment can be performed in electrophile ion reactions as in nucleophile ion reactions where the mass-selection of $16^{+\cdot}$ methane ions was used to detect and quantitate sample components by charge exchange. In one scan, the $E^{+\cdot}$ ion is mass-selected to react with neutral pyridine in the collision cell; while in the next scan, Q1 is scanned over the entire mass range to produce EI-type mass spectra. Since pyridine is present in the collision cell during the Q1MS scan, the electrophile ions entering the collision cell can still undergo reactions with the neutral pyridine. However, since the mass assignment is performed by the scanning quadrupole (Q1) before the collision cell, any product ions formed are assigned the electrophile mass. For instance, if the $76^{+\cdot}$ ion of allyl chloride reacts in the collision cell with pyridine to form the product ion, 120^+, the data system will assign the product ion a mass of 76 because the mass assignment was determined by Q1 before reaction. Note that unless the sample composition is known, a Q1 mass spectrum must be obtained prior to reaction to determine what ions to mass-select at what retention times.

The mass spectrum obtained by alternately scanning Q1, in the same experiment as mass-selecting $76^{+\cdot}$ of allyl chloride to react with pyridine (Figure 3-12b), is shown in Figure 3-13. The Q1 mass spectrum of allyl chloride with pyridine in the collision cell contains identical ions with similar relative abundances (as well as similar absolute intensities) as the Q1 mass spectrum without pyridine in the collision cell. The radical molecular ions of allyl chloride are observed at m/z 76 and 78, and the allyl ion at m/z 41. The mass spectra obtained by scanning
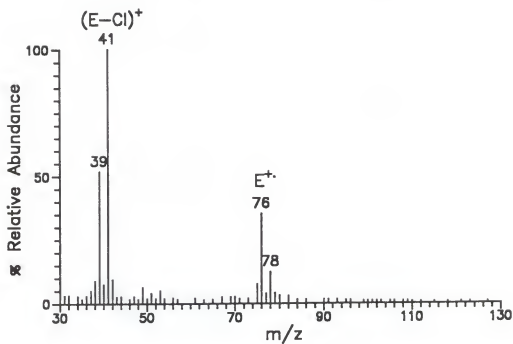
Figure 3-13: The Q1MS mass spectrum of allyl chloride obtained with neutral pyridine in the collision cell.

Q1 while introducing pyridine into the collision cell tend to be noisier than without pyridine. The increased noise levels may be due to the detection of scattered ions and neutrals.

Reactivity of Various Electrophile Ions

The reactivities of the mass-selected electrophile $E^{+\cdot}$ and $[E-X]^+$ ions produced under EI conditions and the $[E+H]^+$, $[E+C_2H_5]^+$, $[E+C_3H_5]^+$, and $[E-H]^-$ ions produced under CI conditions were studied for the electrophiles allyl isothiocyanate, allyl chloride, allyl bromide, and allyl iodide. In the case of these four allyl compounds, all the positive electrophile ions produced a product ion at m/z 120 (P^+) in varying intensities upon reaction with pyridine in the collision cell. Since the electrophile ions produced under CI conditions have potential hydrogen bonding sites, in addition to the 120^+ product ion, several hydrogen bonded adduct ions are observed in the mass spectra. The $[E+H]^+$ ion reacted to produce the $[P+H]^+$ and $[E+H+N]^+$ ions, and the $[E+C_2H_5]^+$ and $[E+C_3H_5]^+$ ions reacted to produce the $[E+C_2H_5+N]^+$ and $[E+C_3H_5+N]^+$ ions, respectively (Table 3-2). No detectable reaction was observed when the $[E-H]^-$ ion was selected for any of the allyl compounds.

The mass spectra shown in Figure 3-14 are obtained by reaction of neutral pyridine with the $E^{+\cdot}$ ion of allyl chloride, allyl bromide, and allyl iodide. The $76^{+\cdot}$ ion (^{35}Cl isotope) of allyl chloride , $122^{+\cdot}$ ion (^{81}Br isotope) of allyl bromide and

Table 3-2: Comparison of product ions obtained by reaction of various electrophile ions with neutral pyridine.

Mass-Selected Electrophile Ions

Electrophile	$E^{+\cdot}$	$[E-X]^+$	$[E+H]^+$	$[E+C_2H_5]^+$ [a]	$[E+C_3H_5]^+$ [a]	$[E-H]^-$ [b]
Allyl isothiocyanate	$P^{+\cdot}$	P^+	P^+	$[E+C_2H_5+N]^+$	$[E+C_3H_5+N]^+$	NR
Allyl chloride	P^+	P^+	P^+	$[E+C_2H_5+N]^+$	$[E+C_3H_5+N]^+$	NR
Allyl bromide	P^+	P^+	P^+	$[E+C_2H_5+N]^+$	$[E+C_3H_5+N]^+$	NR
Allyl iodide	P^+	P^+	P^+	ND^c	ND	NR

[a] mass spectra also contain m/z 120 (P^+).
[b] no detectable reaction.
[c] not determined.
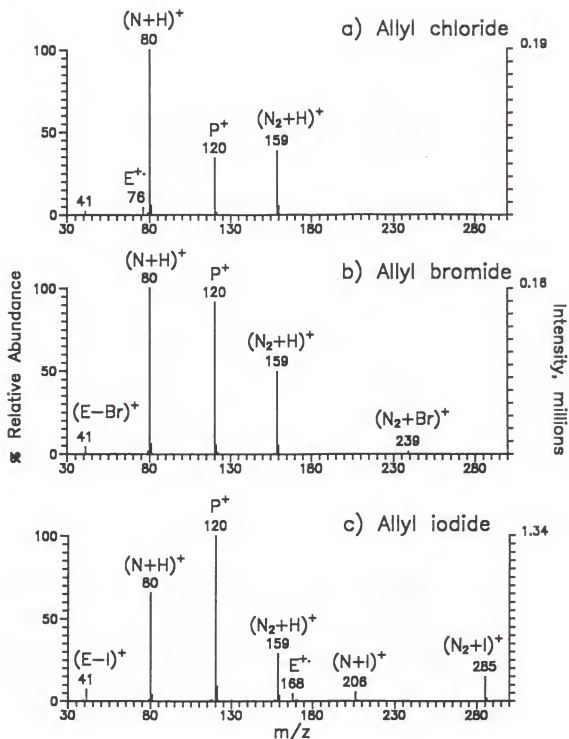
Figure 3-14: The mass spectra obtained by the reaction of neutral pyridine with the $E^{+\cdot}$ ion of a) allyl chloride, b) allyl bromide, and c) allyl iodide.

the $168^{+\cdot}$ ion of allyl iodide were mass-selected by Q1. The $122^{+\cdot}$ ion of allyl bromide was chosen in order to eliminate the possibility of the $120^{+\cdot}$ ion being a combination of the P^+ and $E^{+\cdot}$ ions. The product ion (P^+) is observed at m/z 120 for each electrophile. Comparison of the P^+ ion intensities is complicated by the fact that even though the solution is equimolar, the intensities of the mass-selected $E^{+\cdot}$ ions are not equivalent for each analyte. Fragmentation in the ion source and the distribution of isotope ions will decrease the intensity of the mass-selected electrophile ion.

In addition to product ion formation, as the electrophile ions enter the collision cell, pyridine (with its high proton affinity) abstracts a proton to produce the $[N+H]^+$ ion at m/z 80. This 80^+ ion undergoes further reaction with neutral pyridine to produce the proton-bound dimer of pyridine ($[N_2+H]^+$ ion at m/z 159) observed in each of the mass spectra. The fragment ion $(E-X)^+$ at m/z 41, produced by collisionally activated decomposition (CAD), is also observed in each of the mass spectra. A 239^+ ion is observed in the mass spectrum obtained by the allyl bromide reaction, which is the $[N_2+Br]^+$ ion that was also seen in the nucleophile ion reactions (Figure 3-5b). The $[N+I]^+$ and $[N_2+I]^+$ ions are observed in the mass spectrum obtained by reaction of allyl iodide; however, no corresponding ions are observed for the reaction of allyl chloride.

Since each of these electrophiles has an ionization energy (IE) greater than or nearly equal to that of pyridine, the $E^{+\cdot}$ ion can undergo charge exchange (reaction e) with the neutral pyridine to produce the $N^{+\cdot}$ ion. A small amount of the $79^{+\cdot}$ ion is observed in each of the mass spectra in Figure 3-14.

(e) $E^{+\cdot}$ +   N $\longrightarrow$ E   + $N^{+\cdot}$

However, since very small quantities of the electrophile are introduced into the ion source via GC, not many electrophile neutrals make it into the collision cell. Thus, reactions of the $N^{+\cdot}$ ion with neutral electrophile to produce the product ion is not likely. This is in contrast to the case when much larger quantities of pyridine are leaked into the source for nucleophile ion/electrophile neutral reactions.

Figure 3-15 depicts the mass spectra of the reaction of neutral pyridine with (a) $[E+H]^+$, (b) $[E+C_2H_5]^+$, and (c) $[E+C_3H_5]^+$ ions of allyl chloride (mass-selection of ^{35}Cl isotope). The mass spectrum obtained by reaction of the $[E+H]^+$ ion at m/z 77 in Figure 3-15a has the typical $[E-Cl]^+$, $[N+H]^+$, and $[N_2+H]^+$ ions as described in the reaction of the $E^{+\cdot}$ ions. The product ions produced by the reaction of the $[E+H]^+$ ion are the 120^+ ion (P^+) arising from loss of HCl and the 156^+ proton bound adduct ion, $[N+H+E]^+$. The intensity of 121^+ ion is not significantly greater than the ^{13}C contribution for allyl chloride; thus, little or no $[P+H]^+$ ion is observed. In addition to the ions discussed above, the mass spectra obtained by reaction of the $[E+C_2H_5]^+$ (Figure 3-15b) and $[E+C_2H_5]^+$ (Figure 3-15c) ions with neutral pyridine depict product ions at m/z 184 ($[E+C_2H_5+N]^+$) and m/z 196 ($[E+C_3H_5+N]^+$) ions, as well as the 120^+ ion (P^+). Note that addition of the alkyl groups to the electrophile ion significantly reduces the abundance of the P^+ ion.
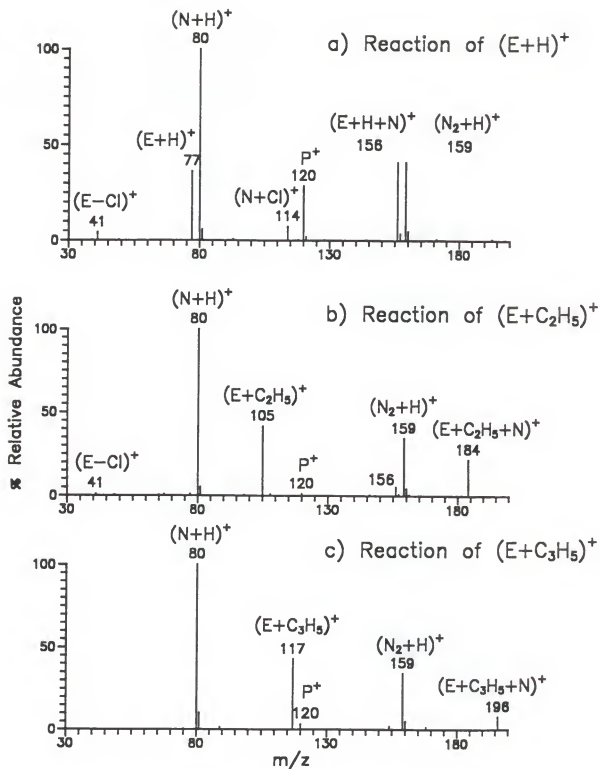
Figure 3-15: The mass spectra obtained by the reaction of neutral pyridine in the collision cell with the mass-selected a) $[E+H]^+$, b) $[E+C_2H_5]^+$, and c) $[E+C_3H_5]^+$ ions of allyl chloride.

Calibration Studies of Allyl Halides

Figure 3-16 depicts the log-log calibration curves obtained for the reaction of the allyl chloride and allyl iodide radical molecular ions ($E^{+\cdot}$) with neutral pyridine in the selected reaction monitoring (SRM) mode. The calibration curves for the reaction of both allyl halides are linear over approximately 3 decades (slope (m) = 0.96 and 0.95 for allyl chloride and allyl iodide, respectively). The calibration curves are just beginning to level off above ≈ 1000 pmol due to saturation of the data system summation algorithms. The average area counts (in millions) for the blanks are 0.0017 and 0.0025 for allyl chloride and allyl iodide, respectively. The reproducibility, calculated as the average relative standard deviation (RSD), of the allyl chloride and allyl iodide reaction product ions (m/z 120) is 6.0% for allyl chloride and 6.4% for allyl iodide over the linear portion of the calibration curves. The offset in the calibration curves between the product ion areas of the allyl iodide and allyl chloride is indicative of the difference in the gas-phase reactivity of the two allyl halides. Note that there appears to be a larger difference in the reactivity of the two compounds when the $E^{+\cdot}$ ions are mass-selected compared to when the $N^{+\cdot}$ ions are mass-selected (Figure 3-7), as indicated by the larger offset between the allyl chloride and allyl iodide calibration curves in Figure 3-16. This larger difference in product ion areas for the $E^{+\cdot}$ ion reaction is due to the mass-selection of the $76^{+\cdot}$ ion of allyl chloride which neglects the ^{37}Cl isotope at m/z 78 (33% abundance relative to m/z 76). Therefore, the allyl chloride product ion areas in Figure 3-16 only reflect reaction with 75% of the amount of allyl

Figure 3-16: The SRM calibration curves obtained by the reaction of the $E^{+\cdot}$ ion of allyl iodide and allyl chloride with neutral pyridine in the collision cell.

Low picogram ($\approx$100 femtomoles) limits of detection (LOD) were observed for the product ions of these two allyl halides. The mass chromatogram at 25 picograms, shown in Figure 3-17, depicts a S/N ratio of $\approx$6 for allyl chloride and $\approx$23 for allyl iodide. The S/N ratios are calculated as the analyte peak height divided by the peak-to-peak noise of the baseline. Note that there are only the two analyte peaks, in contrast to the nucleophile ion chromatograms in the SRM mode (Figure 3-8). Since the analytes elute via GC into the ion source during electrophile ion reactions rather than into the collision cell, the neutrals (including the solvent) are more efficiently pumped away by the differential pumping between the ion source and analyzer regions. Also, the solvent ions are not mass-selected during the experiment, so no peaks due to the solvent are observed.

The log-log calibration curves obtained for the reaction of the allyl chloride and allyl iodide radical molecular ions ($E^{+\cdot}$) with neutral pyridine in the full scan mode (Q3 scanned from 30 to 280 amu) are illustrated in Figure 3-18. The calibration curves for the reaction of both allyl halides are linear over $\approx$2 decades ($m=1.02$ and 1.01 for allyl chloride and allyl iodide, respectively). The calibration curves are just beginning to level off above $\approx$100 pmol due to saturation of the data system summation algorithms. The average area counts (in millions) for the blanks are 0.013 and 0.014 for allyl chloride and allyl iodide, respectively. The reproducibility, calculated as the average relative standard deviation (RSD), of the allyl chloride and allyl iodide reaction product ions (m/z 120) is 10.9% for both compounds over the linear portion of the calibration curves. Full scan calibrations

Figure 3-17: The SRM mass chromatogram (m/z 120) obtained for reaction of the $E^{+\cdot}$ ions of the 25 picogram allyl iodide and allyl chloride solution with neutral pyridine in the collision cell.
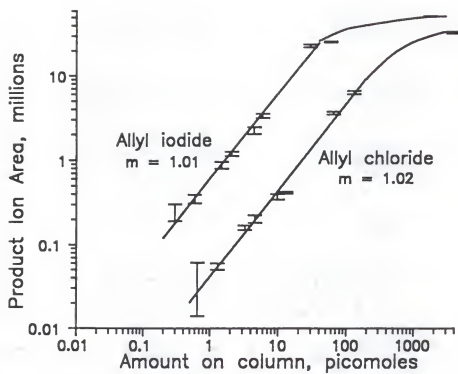
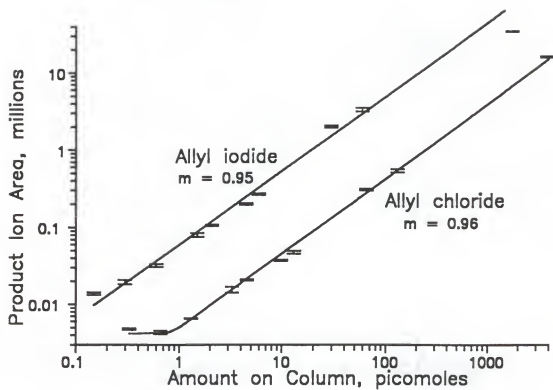Figure 3-18: The full scan calibration curves obtained by the reaction of the $E^{+\cdot}$ ion of allyl iodide and allyl chloride with neutral pyridine in the collision cell.

resulted in LOD's of approximately 100 pg for the two allyl halides with S/N ratios of ≈2 for allyl chloride and ≈10 for allyl iodide as observed in the 100 pg mass chromatograms shown in Figure 3-19. The noise spikes observed in the background of the full scan mass chromatogram, which are not observed in the SRM mass chromatogram, can be explained by ion statistics. The scan time in both cases is constant (0.25 seconds), thus the time spent on one m/z in the full scan mode (1ms) is 1/250 of the time spent in the SRM mode (250 ms). The SRM scan mode results in LOD's which are approximately 5 times better than full scan LOD's.

Gas-Phase vs Solution-Phase Reactivity

Table 3-3 compares the normalized gas-phase reactivities (average of 3 injections) of the various electrophile ions of allyl isothiocyanate, allyl chloride, allyl bromide, and allyl iodide with the mutagenicity determined by the Ames test. All product ions are normalized to the Q1MS electrophile ion areas obtained by the alternate Q1MS scan. Of all the electrophile ions studied, only the $E^{+\cdot}$ ion followed the same order of gas-phase reactivity as the Ames test mutagenicity. Since the $[E-X]^+$ allyl ion has the same composition ($C_3H_5^+$) for each of these four allyl compounds (i.e., the various leaving groups are already gone), no difference in the gas-phase reactivity is expected. This is indeed the case for the $[E-X]^+$ ions produced from allyl chloride, allyl bromide, and allyl iodide; the intensities of the
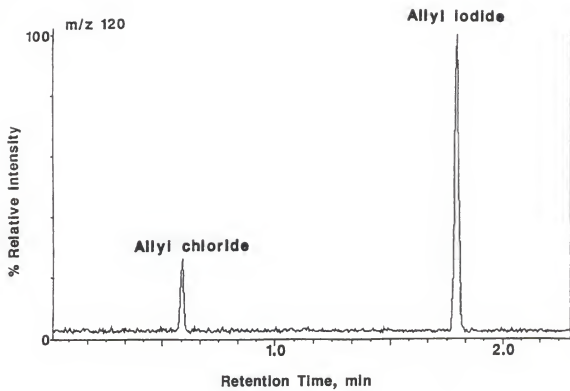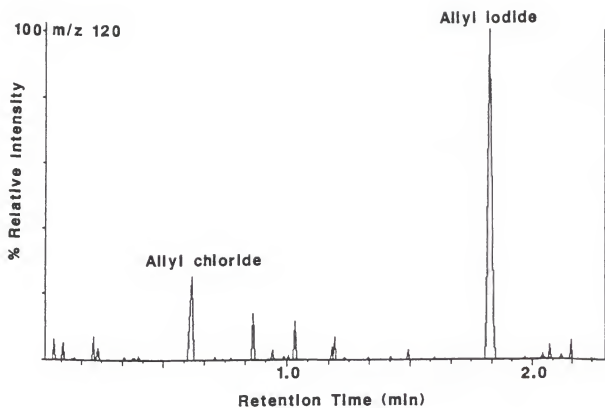
Figure 3-19: The full scan mass chromatogram (m/z 120) obtained for the reaction of the $E^{+\cdot}$ ions of the 100 nanogram allyl iodide and allyl chloride solution with neutral pyridine in the collision cell.

Table 3-3: Comparison of gas-phase reactivity of various electrophile ions and the Ames mutagenicity test.

Reactant Ion	Mass-Selected Electrophile Ions				Mutagenicity[b]
	$E^{+\cdot}$	$[E-X]^+$	$[E+H]^+$		
Allyl isothiocyanate	1[a]	1[a]	1[a]	1[c]	1
Allyl chloride	4.8	2.1	1.2	1.5	9
Allyl bromide	8.8	2.0	0.5	1.6	700
Allyl iodide	16.0	2.0	1.8	1.9	2000

[a] product ion (120^+) areas/Q1MS electrophile ion area, normalized to allyl isothiocyanate = 1.0.

[b] ref: Eder et al., 1982a; Mutagenicity in rev/μL without metabolic activation.

[c] $\Sigma(P^+ + [E+H+N]^+)$ ion areas/Q1MS electrophile ion areas, normalized to allyl isothiocyanate = 1.0.

120^+ ions are equivalent. The gas-phase reactivity of the $[E-X]^+$ ion produced from allyl isothiocyanate is significantly lower than the other three compounds. This may result from internal energy differences in the $[E-X]^+$ fragment ions produced in the ion source, especially for the allyl isothiocyanate fragment ion where the leaving group is polyatomic. In the case of the $[E+H]^+$ ion, the gas-phase reactivity is particularly low when the P^+ (120^+) ion is used to determine the gas-phase reactivity. However, not only is the P^+ ion observed in the mass spectra, but also the proton bound adduct ion, $[N+H+E]^+$. This $[N+H+E]^+$ ion is particularly abundant in the allyl bromide reaction, and its formation is competitive with the formation of the P^+ ion. Thus, for the mass-selected $[E+H]^+$ ion, the gas-phase reactivity may be better defined as the summation of the P^+ ion and $[E+H+N]^+$ ion (normalized to the Q1MS $[E+H]^+$ ion area). Consideration of both product ions triples the allyl bromide reactivity, with very little effect on any other of the allyl compounds. Note that there is very little range in the reactivities (1 to 1.9) of the $[E+H]^+$ ions. Attempts to quantitate the reactivity of the $[E+C_2H_5]^+$ or $[E+C_3H_5]^+$ ions offer little insight into their reactivity.

Table 3-4 compares the gas-phase reactivities of the $E^{+\cdot}$ ion of a series of allyl compounds and two propyl compounds to their solution-phase reactivities determined by the NBP alkylating test and the Ames bacteriological test. The data were obtained by alternating between mass-selecting the $E^{+\cdot}$ ion of the electrophile and a Q1MS scan; thus, the product ions are normalized to the amount of $E^{+\cdot}$ ion produced in the ion source (i.e., isotopic patterns are corrected

Table 3-4: Comparison of the gas-phase E+· ion reactivity to the Ames mutagenicity test and NBP alkylating test.

	E+· m/z [a]	Gas-Phase Reactivity [b]	Mutagenicity [c]	Alkylating Activity [c,f]
Propyl chloride	78	0.001 (RIC)[d]	0	0
Propyl bromide	128	0.001 (RIC)	ND[g]	ND
Allyl isothiocyanate	99	1.0 (120)[e]	1	1
Allyl chloride	76	4.8 (120)	9	10
2,3-dichloropropene	---[h]	---	26	8
Benzyl chloride	126	0.5 (170)	560	98
Allyl bromide	122	8.8 (120)	700	1800
Allyl iodide	168	16.1 (120)	2000	5467

[a] electrophile ion mass-selected with Q1.

[b] product ion areas/Q1MS E+· ion areas for equimolar solutions normalized to allyl isothiocyanate reactivity.

[c] ref: Eder et al., 1982a; Mutagenicity in rev/μmole without metabolic activation; alkylating activity defined as the extinction coefficient at 560 nm.

[d] no detectable peaks, so baseline noise of the RIC is measured.

[e] m/z of product ion measured.

[f] reported values normalized to allyl isothiocyanate.

[g] not determined.

[h] gas-phase reactivity not determined.

also). Similar results were obtained as in the nucleophile ion/electrophile neutral reactions. Compounds mutagenic in the solution-phase tests were reactive in the gas phase. The $E^{+\cdot}$ ions of propyl chloride and propyl bromide were non-reactive in the gas phase as expected. Due to the barely baseline chromatographic resolution between 2,3-dichloropropene and allyl iodide, 2,3- dichloropropene was not tested. Attempting to acquire scans over the entire 2,3-dichloropropene chromatographic peak before switching to the $E^{+\cdot}$ ion of allyl iodide resulted in a portion of the allyl iodide peak being missed. There does not appear to be a simple mathematical correlation between the gas-phase reactivity of the $E^{+\cdot}$ ion of the allyl compounds and the Ames mutagenicity test or NBP alkylating test.

As mentioned previously, many chemicals (e.g., polycyclic aromatic hydrocarbons (PAH)) require metabolic activation to become mutagens or carcinogens. Two pathways have been reported for metabolic activation of PAH's to reactive electrophiles: 1) one-electron oxidation to yield radical cations and 2) monooxygenation to produce diol epoxides (Sims and Grover, 1981). A brief investigation was performed to determine if forming the radical ion in the ion source would be sufficient activation in the gas phase to produce a reaction with neutral pyridine in the collision cell. Benzo(a)pyrene (121 rev/nmol) and benzo(e)pyrene (0.6 rev/nmol) were chosen since their mutagenicities with rat liver activation vary by a factor of 200 (McCann et al., 1975). The mass spectra obtained by mass-selecting the radical molecular ions ($E^{+\cdot}$) of each PAH to react with the neutral pyridine in the collision cell are shown in Figure 3-20. The
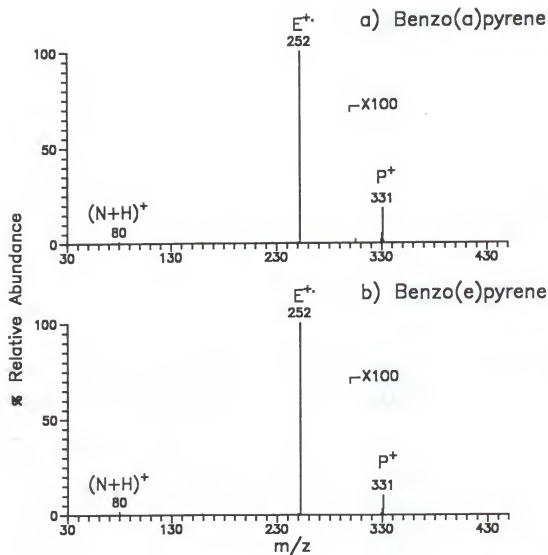
Figure 3-20: The mass spectra obtained by the reaction of the $E^{+\cdot}$ ion $(252^{+\cdot})$ of a) benzo(a)pyrene and b) benzo(e)pyrene with neutral pyridine in the collision cell.

intensities of the product ion (331^+) are approximately equal, thus benzo(a)pyrene does not appear to be activated simply by producing a radical ion.

Conclusions

The ability to detect product ions of nucleophile/electrophile reactions in the collision cell has been demonstrated. The mass spectra obtained are simpler than reactions in the ion source, since only one ion is mass-selected to react with the neutrals in the collision cell. Only the radical molecular ion of the nucleophile reacted to form a product ion in the gas phase, whereas all of the positive electrophile ions reacted. None of the negative ions investigated in these studies reacted. Qualitatively, similar mass spectra are obtained for electrophile ion and nucleophile ion reactions. Low picogram limits of detection were obtained in the SRM mode for electrophile ion and nucleophile ion reactions; ≈5 times higher full scan limits of detection were obtained. Compared to the Ames test in which mutagens are detected in low microgram or in some cases in nanogram amounts (Ames, 1984), the detection limits obtained by this method are better by orders of magnitude, and are adequate to detect potential carcinogens in environmental mixtures.

The selected set of allyl compounds investigated that are mutagenic in the Ames test and alkylating agents in the NBP test were observed to react with pyridine ions in the gas phase; the two non-mutagenic compounds did not react

in the gas phase with pyridine ions. No simple mathematical correlation was found between gas phase reactivity and mutagenicity or alkylating activity. Further studies are necessary to assess the capability of these ion-molecule reactions to detect potential carcinogens. The gas-phase reactivities of a larger set of electrophiles and nucleophiles are presented in Chapter 5.

At the present time, the nucleophile ion reactions are limited to volatile electrophiles (boiling point <200°C) because of the unheated portion of the GC column inside the vacuum chamber. However, in terms of a screening technique for potential carcinogens in complex environmental mixtures, the nucleophile ion reactions offer important advantages over the electrophile ion reactions. It is not necessary to know the identity of the sample components in nucleophile ion reactions, unlike electrophile ion reactions where prior knowledge of the eluates is necessary to determine the electrophile ion to mass select. Also, in electrophile ion reactions, a chromatographic peak will be observed for every GC eluate whether or not reaction with the neutral nucleophile occurs; whereas, in nucleophile ion reactions, chromatographic peaks are observed only when reaction (including charge exchange) between the electrophile and nucleophile occurs.

CHAPTER 4
COLLISION ENERGY AND PRESSURE EFFECTS ON NUCLEOPHILE/ELECTROPHILE REACTIONS IN THE COLLISION CELL

Introduction

Ion-molecule reactions carried out in the collision cell of a triple quadrupole mass spectrometer are characterized by several important factors. The ability to spatially separate the formation of the reactant ions and their subsequent reaction with the neutral species in the tandem-in-space triple quadrupole mass spectrometer is an advantage over tandem-in-time instruments. Further, ion-molecule reactions in the collision cell allow for control of the axial kinetic energy (collision energy) of the reactant ion. Finally, the type and quantity of the ion-molecule reaction products are also a function of the reactant pressures. This chapter presents the results of the collision energy studies and the optimization of the pyridine pressure in the ion source or in the collision cell for nucleophile ion/electrophile neutral and electrophile ion/nucleophile neutral reactions. Variation of the electrophile amount (introduced by GC) was discussed in the calibration sections of Chapter 3.

Nucleophile Ion/Electrophile Neutral Mass-Selected Reactions in the Collision Cell

Experimental

All experiments were performed on a Finnigan MAT TSQ 70 (with an octapole collision cell) equipped with a Varian 3400 gas chromatograph. Pyridine was constantly introduced into the ion source with a Granville Phillips fine-metering valve (Boulder, CO) and ionized under electron ionization (EI) conditions. The uncorrected pyridine ion source pressure was measured with a Varian Bayard-Alpert ionization gauge (Palo Alto, CA) mounted on a flange in the ion source region of the vacuum manifold. All experiments were performed at an emission current of 200 μA, electron energy of 70 eV, a manifold temperature of 100°C, and an ion source temperature of 170°C.

Gas chromatography was carried out on a J & W Scientific (Folsom, CA) DB-5 (20 m long, 0.178 mm i.d., 0.4 μm film thickness) capillary column in the split mode (split ratio (SR) = 100:1) with helium carrier gas at an inlet pressure of 5 psig. The GC oven was temperature programmed from 50°C to 100°C at 20°C/min with an injection port temperature of 200°C and a transfer line temperature of 200°C. In the pyridine optimization and collision energy studies, 1 μL injections were made in duplicate of a mixture containing 5 μg/μL each of allyl chloride, allyl bromide, and allyl iodide in pentane. The piperidine optimization studies involved 1 μL injections, made in duplicate, of a 59.8 nmol/μL equimolar mixture containing allyl chloride, allyl bromide, and allyl iodide in pentane.

The radical molecular ion of pyridine ($N^{+\cdot}$, m/z 79) was mass-selected by Q1 and reacted in the collision cell with the neutral electrophiles introduced into the collision cell via the GC column. The product ions (120^+) were mass analyzed with Q3 scanned from 10 to 300 amu in 0.20 seconds at an electron multiplier (EM) voltage of -1000 V (dynode: -5 kV). Since the mass-selected reactant ion signal is saturated at the EM voltage necessary to observe the product ions, in order to assess the quantity of reactant ion present, the EM voltage was lowered to -600 V during the first 60 scans of the mass chromatograms (no eluates in this region).

In the piperidine studies, the radical molecular ion of piperidine ($N^{+\cdot}$, m/z 85) was mass-selected by Q1 and reacted in the collision cell with the neutral electrophiles introduced into the collision cell via the GC column. The product ions (126^+) were mass analyzed with Q3 scanned from 30 to 350 amu in 0.30 seconds at an EM voltage of -1400 V. The EM voltage was lowered to -700 V during the first 60 scans of the mass chromatograms (no eluates in this region).

The mass spectrometer was mass-calibrated with perfluorotributylamine (FC43) and then tuned for ion-molecule reactions in the collision cell. Allyl chloride was constantly introduced into the collision cell with a Negretti fine-metering valve (Hampshire, England) via the collision gas inlet. The collision energy, collision cell rf potential, and the potentials on the lenses immediately before and following the collision cell were optimized for maximum transmission of the reactant ion ($N^{+\cdot}$) and product ion (120^+).

Allyl chloride, allyl iodide, and allyl bromide were purchased from Aldrich Chemical Company (Milwaukee, WI); pyridine, piperidine, and HPLC grade pentane were obtained from Fisher Scientific (Fair Lawn, NJ).

Effect of Nucleophile Pressure on the Product Ions

The utility of these ion-molecule reactions between the pyridine ion and electrophiles is their potential ability not only to detect possible mutagens, but also to predict their relative order of mutagenicity. The mass chromatograms of the product ions (120^+) in Figure 4-1 illustrate the effect of pyridine pressure in the ion source (thus, the pyridine $N^{+\cdot}$ ion intensity) on the relative reactivity of allyl chloride, allyl bromide, and allyl iodide. Although the test mixture is not equimolar (i.e, there are twice as many moles of allyl chloride than allyl iodide), the expectation is that the product ion intensity for all the analytes would increase the same amount as the pyridine pressure is increased. However, at a pyridine pressure of 2×10^{-5} torr in the ion source, the gas-phase reactivity is reversed compared to tabulated Ames test mutagenicities (allyl chloride < allyl bromide < allyl iodide), while at an ion source pyridine pressure 15 times higher, the gas-phase reactivity of the allyl iodide product ion is increased dramatically compared to allyl chloride and allyl bromide product ions. At these higher pressures, the gas-phase reactivities (if normalized to the number of moles of analyte present) agree with the mutagenicities observed with the Ames test.
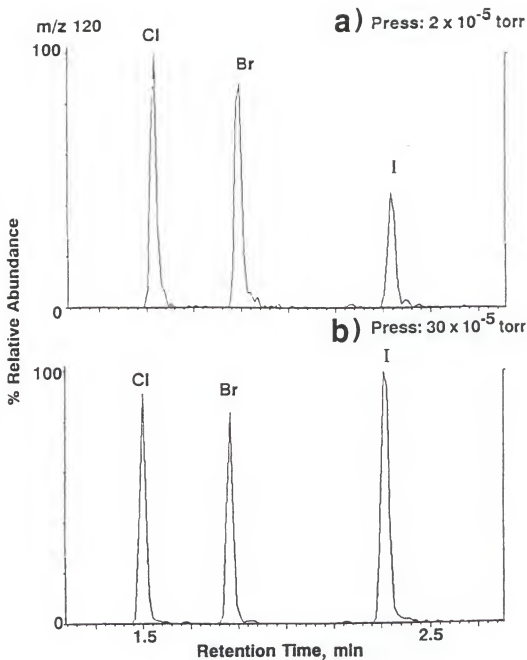
Figure 4-1: Mass chromatograms of the product ion (120⁺) of the reaction of allyl chloride, allyl bromide, and allyl iodide with the N⁺· ion of pyridine at a) 2×10^{-5} torr and b) 30×10^{-5} torr ion source pyridine pressures. Note that the allyl halide mixture is not equimolar. The order of Ames test mutagenicities is allyl chloride < allyl bromide < allyl iodide.

In an attempt to determine the dependence of relative gas-phase reactivity on pyridine pressure, optimization of the pyridine pressure in the ion source was undertaken for the reaction with allyl chloride, allyl bromide, and allyl iodide at a collision energy of 2 eV. The radical molecular ion of pyridine ($N^{+\cdot}$) is mass-selected to react with the neutral allyl halides eluting into the collision cell via a GC column. Figure 4-2 depicts the effect of increasing the pyridine pressure in the ion source on the product ion (120^+) (average of two injections) produced in the collision cell. Since the test mixture is not equimolar, the product ions for each component are normalized to the number of moles of each analyte in the mixture. Formation of the product ion for all three allyl halides optimizes at an indicated pyridine pressure of $\approx 15 \times 10^{-5}$ torr in the ion source. The dashed line represents the intensity of the pyridine ion (average intensity over 5 scans) early in the mass chromatogram before elution of the analytes. Note that the electron multiplier (EM) voltage is lowered so that the reactant ion signal is not saturated in these early scans, but raised before elution of the analytes. Thus, absolute intensities of the product ion and the pyridine reactant ion can only be compared if the difference in EM gain due to the different EM voltages is included, as discussed later in this chapter.

At pyridine ion source pressures of $>30 \times 10^{-5}$ torr the pyridine ion and product ion intensities (as well as the other ions formed in the collision cell) decrease due to scattering effects at these high pressures ($>2 \times 10^{-5}$ torr in the analyzer region). As expected, the intensities of the product ions obtained by reaction of allyl chloride and allyl bromide maximize at the same pressure as the
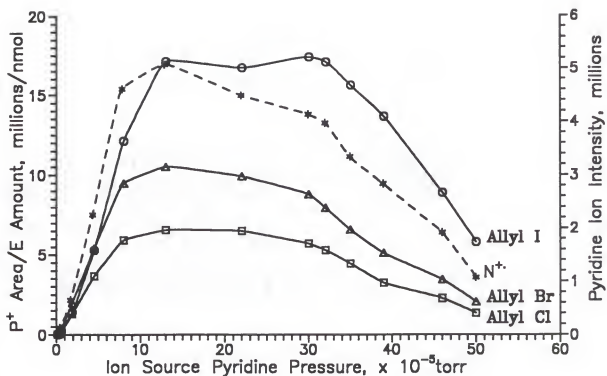
Figure 4-2: Effect of ion source pyridine pressure (uncorrected ionization gauge reading) on the product ion (120^+) of reaction of the $N^{+\cdot}$ ion with allyl chloride, allyl bromide, and allyl iodide. The product ion intensities have been normalized to the number of moles of the electrophile in the mixture. The dashed line represents the intensity of the $N^{+\cdot}$ ions (at a lower EM voltage) before elution of the electrophiles into the collision cell.

$N^{+\cdot}$ reactant ion (dashed line). In contrast, the intensity of the product ion obtained from the reaction of allyl iodide does not follow the pyridine $N^{+\cdot}$ ion trace, but rather appears to reach a second maximum at a pyridine pressure of 35×10^{-5} torr. This is an indication that two types of reactions may be occurring in the case of allyl iodide:

$$\text{(a)} \quad N^{+\cdot} \; + \; E \; \longrightarrow \; P^{+} \; + \; X^{\cdot}$$

$$\text{(b)} \quad N^{+\cdot} \; + \; E \; \xrightarrow{\text{CE}} \; N \; + \; E^{+\cdot} \; \xrightarrow{\text{N}} \; P^{+}$$

Equation (a) is the expected reaction of the radical molecular ion of pyridine ($N^{+\cdot}$) and neutral allyl iodide (E) to produce the product allyl pyridine (P^{+}) with the subsequent loss of a neutral iodine radical ($X^{\cdot}$). In addition to the reaction shown in equation (a), the P^{+} ion can be produced by the mechanism depicted in equation (b). Since the ionization energy (IE) of pyridine is 9.25 eV (Lias et al., 1988), the radical molecular ion of pyridine ($N^{+\cdot}$) can undergo charge exchange (CE) with the neutral allyl iodide (IE=9.298) to produce the radical molecular ion of allyl iodide ($E^{+\cdot}$). The $E^{+\cdot}$ ion of allyl iodide can undergo further reaction with the neutral pyridine present in the collision cell to produce the allyl pyridine product ion. Although the analyzer region (in which the collision cell resides) and the ion source are differentially pumped, it is possible for some of the neutral pyridine to enter the collision cell. As the pyridine pressure in the ion source is

increased, the amount of neutral pyridine which makes it into the collision cell increases. The reaction of the $E^{+\cdot}$ ion with neutral pyridine to form the P^+ product ion has been shown to occur in Chapter 3. Allyl chloride and allyl bromide are not ionized by charge exchange with the pyridine ion because their ionization enerigies are significantly greater than the IE of pyridine (9.9 and 10.06 eV, respectively) (Lias et al., 1988).

In the case of equation (a), a linear relationship between the product ion intensity and pyridine ion intensity is expected; thus dividing the product ion area by the pyridine ion intensity should yield a horizontal line. In Figure 4-3, the ratio of the product ion area to the pyridine ion area ($P^+/N^{+\cdot}$) is plotted versus the ion source pressure of pyridine. The allyl chloride and allyl bromide traces are essentially horizontal as expected, except at very low pressures where determination of the pyridine ion area is not very reproducible. The $P^+/N^{+\cdot}$ ratio for allyl iodide does not level off, but continues to increase with increasing pyridine pressure in the ion source. This implies that a neutral pyridine molecule can also be involved in the formation of this product ion, as shown in equation (b). Crossover points are observed in this plot where the gas-phase reactivity of allyl iodide becomes greater than that of allyl chloride at $\approx 2 \times 10^{-5}$ torr and allyl bromide at 5×10^{-5} torr.

Note that the $P^+/N^{+\cdot}$ ratio in Figure 4-3 is greater than one, which is due to the different electron multiplier voltages used to determine the product ion and reactant ion areas. The approximate ratio of the gain of the electron multiplier at
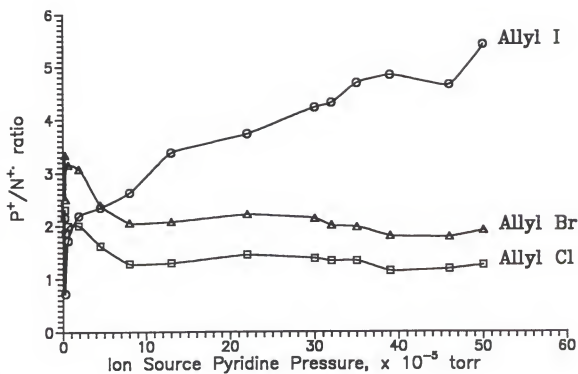
Figure 4-3: Ratio of the product ion intensities to the pyridine reactant ion intensities ($P^+/N^{+\cdot}$) at various ion source pyridine pressures for the allyl chloride, allyl bromide, and allyl iodide reactions.

the two voltages is calculated in Table 4-1 for several ions not saturated at either electron multiplier setting. The $[N-HCN]^+$ (m/z 52) and the $N^{+\cdot}$ ion are not saturated at low pyridine ion source pressures. The intensities of these ions (averaged over 5 scans) at the two EM voltages can be divided to yield the approximate increase in the gain of the electron multiplier. The average gain ratio of 138 may be used to correct the pyridine ion intensity at the optimum pressure (13×10^{-5} torr) in Figure 4-2. Thus, the $P^+/N^{+\cdot}$ ratios at the optimum pyridine pressure can be corrected to 0.011, 0.016, and 0.027 for allyl chloride, allyl bromide, and allyl iodide, respectively, corresponding to 1.1% to 2.7 % conversion of the incident $N^{+\cdot}$ ions into P^+ ions.

In addition to the charge exchange discussed above, there are several other competitive reactions occurring during these collision cell ion-molecule reactions. The background-subtracted mass spectra obtained by the mass-selected reaction of the $N^{+\cdot}$ ion of pyridine with neutral allyl chloride, allyl bromide, and allyl iodide eluting into the collision cell are shown in Figure 4-4. The product ions of the collision cell reactions are observed at m/z 120 as are the allyl fragment ions at m/z 41. Only in the case of allyl iodide is the $E^{+\cdot}$ ion produced by charge exchange with the $N^{+\cdot}$ ion of pyridine observed (at m/z 168). The presence of the $168^{+\cdot}$ ion in the mass spectra supports the occurrence of reaction (b) for allyl iodide. The allyl bromide mass spectrum includes an $[N+^{79}Br]^+$ ion at m/z 158 (and an $[N+^{81}Br]^+$ at m/z 160) which undergo further reaction with the neutral pyridine present in the collision cell to form the $[N_2+Br]^+$ ions at m/z 237 and 239.

Table 4-1: Estimation of the increase in gain from an increase of electron multiplier voltage from -600 V to -1200 V.

Structure	m/z	Pressure x 10^{-5} torr	Ion Areas (millions) EM -600 V	Ion Areas (millions) EM -1200 V	Increase in Gain
[N-HCN]$^+$	52	4.50	0.0450	6.164	137
[N-HCN]$^+$	52	4.50	0.0420	5.779	138
[N-HCN]$^+$	52	8.50	0.0965	13.485	140
[N-HCN]$^+$	52	8.50	0.0978	13.594	139
N$^{+\cdot}$	79	0.26	0.0418	5.748	138
N$^{+\cdot}$	79	0.26	0.0343	4.589	134
				Average:	138 ± 2
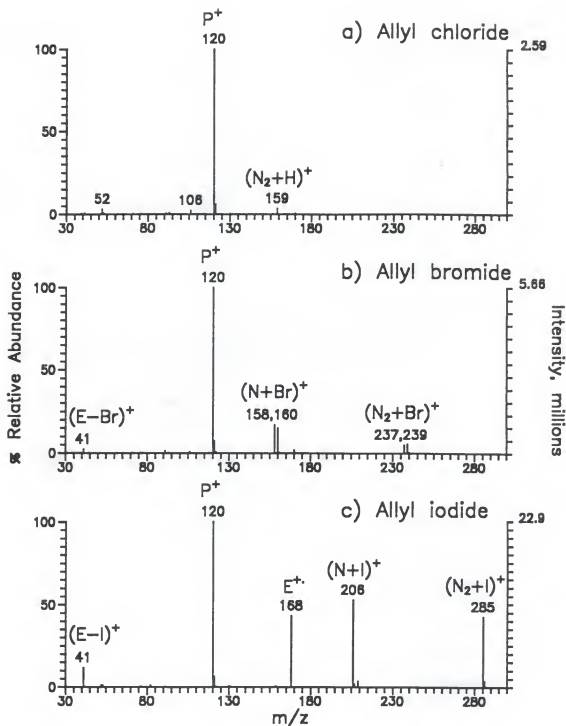
Figure 4-4:   Background-subtracted mass spectra obtained from the reaction of $N^{+\cdot}$ ion of pyridine with a) allyl chloride, b) allyl bromide, and c) allyl iodide.

Allyl iodide is observed to undergo analogous reactions to produce ions at m/z 206 and 285, $[N+I]^+$ and $[N_2+I]^+$, respectively. No $[N+Cl]^+$ or $[N_2+Cl]^+$ ions are detected in the allyl chloride reactions. The $[N+X]^+$ ions (X=halide) are produced by reaction of the $N^{+\cdot}$ ion with the neutral allyl halide followed by loss of a $C_3H_5\cdot$ neutral radical. Formation of the $[N_2+X]^+$ ions must involve reaction of the $[N+X]^+$ ion with a neutral pyridine molecule. These pyridine-halide adduct ions can be utilized to further aid in understanding the mechanisms involved in the formation of the product ions (120^+).

Figure 4-5 illustrates the effect of the ion source pyridine pressure on the pyridine-halide adducts described above. The $[N+Br]^+$ and $[N+I]^+$ ions maximize at $\approx 15 \times 10^{-5}$ torr, which is also the maximum of the pyridine ion and the maxima of the allyl chloride and allyl bromide product ions (Figure 4-2). This indicates that the product ion obtained by reaction with allyl chloride and allyl bromide do not involve reaction with a neutral pyridine. In contrast, the $[N_2+Br]^+$ and $[N_2+I]^+$ ions optimize at 35×10^{-5} torr which is indicative of neutral pyridine being involved in the reaction. The $[N_2+X]^+$ ions in Figure 4-5 maximize at the same pyridine pressure as the second optimum of the product ion of the allyl iodide reaction in Figure 4-2. Dividing the pyridine-halide adduct ion areas by the pyridine ion area yields reasonably horizontal lines above 5×10^{-5} torr for the $[N+Br]^+$ and $[N+I]^+$ ions, as depicted in Figure 4-6. Similar horizontal lines were obtained for the $P^+/N^{+\cdot}$ ratios for allyl chloride and allyl bromide, indicating that these product ions obtained by the reaction of allyl chloride and allyl bromide are dependent only on
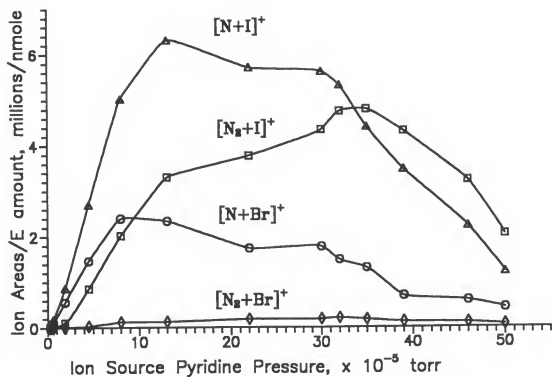
Figure 4-5: The effect of the ion source pyridine pressure on the pyridine-halide adduct ions of the allyl bromide and allyl iodide reactions. The adduct ion areas have been normalized to the number of moles of the electrophile in the mixture. Note that in the case of the allyl bromide ions, the area of the pyridine-bromide adducts is the sum of both isotopes.
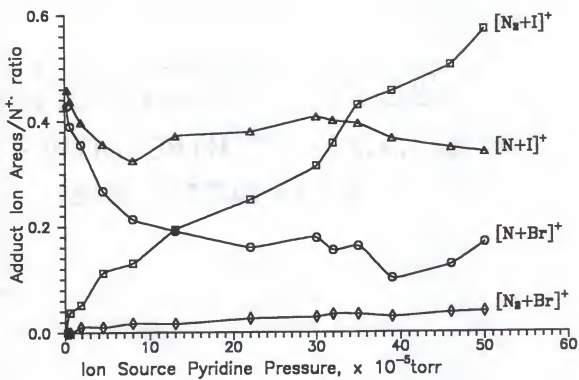
Figure 4-6: Ratio of the pyridine-halide adduct ion intensities to the pyridine reactant ion intensities at various ion source pyridine pressures for the allyl bromide and allyl iodide reactions.

the amount of the $N^{+\cdot}$ ion. However, the curves for $[N_2+Br]^+$ and $[N_2+I]^+$ ions steadily increase with pyridine pressure in the ion source. These ions, each containing two pyridines, clearly require reaction with a neutral pyridine molecule in the collision cell. The $[N_2+Br]^+$ and $[N_2+I]^+$ curves are similar to the curve obtained for the allyl iodide product ion of interest (120^+), which is further indication that to some extent the allyl iodide reaction involves neutral pyridine. Also note that at very low pyridine pressures in the ion source the ratio of the $[N_2+I]^+$ ion area/$N^{+\cdot}$ intensity is essentially zero. However, in the plot of the $P^+/N^{+\cdot}$ ratios (Figure 4-3), the allyl iodide product ion is present even at low pressures of pyridine in the ion source. This indicates that at low pressures, reaction (a) is the dominant reaction occurring, while at high pressures reaction (b), involving neutral pyridine, becomes significant.

Since it has been determined that charge exchange between the electrophile and nucleophile plays a role in the gas-phase reactivity, another volatile nucleophile, piperidine (the saturated analog of pyridine, $C_5H_{11}N$), was investigated. Piperidine was chosen because its ionization energy is 8.05 eV; thus the piperidine $N^{+\cdot}$ ion (m/z 85) is not capable of charge exchange with allyl iodide (IE=9.298 eV) or any of the other allyl compounds. The plot in Figure 4-7 depicts the effect of piperidine pressure in the ion source on the product ion (126^+) intensities (average of two injections). The product ion areas for all three electrophiles maximize at $\approx 35 \times 10^{-5}$ torr which is also the piperidine ion ($N^{+\cdot}$) optimum. Note that no normalization of the product ions is necessary since the allyl halide mixture used is equimolar.
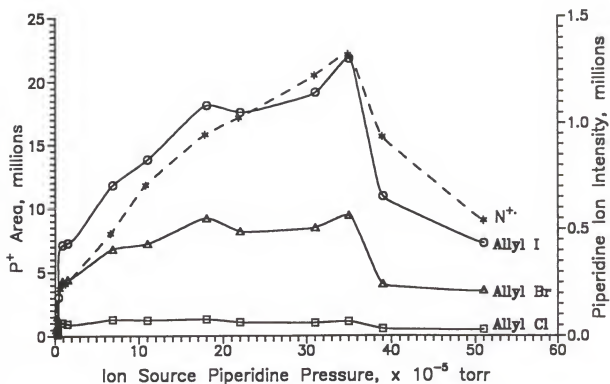
Figure 4-7: Effect of ion source piperidine pressure (uncorrected ionization gauge reading) on the product ion (126$^+$) of the reaction of the N$^{+\cdot}$ ion with allyl chloride, allyl bromide, and allyl iodide. The dashed line represents the N$^{+\cdot}$ ion intensity (at a lower EM voltage) before elution of the electrophiles into the collision cell.

Dividing the product ion areas by the piperidine ion areas yields curves in Figure 4-8 that are essentially horizontal even for allyl iodide, unlike the allyl iodide curve in Figure 4-3 produced by the reaction with pyridine. This indicates that there is little or no piperidine neutral involved in the reaction. No piperidine-halide adduct ions ($[N+X]^+$ or $[N_2+X]^+$) are detected at any piperidine pressures, although the $[N_2+H]^+$ ion is formed, indicating that some neutral piperidine does make it from the ion source to the collision cell. The reduction in the number of competitive reactions with the use of piperidine as the nucleophile simplifies the resulting spectra.

Note also that the gas-phase reactivities of these allyl halides with piperidine follow the same order as mutagenicities from the Ames test (allyl chloride < allyl bromide < allyl iodide) at all pressures. The reason the allyl iodide reactivity with the pyridine $N^{+\cdot}$ ion is low at low pressures (but not with the piperidine $N^{+\cdot}$ ion) could be that charge exchange to form the $E^{+\cdot}$ ion is favored over product ion formation; at low pyridine pressures in the ion source, there is little neutral pyridine present in the collision cell to produce the product ion by reaction with the $E^{+\cdot}$ ion formed by charge exchange.

Effect of Collision Energy on the Product Ions

In the tandem mass spectrometer used, the collision energy (axial kinetic energy) of the reactant ion is controlled by varying the quadrupole offset potential
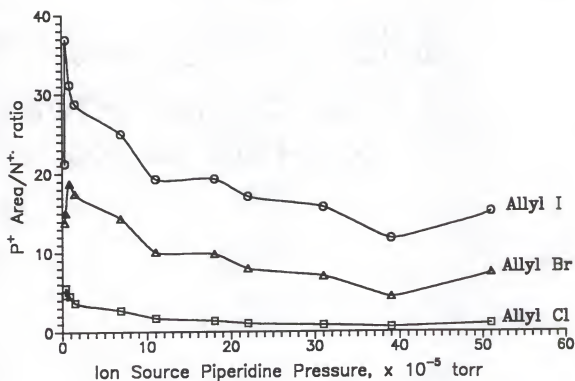
Figure 4-8: Ratio of the product ion intensities ($P^+/N^{+\cdot}$) to the piperidine reactant ion intensities at various ion source piperidine pressures for the allyl chloride, allyl bromide, and allyl iodide reactions.

of the collision cell (quadrupole 2) with respect to the ion source potential (ground). Varying the collision energy of the reactant ion controls the amount of energy deposited into the product ions; thus, low collision energies should favor associative ion-molecule reactions in the collision cell. Adjusting the collision energy of the reactant ion also effectively controls the residence times of the reactant ions in the collision cell.

Figure 4-9 illustrates the effect of collision energy on the reactant ion (essentially a function of transmission of the mass-selected reactant ion) and on the product ion intensities of the allyl chloride, allyl bromide, and allyl iodide reactions. With increasingly negative offset potential, the intensity of the $N^{+\cdot}$ ion continues to increase up to ≈ 7 V and levels off above 7 V. Note that the $N^{+\cdot}$ ion intensity is measured by lowering the electron multiplier voltage in the first 60 scans of the analysis. As the collision offset becomes more negative than -2 V, the product ions obtained by reaction with allyl chloride and allyl bromide decrease dramatically, while the product ion of allyl iodide decreases to a lesser extent. The product ion obtained by reaction with allyl iodide occurs by the two previously mentioned mechanisms (equations a and b) which may account for the greater stability of the allyl iodide product ion. The radical molecular ion of allyl iodide ($E^{+\cdot}$) produced by charge exchange with the mass-selected $N^{+\cdot}$ ion of pyridine (equation b) will have less kinetic energy than the original $N^{+\cdot}$ ion. Thus, the portion of the product ion obtained by reaction of the $E^{+\cdot}$ with neutral pyridine would be more stable at higher axial kinetic energies of the $N^{+\cdot}$ ion.
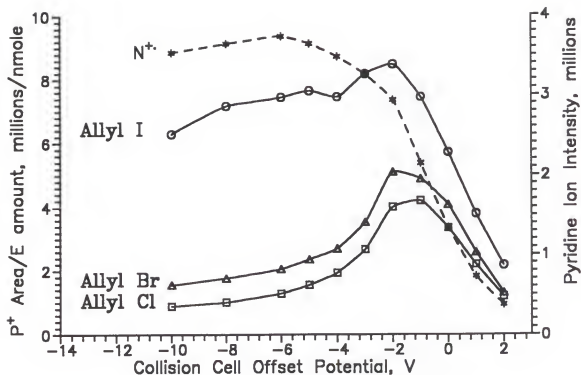
Figure 4-9: The effect of collision energy (collision cell offset potential) on the reactant ion ($N^{+\cdot}$) and product ion (120^+) intensities obtained by the reaction of the $N^{+\cdot}$ ion of pyridine with allyl chloride, allyl bromide, and allyl iodide. The product ion areas have been normalized to the number of moles of the electrophile in the mixture. The dashed line represents the $N^{+\cdot}$ ion intensity (at a lower EM voltage) before elution of the electrophiles into the collision cell.

Figure 4-10 illustrates the effect of collision energy on the pyridine-halide adduct ions and allyl fragment ions formed during the reaction of the allyl halides with the $N^{+\cdot}$ ion of pyridine. The $[N+X]^+$ and $[N_2+X]^+$ ions of allyl bromide and allyl iodide in Figure 4-10a maximize at the same low collision energies (1.5 to 2 eV) as the 120^+ product ions. In contrast, the allyl fragment ions (41^+) are observed in Figure 4-10b to steadily increase with increasing collision energy. The more internal energy deposited into the 120^+ product ion formed at higher collision energies would cause increased fragmentation of the product ion to the allyl ion due to unimolecular decomposition of the product ion. At higher collision energies, the product ion would also retain greater kinetic energy, increasing the probability of collisionally activated decomposition (CAD).

<u>Electrophile Ion/Nucleophile Neutral
Mass-Selected Reactions in the Collision Cell</u>

<u>Experimental</u>

All experiments were performed on a Finnigan MAT TSQ 70 equipped with a Varian 3400 gas chromatograph. Note that the collision energy studies were performed with a quadrupole collision cell, while the pyridine pressure studies utilized an octapole collision cell. The electrophiles were introduced into the ion source via a GC column and ionized under electron ionization (EI) conditions. All
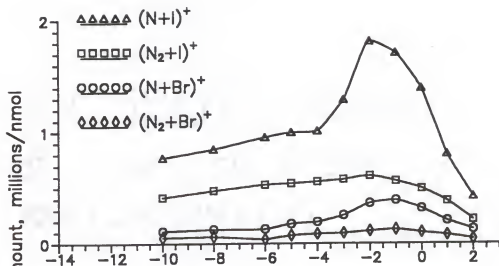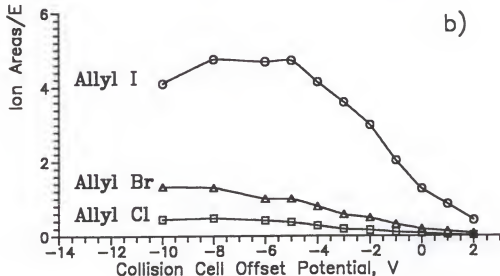
Figure 4-10: Plots depicting the effect of collision cell offset potential on a) the pyridine-halide adduct ion intensities and b) the allyl ion (41^+) intensities for the reactions of allyl chloride, allyl bromide, and allyl iodide with the $N^{+\cdot}$ ion of pyridine.

experiments were performed at an emission current of 200 μA, electron energy of 70 eV, manifold temperature of 100°C, and an ion source temperature of 170°C.

Gas chromatography was carried out on a J & W Scientific DB-5 (20 m long, 0.178 mm i.d., 0.4 μm film thickness) capillary column in the split mode (SR=100:1) with helium carrier gas at an inlet pressure of 5 psig. The GC oven was temperature programmed from 50°C to 100°C at 20°C/min with an injection port temperature of 200°C and transfer line temperature of 200°C. One-microliter injections were made in duplicate of a mixture containing 10 μg/μL each of allyl chloride, allyl bromide, and allyl iodide in pentane.

In the pressure study, the radical molecular ion of the electrophile ($E^{+\cdot}$) was mass-selected by Q1 and reacted in the collision cell with neutral pyridine introduced via a Granville Phillips fine-metering valve (Boulder, CO). The product ions were mass-analyzed with Q3 scanned from 30 to 300 amu in 0.25 seconds and detected with an electron multiplier (EM) voltage of -1100 V (dynode: -5 kV). The uncorrected pyridine pressure in the collision cell was measured with a Granville Phillips convectron gauge. The mass-selected $E^{+\cdot}$ ions were $76^{+\cdot}$ of allyl chloride, $122^{+\cdot}$ of allyl bromide, and $168^{+\cdot}$ of allyl iodide. Computer control of the mass-selected ions as a function of time allowed for mass-selection of each electrophile ion during the retention time window for elution of its parent compound.

In the collision energy studies, the radical molecular ion and allyl fragment ion of the electrophile ($E^{+\cdot}$ or $[E-X]^{+}$) was mass-selected by Q1 (by retention

time), and reacted in the collision cell with neutral pyridine introduced into the collision cell. The product ions were mass analyzed with Q3 scanned from 30 to 280 amu in 0.25 seconds and detected with an electron multiplier (EM) voltage of -1000 V. The same electrophile ions were mass-selected as in the pressure study.

The mass spectrometer was mass-calibrated with FC43, then tuned for ion-molecule reactions in the collision cell. Allyl chloride was constantly introduced into the ion source with a Negretti fine-metering valve (Hampshire, England). The collision energy, collision cell rf potential, and the potential of the lenses immediately before and following the collision cell were optimized for maximum transmission of the reactant ion (E^+) and the product ion (120^+).

Effect of Nucleophile Pressure on the Product Ions

Figure 4-11a illustrates the effect of pyridine pressure in the collision cell on the 120^+ product ions obtained by mass-selection of the $E^{+\cdot}$ ions of allyl chloride, allyl bromide, and allyl iodide. The product ion areas (the average of two injections) are normalized to the mass-selected $E^{+\cdot}$ ion intensities with no pyridine present in the collision cell (E_0^+). Normalizing to the $E_0^{+\cdot}$ intensity corrects for differences in the intensity of the $E^{+\cdot}$ ion formed from EI of the allyl halides in the ion source resulting from different extents of fragmentation and different isotopic distributions. The product ion intensities (120^+) of the allyl halides maximize in Figure 4-11a at approximately 1.3 mtorr (uncorrected) of pyridine in the collision cell. At pyridine pressures above ≈ 2 mtorr, the decrease in the intensity of the
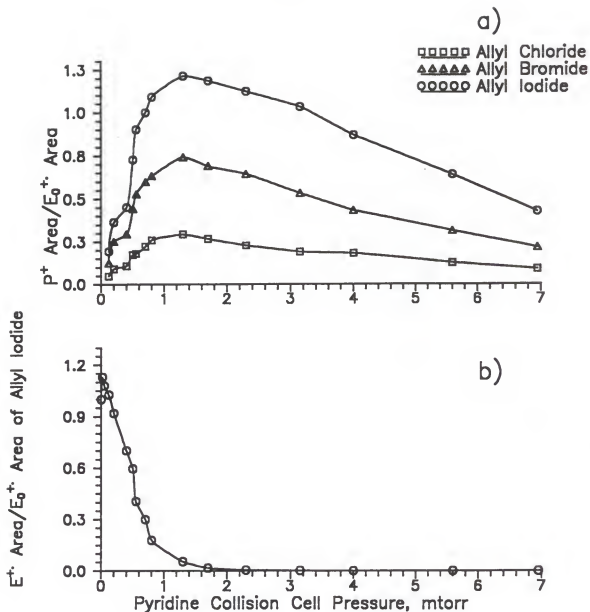
Figure 4-11: a) Effect of collision cell pyridine pressure (uncorrected convectron gauge reading) on the product ion (120$^+$) of the reactions of the E$^{+\cdot}$ ion of allyl chloride, allyl bromide, and allyl iodide with neutral pyridine. The product ion intensities have been normalized to the electrophile ion intensities with no pyridine in the collision cell (E$_o^{+\cdot}$). b) Plot of the unreacted E$^{+\cdot}$ ion intensities of allyl iodide (normalized to E$_o^{+\cdot}$) as a function of pyridine pressure in the collision cell.

product ions is most likely due to scattering of the ions at these high pyridine pressures. Note that the order of gas-phase reactivity is allyl chloride < allyl bromide < allyl iodide over the entire pyridine pressure range.

The maximum efficiencies of product ion formation (at the optimum pyridine pressure), indicated by the maximum $P^+/E_o^{+\cdot}$ ratio in Figure 4-11a, are 29, 74, and 121% for allyl chloride, allyl bromide, and allyl iodide, respectively. These values are higher than expected, especially when compared to the nucleophile ion reactions. Due to GC introduction of the electrophiles into the ion source in nanogram quantities and the low ionization efficiency, the $E^{+\cdot}$ ion is present in much smaller quantities than is neutral pyridine in the collision cell. Figure 4-11b illustrates that 99% of the $E^{+\cdot}$ ion is depleted at the optimum pyridine pressure. In Figure 4-11b, the unreacted $E^{+\cdot}$ ion of allyl iodide (normalized to the $E_o^{+\cdot}$ ion intensity) decreases with increasing pyridine pressure with one exception. The unreacted $E^{+\cdot}$ ion at the first pyridine pressure is 1.2 times greater than the $E^{+\cdot}$ ion without pyridine present in the collision cell ($E_o^{+\cdot}$). This increase in the mass-selected reactant ion upon adding pyridine in the collision cell could be due to a buffering effect of the collision gas. This buffering effect, reflected in the increased transmission efficiency of the ions, could arise from decreased axial kinetic energy (recall that the instrument was tuned to maximize transmission of ion-molecule reaction product ions which have very low axial kinetic energies) or from decreased off-axis kinetic energy and concomitant reduced loss of ions in the collision cell and into Q3.

Examination of the reconstructed ion current (RIC) areas of the allyl halide reactions (i.e., the summation of all ions) in Figure 4-12 provides further evidence that the pyridine collision gas is increasing the overall collection efficiency of all ions. Disregarding scattering effects at high pressures, it is expected that for every product ion formed, an electrophile ion would be used up; thus the RIC areas should be constant over the pyridine pressure range. However, the RIC areas are not constant, but rather increase by as much as 69% with increasing pyridine pressure in the collision cell up to 1.3 mtorr. Above 1.3 mtorr, scattering effects begin to dominate, causing the RIC areas to decrease.

The effect of pyridine pressure in the collision cell on the pyridine-halide adduct ions are examined in Figure 4-13a. Similar to the trends noted in the nucleophile ion reactions, the $[N_2+X]^+$ ions maximize at higher neutral pyridine pressures (1.6 mtorr), than do the $[N+X]^+$ ions (0.5-1.2 mtorr), since two neutral pyridines are involved in the reactions to form the $[N_2+X]^+$ ion, but only one is needed to form the $[N+X]^+$ ion. It is also interesting to note that, while the $[N+Br]^+$ ion intensity is greater than the $[N_2+Br]^+$ ion intensity at all pyridine pressures, the $[N_2+I]^+$ ion intensity becomes larger than the $[N+I]^+$ ion intensity above 1 mtorr of pyridine in the collision cell. These differences in the allyl iodide and allyl bromide reactions could be due to kinetic or thermodynamic effects which have not been investigated.

The pyridine-halide ion maxima can be compared to those for the $[N+H]^+$ and $[N_2+H]^+$ ions of pyridine produced by proton transfer as the mass-selected
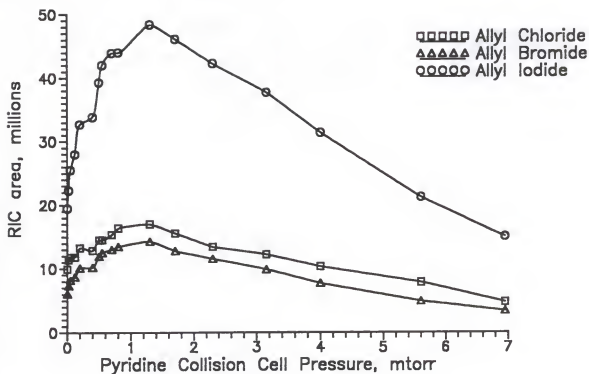
Figure 4-12: Plot of the reconstructed ion current (RIC) areas of the reactions of allyl chloride, allyl bromide, and allyl iodide as a function of pyridine collision cell pressure.
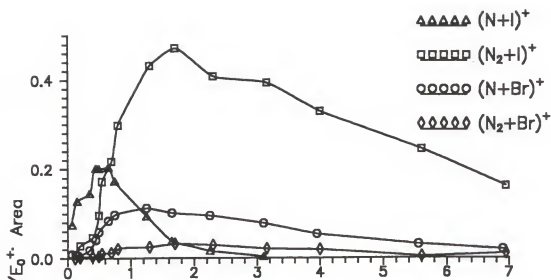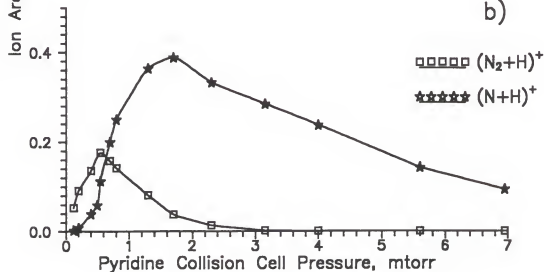
Figure 4-13: Plots illustrating the effect of the collision cell pyridine pressure on a) the pyridine-halide adduct ions and b) the $[N+H]^+$ and $[N_2+H]^+$ ion of pyridine produced upon reaction with the $E^{+\cdot}$ ion of allyl chloride.

$E^{+\cdot}$ ions enter the collision cell. The $[N+H]^+$ ion produced when the $E^{+\cdot}$ ion of allyl chloride enters the collision cell maximizes in Figure 4-13b at ≈ 0.5 mtorr of pyridine, similar to the $[N+X]^+$ ions in Figure 4-13a. In contrast, the $[N_2+H]^+$ ion maximizes at ≈ 1.6 mtorr, which is also the optimum of the $[N_2+X]^+$ ions. Although not shown, the $[N+H]^+$ and $[N_2+H]^+$ ions produced when the $E^{+\cdot}$ ions of allyl bromide and allyl iodide are mass-selected maximize at the same pressures as those formed from the allyl chloride $E^{+\cdot}$ ions. Approximately similar ion intensities are obtained for the $[N+H]^+$ ions of all three allyl halides. In contrast, the intensities of the $[N_2+H]^+$ ions decrease in the order allyl chloride > allyl iodide > allyl bromide. All three allyl halide ions can charge exchange with the neutral pyridine to form $N^{+\cdot}$ ions; however, since the electrophile is introduced by GC in low nanogram amounts into the ion source, few electrophile neutrals are present in the collision cell to react with the $N^{+\cdot}$ ion.

Effect of Collision Energy on the Product Ions

Figure 4-14 illustrates the effect of collision energy on the product ions (average of two injections) obtained by reaction of the (a) $E^{+\cdot}$ and (b) $[E-X]^+$ ions of allyl chloride, allyl bromide, and allyl iodide with neutral pyridine at a collision cell pyridine pressure of 1.2 mtorr. The product ions in these collision energy studies are not normalized to the $E_0^{+\cdot}$ ion intensity because no attempt was made to determine the $E^{+\cdot}$ ion intensity at each collision energy with no pyridine in the

Figure 4-14: The effect of the collision cell offset potential on the product ions (120$^+$) produced by the reaction of neutral pyridine in the collision cell with the mass-selected a) E$^{+\cdot}$ ions and b) [E-X]$^+$ ions of allyl chloride, allyl bromide, and allyl iodide.

collision cell. Mass-selection of the $E^{+\cdot}$ ion of the allyl halides followed by reaction with neutral pyridine in the collision cell gives rise to the product ion (120^+). The product ions of all three allyl halides maximize at a collision energy of approximately 4 eV in Figure 4-14a and remain stable up to >10 eV. In Figure 4-14b, the $[E-X]^+$ electrophile ion is mass-selected to react with the neutral pyridine in the collision cell, resulting in the 120^+ product ion. The product ions obtained by reaction of the allyl ions also maximize at a collision energy of approximately 4 eV, but the product ion intensities decrease significantly above 6 eV. The difference in the product ion stability at kinetic energies >6 eV when the $E^{+\cdot}$ is chosen is likely due to the leaving group removing excess internal energy, thus, stabilizing the product ions. The product ions formed by reaction with the mass-selected $[E-X]^+$ ions have no halide leaving group to remove excess internal energy and stabilize the product.

Figure 4-15 illustrates the effect of collision energy on the allyl fragment ion (41^+) produced during these allyl halide reactions. As the collision energy increases, more internal energy is deposited into the product ion, causing increased fragmentation to the allyl ion due to unimolecular decomposition or collisionally activated decomposition (CAD) of the product ions.

It is important to point out that the two collision energy curves depicted in Figure 4-14 were obtained under identical operating conditions. When optimizing the collision energy at a later date for electrophile ion reactions with a constant source of allyl chloride in the ion source, the collision energy curve obtained by
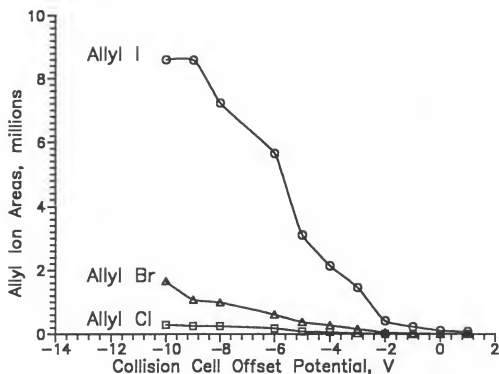
Figure 4-15: The effect of the collision cell offset potential on the allyl fragment ion (41$^+$) produced by the reaction of neutral pyridine in the collision cell with the mass-selected E$^{+\cdot}$ ions of allyl chloride, allyl bromide, and allyl iodide.

mass-selecting the $E^{+\cdot}$ ion of allyl chloride was similar to the one obtained by mass-selecting the $[E\text{-}Cl]^+$ ion. In contrast to the reaction of the $E^{+\cdot}$ ion in Figure 4-14a where the product ions remain stable up to a collision energy of 10 eV, with the new set of tuning parameters, the intensity of the product ion obtained by reaction of the $E^{+\cdot}$ ion decreased dramatically above 6 eV as shown in Figure 4-16.

The tuning parameters of the TSQ 70 are saved in tune tables which can be restored for comparison. The major difference between the tune table which generated the collision energy curve in Figures 4-14 and Figure 4-16 was the lens voltage on the second lens past the collision cell (L32): -30 V for Figure 4-14 and -130 V for Figure 4-16. The lens potentials on the adjacent lenses (L31 and L33) in both cases are -15 V. Figure 4-17 illustrates the effect of L32 voltage on the collision energy curves for the product ion of the allyl chloride reaction. At L32 values more negative than -60 V the product ions maximizes at a collision energy of 3 eV and decreases to ≈50% at 10 eV. At L32 voltages less negative than -30 V, product ion intensity maximizes at a collision energy of 2 eV and remains level up to 10 eV. Note that the optimum product ion intensity at the smaller L32 voltages is ≈50% less than at the higher L32 voltages. Thus, when tuning for the product ion at low collision energies (2-3 eV), the more negative L32 voltages would be utilized to maximize the product ion intensity.

A possible explanation for this lens effect is that at low collision energies, more negative lens voltages are required to extract product ions of associative ion-
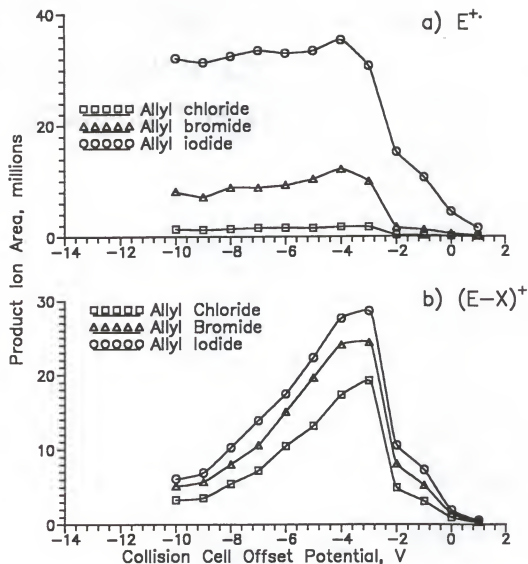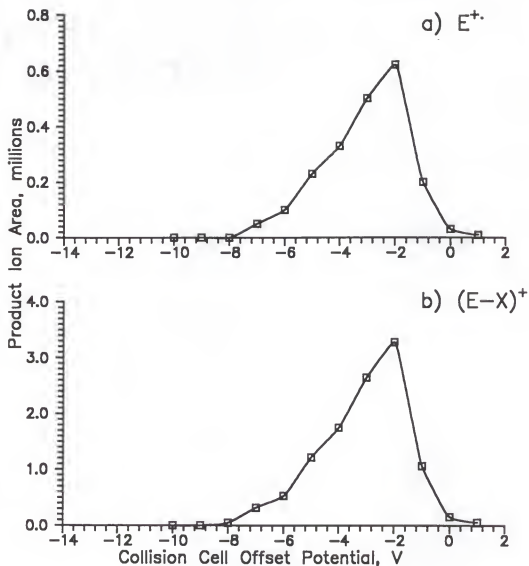
Figure 4-16: The effect of the collision cell offset potential on the product ions (120$^+$) produced by the reaction of neutral pyridine in the collision cell with the mass-selected a) E$^{+\cdot}$ ions and b) [E-X]$^+$ ions of allyl chloride. Performed with a new set of tuning parameters.
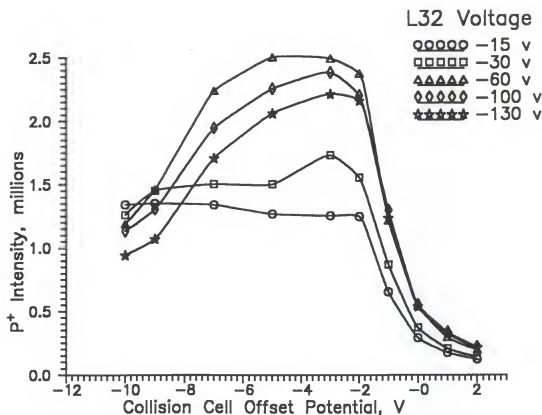
Figure 4-17: Plot of the product ion intensity (120$^+$) as a function of the collision cell offset potential for various L32 voltages. The product ion is produced by reaction of the E$^{+ \cdot}$ ion of allyl chloride with neutral pyridine in the collision cell. The voltages on the two adjacent lenses (L31 and L33) are kept constant at -15 V.

molecule reactions, which have very low kinetic energy. The use of a low L32 potential, as in the experiments for Figure 4-14, may make for less efficient transmission of low kinetic energy product ions relative to that for higher kinetic energy product ions such as those formed at more negative collision cell offsets. Thus, the shape of the collision energy curves is dependent to some extent on the tuning parameters; however, in-depth studies (e.g. computer simulations) of all the lens voltages and their interactions with each other would be necessary to completely characterize this effect. It has been recommended that the tuning parameters be optimized for each collision energy to obtain maximum ion transmission (Hail, 1990). Note that these lens effects only become important when varying the collision energy. Normally the collision energy is set at a low value of -2 or -3 eV; the lens voltages before and after the collision cell are then optimized for maximum product ion intensity.

A rather interesting phenomenon was discovered involving the entrance (L23) and exit (L31) lenses of the collision cell during these lens optimization studies. A plot of the product ion intensity for the allyl chloride reaction versus collision energy for various voltages on L23 is shown in Figure 4-18. The product ion intensities lie approximately on top of one another until the point when the collision cell offset potential equals the potential on L32. The product ion intensity is observed to increase dramatically when the collision cell offset voltage is equivalent to the voltage on L23 (L31 demonstrates a similar effect). Thus, as the collision cell offset voltage is increased, the optimum L23 voltage increases.
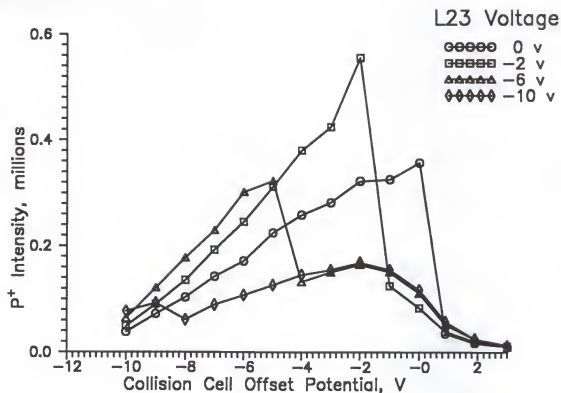
Figure 4-18: Plot of the product ion intensity (120$^+$) as a function of the collision cell offset potential for various L23 voltages. The product ion is produced by reaction of the E$^{+\cdot}$ ion of allyl chloride with neutral pyridine in the collision cell.

Similar results have been reported for the collisionally activated decomposition (CAD) of the 219^+ ion of the FC43 calibration compound (Hail, 1990). Indeed, a linear relationship was discovered between collision offset voltages and L23 optima. The reason for this behavior is not understood at this time; however, the L23 and L31 voltages become very important when studying a range of collision energies, since the lens voltages are initially optimized at low collision energies (2-3 eV) for these ion-molecule reactions.

Conclusions

Optimization of the pyridine ion source pressure in nucleophile ion reactions led to the discovery that the presence of neutral nucleophile in the collision cell at high ion source pressures allows for reactions with electrophile ions formed by charge exchange. These competitive reactions involving charge exchange and subsequent reaction with neutral pyridine in the collision cell affect the gas-phase reactivity of allyl iodide. Selection of a nucleophile which has an IE low enough that its molecular ion cannot undergo charge exchange (e.g. piperidine) with the electrophiles can minimize competitive reactions and dependence of reactivity on the neutral nucleophile pressure.

In the electrophile ion reactions, the product ions of all three allyl halides optimized at the same neutral pyridine pressure in the collision cell. Charge exchange between the electrophile ions and the neutral pyridine in the collision cell

can occur. However, because the electrophile is introduced in small quantities into the ion source, there are few electrophile neutrals in the collision cell for the pyridine charge exchange product to react with to produce the P^+ ion. At all neutral pyridine pressures in the collision cell, the order of relative gas phase reactivities of the $E^{+\cdot}$ ion is allyl chloride < allyl bromide < allyl iodide.

The product ions of both nucleophile ion and electrophile ion reactions optimize at low collision energies (2-3 eV). It is important to realize that the potentials on the lenses before and after the collision cell will affect the shape of the collision energy curves. For maximum collection of the product ions, the lenses before and after the collision cell should be optimized at the optimum collision energy.

CHAPTER 5
EVALUATION OF THE GAS-PHASE REACTIVITY
OF A SERIES OF ELECTROPHILES
WITH VARIOUS NUCLEOPHILES

Introduction

As discussed in Chapter 4, pyridine is not an ideal choice of nucleophile due to the possibility of charge exchange between pyridine and electrophiles with ionization energies (IE) less than 9.25 eV (IE of pyridine). This chapter presents results of nucleophile ion and electrophile ion reactions of two other nucleophiles (piperidine and aniline) with thirty electrophiles. Piperidine and aniline have IE's below the IE's of any of the electrophiles studied. A preliminary study of the types of product ions observed in the mass spectra is undertaken. Also, the gas-phase reactivity (intensity of major product ions) is compared to the Ames test classification (mutagen or non-mutagen) of these analytes. In some cases, the Ames test mutagenicities were not found in the literature; however, a cooperative agreement with U.S. Environmental Protection Agency (EPA) in Duluth, MN, may lead to correlations of these compounds with toxicological data acquired by the EPA.

Nucleophile Ion/Electrophile Neutral Mass-Selected Reactions in the Collision Cell

Experimental

All experiments were performed on a Finnigan MAT TSQ 70 (octapole collision cell) equipped with a Varian 3400 gas chromatograph. The nucleophile (e.g. piperidine or aniline) and methane were constantly introduced into the ion source with a Granville Phillips fine-metering valve (Boulder, CO) and ionized under electron ionization (EI) conditions. The uncorrected ion source pressure of piperidine or aniline was 2.0×10^{-4} torr as measured by a Varian Bayard-Alpert ionization gauge (Palo Alto, CA) mounted on a flange on the ion source vacuum chamber. The methane ion source pressure was 1.25 mtorr (without the nucleophile present) as measured by a Granville Phillips convectron gauge (Boulder, CO). All experiments were performed at an emission current of 200 μA, electron energy of 70 eV, a manifold temperature of 100°C, and ion source temperature of 170°C.

Gas chromatography was carried out on a J & W Scientific (Folsom, CA) DB-5 (20 m long, 0.178 mm i.d., 0.4 μm film thickness) capillary column in the split mode (SR=100:1) with helium carrier gas at an inlet pressure of 5 psig. The GC oven was temperature programmed from 35°C to 150°C at 10°C/min after an initial hold time of 1.5 minutes. The injection port and collision cell transfer line were held at a temperature of 200°C. One μL injections were made of three equimolar

mixtures (59.6 nmoles/μL) prepared in octane (purchased from Chem Service in West Chester, PA). The contents of the three mixtures are listed in Table 5-1, along with the ionization energy (IE) of each analyte. Note that the IE's of the nucleophiles (also in Table 5-1) are less than all of the known IE's of the analytes; thus, charge exchange between the nucleophile ion and the neutral analyte is not favorable.

The experiments were performed by alternately mass-selecting (with Q1) between the radical molecular ion ($N^{+\cdot}$) of the nucleophiles (or the $[N+H]^+$ ion) and the radical molecular ion of methane ($CH_4^{+\cdot}$) to react in the collision cell with the neutral analytes introduced into the collision cell via a GC column. The product ions (P^+) of the $N^{+\cdot}$ reactions were mass analyzed with Q3 scanned from 90 to 350 amu in 0.25 seconds (95 to 350 amu in 0.25 seconds for aniline) at an electron multiplier (EM) voltage of -1200 V (dynode: -5 kV). Since the mass-selected reactant ion is saturated at the EM voltage necessary to observe the product ion, in order to assess quantity of reactant ion present, the EM voltage was lowered to -700 V during the first 30 scans of the chromatograms (no eluates in this region). The ions produced by charge exchange with methane were mass analyzed with Q3 scanned from 30 to 350 amu in 0.25 seconds at an electron multiplier voltage of -1200 V.

The mass spectrometer was mass-calibrated with perfluorotributylamine (FC43), then tuned for ion-molecule reactions in the collision cell. Allyl chloride is constantly introduced into the collision cell with a Negretti fine-metering valve

Table 5-1:   Properties of the nucleophiles and the analytes comprising the three
equimolar GC mixtures, listed in order of their GC elution.

Electrophile	MW[b]	IE (eV)[c]	Source
Mix 1:			
Acrolein	56	10.10	Fluka (Buchs, Switzerland)
Pentane[a]	72	10.35	Fisher Scientific (Fair Lawn, NJ)
Allyl chloride	76	9.90	Aldrich (Milwaukee, WI)
Propyl chloride	78	10.82	Eastman Kodak (Rochester, NY)
Propyl bromide	122	10.18	Eastman Kodak
Allyl bromide	120	10.16	Aldrich
Benzene	78	9.25	Fisher Scientific
Cyclohexane	84	9.86	Fisher Scientific
2,3-dichloropropene	110	NR[d]	Aldrich
Allyl iodide	168	9.30	Aldrich
Epichlorohydrin	92	NR	Eastman Kodak
Allyl isothiocyanate	99	NR	Aldrich
o-Xylene	106	8.56	Chem Service (Media, PA)
Decane	142	9.65	Alfa Products (Danvers, MA)
Benzyl chloride	126	9.14	Eastman Kodak
Benzyl bromide	170	9.00	Eastman Kodak
Mix 2:			
t-Butyl bromide	136	9.92	Aldrich
sec-Butyl bromide	136	9.98	Aldrich
n-Butyl bromide	136	10.13	Aldrich
Chlorobenzene	116	9.06	Chem Service
Ethyl benzene	106	8.77	Fisher Scientific
Styrene	104	8.43	Fisher Scientific
Nonane	128	9.72	Alltech (Deerfield, IL)
Bromobenzene	156	8.98	J.T. Baker (Phillipsburg, NJ)
Benzoyl chloride	140	9.54	Eastman Kodak
Mix 3:			
m-Difluorobenzene	114	9.23	Aldrich
t-Butyl iodide	184	9.02	Aldrich
sec-Butyl iodide	184	9.09	Aldrich
n-Butyl iodide	184	9.09	Eastman Kodak
m-Dichlorobenzene	146	9.11	Aldrich
Nucleophile:			
Piperidine	85	8.05	Fisher Scientific
Aniline	93	7.72	Eastman Kodak

[a]Pentane not present in mixture 1 during piperidine $N^{+\cdot}$ ion studies.
[b]molecular weight of most abundant isotope.
[c]ionization energies from Lias et al., 1988.
[d]no literature reference found for the IE.

(Hampshire, England) via the collision gas inlet. The collision energy, collision cell rf potential, and the potentials on the lenses immediately before and following the collision cell were optimized for maximum transmission of the reactant ion ($N^{+\cdot}$) and product ion (120^{+}).

Reactions with the $N^{+\cdot}$ Ion of Piperidine

The chromatograms shown in Figure 5-1 are obtained by alternately mass-selecting between the radical molecular ion of piperidine ($85^{+\cdot}$) and the radical molecular ion of methane ($16^{+\cdot}$) with Q1 to react with the components of mixture 1 eluting from the gas chromatograph into the collision cell. Thus, chromatograms are obtained that either depict only reactive compounds (reaction with $85^{+\cdot}$ of piperidine) or depict all the compounds in the mixture (charge exchange reaction with $16^{+\cdot}$ of methane).

Chromatogram (b) in Figure 5-1 displays the reconstructed ion current (RIC) resulting from the mass-selection of the $16^{+\cdot}$ ion of methane and subsequent reaction with the equimolar GC eluates of mixture 1. This chromatogram illustrates the ability to detect all compounds in the mixture regardless of whether the compounds react with the nucleophile. As discussed in Chapter 3, the mass spectra obtained by $CH_4^{+\cdot}$ charge exchange with the neutral electrophiles are similar to the mass spectra obtained when the $N^{+\cdot}$ ion is mass-selected, since the neutral nucleophile present in the collision cell allows for reaction with the

Figure 5-1: Chromatograms obtained by mass selected reactions of (a) the $N^{+\cdot}$ ion of piperidine ($85^{+\cdot}$) and (b) the $16^{+\cdot}$ ion of methane with the following neutral analytes (mix 1) introduced into the collision cell via a GC column: (1) acrolein, (2) allyl chloride, (3) propyl chloride, (4) propyl bromide, (5) allyl bromide, (6) co-elution of benzene and cyclohexane, (7) 2,3-dichloropropene, (8) allyl iodide, (9) epichlorohydrin, (10) 7-methyl heptane, (11) octane (solvent), (12) allyl isothiocyanate, (13) o-xylene, (14) decane, (15) benzyl chloride, and (16) benzyl bromide. (* RIC minus m/z 169 to 172; see text)

electrophile ions resulting in product ions. However, the charge exchange reactions of $CH_4^{+\cdot}$ with the neutral electrophiles can be used to correct for varying amounts of analytes in an unknown mixture and to detect analytes which do not react with the nucleophile ion.

The elevated background in chromatogram (b) is most likely due to proton transfer between the mass-selected $16^{+\cdot}$ ion of methane and neutral piperidine which makes it into the collision cell from the ion source. The proton affinity (PA) of the $CH_3^\cdot$ radical species (8.29 eV) is significantly lower than the PA of piperidine (9.77 eV), thus proton transfer can occur between the $CH_4^{+\cdot}$ ion and neutral piperidine to form the $[N+H]^+$ ion of piperidine and $CH_3^\cdot$ species of methane. The major ions observed in the background mass spectrum are the $[N+H]^+$, $[N-H]^+$, $[N_2+H]^+$, and $[N_2-H]^+$ ions, with m/z (and relative abundances) of 86 (100%), 84 (18%), 171 (26%), 169 (2%), respectively.

Chromatogram (a) in Figure 5-1 illustrates the RIC (minus signals due to the m/z 169-172 ions ($[N_2+H]^+$ and $[N_2-H]^+$ of piperidine) resulting from the mass-selection of the $85^{+\cdot}$ ion of piperidine with Q1 and subsequent reaction with the GC eluates of mixture 1. During mass-selection of the $85^{+\cdot}$ ion of piperidine, Q3 is scanned from 90 to 350 amu in order to avoid scanning over the saturated reactant ion. This chromatogram illustrates the capability to monitor eluates that react in any way with the piperidine reactant ion. Comparison of the two chromatograms in Figure 5-1 illustrates several compounds which are present in the $16^{+\cdot}$ chromatogram, but demonstrate very little or no reactivity with the $85^{+\cdot}$

ion of piperidine. Propyl chloride (peak 3), benzene and cyclohexane (co-elution in peak 6), and decane (peak 14) show little or no reaction with piperidine $N^{+\cdot}$ ion relative to the other electrophiles. Co-elution of benzene and cyclohexane (peak 6) is confirmed by the mass spectra obtained by charge exchange with the $16^{+\cdot}$ ion of methane. The reactivity of octane (solvent, peak 11) is observed to be small, especially considering the enormous quantity of octane entering the collision cell. In fact, the mass spectrum obtained for the reaction of octane consists mostly of noise due to the neutrals hitting the multiplier when the large amount of octane elutes into the collision cell. The chromatographic peak (10) immediately before the elution of octane is an impurity in the octane solvent. The impurity has been identified as 7-methyl heptane by its EI mass spectrum.

The intensity of an analyte's peak in chromatogram 5-1a reflects its electrophilic reactivity and its concentration, whereas its intensity in chromatogram 5-1b reflects primarily its concentration (since the charge exchange reactivities with the $CH_4^{+\cdot}$ ion should be similar). Hence, a ratio of the intensities of the peaks produced upon reaction with $85^{+\cdot}$ to reaction with $16^{+\cdot}$ would correct for varying concentrations and reflect largely the relative electrophilic reactivity.

Similar chromatograms of the equimolar mixtures 2 and 3 (Table 5-1) are illustrated in Figures 5-2 and 5-3. In Figure 5-2, comparison of chromatograms obtained by reaction with the $16^{+\cdot}$ ion and reaction with $85^{+\cdot}$ ion illustrates the low to no reactivity of *t*-butyl bromide (peak 1), chlorobenzene (peak 6), nonane (peak 9) and bromobenzene (peak 10). In Figure 5-3, *m*-difluorobenzene (peak 1),
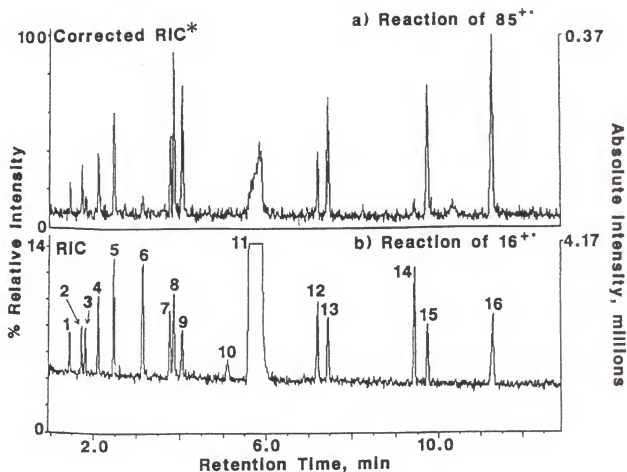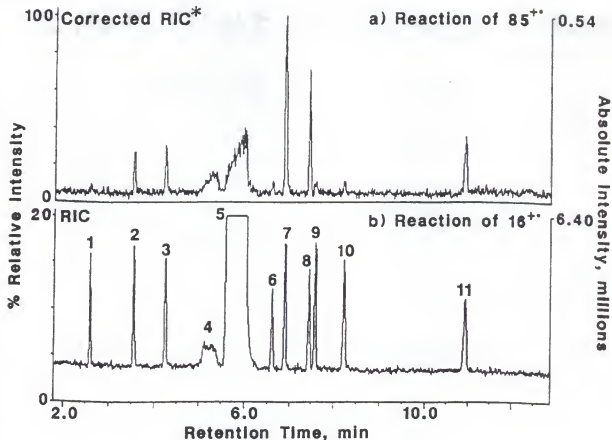
Figure 5-2: Chromatograms obtained by mass-selected reactions of (a) the N$^{+ \cdot}$ ion of piperidine (85$^+$) and (b) the 16$^{+ \cdot}$ ion of methane with the following neutral analytes (mix 2) introduced into the collision cell via a GC column: (1) *t*-butyl bromide, (2) *sec*-butyl bromide, (3) *n*-butyl bromide, (4) 7-methyl heptane, (5) octane (solvent), (6) chlorobenzene, (7) ethyl benzene, (8) styrene, (9) nonane, (10) bromobenzene and (11) benzoyl chloride. (* RIC minus m/z 169 to 172)
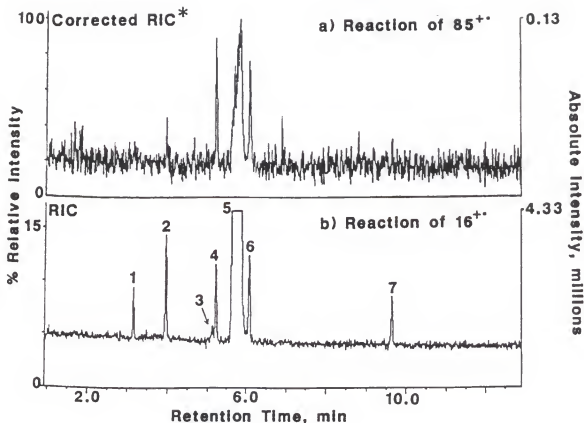
Figure 5-3: Chromatograms obtained by mass-selected reactions of (a) the N$^{+\cdot}$ ion (85$^{+\cdot}$) of piperidine and (b) the 16$^{+\cdot}$ ion of methane with the following neutral analytes (mix 3) introduced into the collision cell via a GC column: (1) *m*-difluorobenzene, (2) *t*-butyl iodide, (3) 7-methyl heptane, (4) *sec*-butyl iodide, (5) octane (solvent), (6) *n*-butyl iodide, and (7) *m*-dichlorobenzene. (* RIC minus m/z 169 to 172)

m-dichlorobenzene (peak 7) and *t*-butyl iodide (peak 2), demonstrate essentially no reactivity towards the $85^{+ \cdot}$ ion of piperidine. Thus, visual inspection of the chromatograms obtained by alternately mass-selecting between the $N^{+ \cdot}$ ion of the nucleophile and $CH_4^{+ \cdot}$ of methane yields information on the number of reactive analytes (i.e., potential carcinogens) versus the total number of analytes in the GC mixtures.

The mass spectral data obtained by the reaction of the $85^{+ \cdot}$ ion of piperidine with the GC eluates in the collision cell are presented in Table 5-2, including the major ions (≥ 0.01 million counts), their structures and their peak areas (in millions). The electrophiles are grouped according to similarities in their structures. The product ions (P^+) are defined as the ion(s) produced by the substitution reaction of the $N^{+ \cdot}$ ion and the neutral E with subsequent loss of a neutral X radical to form the $[N+(E-X)]^+$ ion (equation a).

$$\text{(a)} \quad N^{+ \cdot} \quad + \quad E \quad \longrightarrow \quad [N+(E-X)]^+ \quad + \quad X^\cdot$$

For example, the reaction of allyl chloride with the $85^{+ \cdot}$ ion of piperidine forms the N-allyl pyridine product ion at m/z 126 with the loss of a neutral chlorine radical.

Due to the lack of a suitable leaving group, acrolein, cyclohexane, benzene and styrene might be expected to undergo an addition reaction, if any reaction at all, rather than a substitution reaction. The reaction of acrolein with piperidine forms a loosely bound $[P+H]^+$ product ion at m/z 142 which is most likely the

Table 5-2: The major ions observed in the mass spectra obtained by reaction with the $N^{+\cdot}$ ion of piperidine.

Electrophiles	MW[a]	P[+b]	$[N_2+H]^+$	$[E-X]^+$	Others
Allyl isothiocyanate	99	126 (0.10)	(0.80)	ND[d]	166 (0.01) $[N+C_6H_9]^+$
Allyl chloride	76	126 (0.12)	(0.22)	ND	124 (0.05) $[P \cdot HCl]^+$
2,3-dichloropropene	110	160, 162 (0.20)	(0.23)	ND	
Epichlorohydrin	92	142 (0.02)	(0.25)	ND	98 (0.48) $[P \cdot C_2H_4O]^+$
Allyl bromide	120	126 (0.33)	(0.44)	ND	166 (0.03) $[N+C_6H_9]^+$
Allyl iodide	168	126 (0.54)	(0.33)	ND	166 (0.02) $[N+C_6H_9]^+$
Acrolein	56	NL[c]	(0.31)	ND	142 (0.04) $[N+H+E]^+$
Benzyl chloride	126	176 (0.44)	(0.28)	91 (0.06)	
Benzyl bromide	170	176 (1.01)	(0.17)	91 (0.07)	
Propyl chloride	78	128 (0.03)	(0.15)	ND	
Propyl bromide	122	128 (0.18)	(0.25)	ND	
t-Butyl bromide	136	142 (0.04)	(0.46)	ND	
sec-Butyl bromide	136	142 (0.25)	(0.79)	ND	
n-Butyl bromide	136	142 (0.28)	(0.72)	ND	
t-Butyl iodide	184	142 (0.04)	(0.60)	ND	
sec-Butyl iodide	184	142 (0.20)	(0.41)	ND	
n-Butyl iodide	184	142 (0.10)	(0.38)	ND	

Table 5-2: continued

Electrophiles	MW[a]	P[+b]	[N$_2$+H]$^+$	[E-X]$^+$	Others
Nonane	128	128 (0.01) 142 (0.03)	(0.80)	ND	
Decane	142	128 (0.01) 142 (0.02)	(0.76)	----	
Cyclohexane	84	154 (0.03)	(0.49)	ND	
Benzene	78	NL	(0.49)	ND	
Ethyl benzene	106	176 (0.66)	(0.76)	91 (0.45)	190 (0.14) 204 (0.26)
Chlorobenzene	116	162 (----)[e]	(0.73)	ND	
Bromobenzene	156	162 (0.02)	(1.37)	ND	
m-Difluorobenzene	114	95 (----)	(0.36)	----	
m-Dichlorobenzene	146	196,198 (----)	(0.49)	----	
o-Xylene	106	176 (0.28)	(0.20)	91 (0.13)	190 (0.04) 204 (0.12)
Styrene	104	NL	(0.85)	ND	189 (0.69) [N+E]$^+$ 274 (0.02) [N$_2$+E]$^+$
Benzoyl chloride	140	190 (----)	(1.10)	105 (0.03)	275 (0.42) [N$_2$+(E-X)]$^+$

[a] molecular weight of most abundant isotope.
[b] m/z of P$^+$ ion defined as [N+(E-X)]$^+$; peak area (in millions) in parenthesis.
[c] no suitable leaving group.
[d] m/z is below the first mass scanned (90 amu).
[e] ion area <0.01 million.

proton hydrogen bound complex $[N\cdots H\cdots E]^+$. As observed in Table 5-2, cyclohexane and benzene do not undergo any significant addition reactions to produce the anticipated 169^+ and 163^+ ions, respectively. The reaction of cyclohexane demonstrates a product ion at m/z 154 which appears to be addition of C_5H_9 to the piperidine ion. The EI mass spectrum of cyclohexane contains a fragment ion at m/z 69 which is loss of $CH_3^{\cdot}$ from the radical molecular ion of cyclohexane. The reaction of styrene forms a rather large 189^+ ion in the gas-phase which is probably the $[N+E]^{+\cdot}$ ion.

Certain electrophiles have more than one possible leaving group. For example, the reaction of nonane and decane could involve loss of C_6H_{13} or C_5H_{11} from nonane and C_7H_{15} or C_6H_{13} from decane resulting in the observed $[N+C_3H_7]^+$ (m/z 128) and $[N+C_4H_9]^+$ (m/z 142) product ions. In the case of nonane, the 128^+ product ion could be the $E^{+\cdot}$ ion; however charge exchange is not favorable between nonane (IE=9.72 eV) and piperidine (IE=7.72 eV); the same is true for 142^+ product ion of decane.

Rather than the predicted $[N+(E-X)]^+$ product ions, the mass spectra of epichlorohydrin and benzoyl chloride demonstrate several interesting ions. The reaction of epichlorohydrin with piperidine the $N^{+\cdot}$ ion results in a small amount of the $[N+(E-Cl)]^+$ product ion; however a rather large ion is observed in the mass spectra at m/z 98 which could be due to loss of C_2H_4O from the product ion. The reaction of benzoyl chloride with piperidine produced no significant amount of $[N+(E-Cl)]^+$ product ion; however an abundant ion at m/z 275 is observed whose

structure may be $[N_2+(E-X)]^+$. Comparison of the reaction of benzyl chloride with the $N^{+\cdot}$ ion of piperidine and the $N^{+\cdot}$ ion of pyridine (Chapter 3) illustrates the importance of choosing a nucleophile which cannot undergo charge exchange with the analytes. Reaction of benzyl chloride with the $N^{+\cdot}$ ion of pyridine resulted in primarily the $E^{+\cdot}$ ion produced by charge exchange ($126^{+\cdot}$, $128^{+\cdot}$); however, reaction with the $N^{+\cdot}$ ion of piperidine results in a significant amount of the product ion with no charge exchange ions present.

As each electrophile elutes into the collision cell, proton transfer between the nucleophile and the electrophile causes increased formation of the $[N_2+H]^+$ ion at m/z 171. The absolute intensity of the $[N_2+H]^+$ ion varies as each eluate enters the collision cell as shown in Table 5-2, due to the proton transfer between the analytes and the nucleophile ion as shown in equation (b). The $[N+H]^+$ then undergoes further reaction (equation c) with the neutral piperidine present in the collision cell to form the $[N_2+H]^+$ ion.

$$(b) \quad N^{+\cdot} \quad + \quad E \quad \longrightarrow \quad [N+H]^+ \quad + \quad [E-H]^{\cdot}$$

$$(c) \quad [N+H]^+ \quad + \quad N \quad \longrightarrow \quad [N_2+H]^+$$

The intensity of the $[N_2+H]^+$ ion will depend on the proton affinity (PA) of the $[E-H]^{\cdot}$ radical species and the kinetics of the proton transfer reaction.

The product ions produced in the collision cell can undergo unimolecular decomposition or collisionally activated decomposition (CAD) to produce the

$[E-X]^+$ fragment ion. In most cases, the $[E-X]^+$ fragment ions are below the scan range used (90 to 350 amu); however benzyl chloride, benzyl bromide, ethyl benzene and *o*-xylene demonstrate appreciable $[E-X]^+$ ions at m/z 91.

Table 5-3 compares the gas-phase reactivity of the various equimolar analytes with the radical molecular ion of piperidine to their mutagenicity (+/-) determined by the Ames test (without metabolic activation). The gas-phase reactivity is defined as the product ion areas of the electrophiles normalized to the weakly mutagenic allyl isothiocyanate for ease of comparison. Considering the compounds for which references to mutagenicity were found, seven of the eight mutagens were observed to react appreciably (≥ 1.0) in the gas-phase with the $N^{+\cdot}$ ion of piperidine. Reaction of acrolein with the $N^{+\cdot}$ ion of piperidine appears as a false negative in these gas-phase reactions. The detection of product ions for addition reactions (e.g., acrolein) may be less sensitive than substitution reactions in the gas-phase, although the reaction of styrene contradicts this. If the gas-phase reactivity threshold is assigned a value of 1.0, then six of the eleven non-mutagens would be classified as non-reactive or weakly reactive with the $N^{+\cdot}$ ion of piperidine. The gas-phase reactivities of ethyl benzene, *o*-xylene, styrene, propyl bromide and benzoyl chloride with piperidine are false positives in this method. It is interesting to note that, in the case of ethyl benzene and *o*-xylene, the abundant product ions are a result of the addition of the C_7H_7 ([E-X]) species to piperidine. As discussed in Chapter 2, benzoyl chloride is a suspected carcinogen to humans; however, its estimated mutagenicity may be limited due to

Table 5-3: Comparison of gas-phase reactivities of various analytes with the $N^{+\cdot}$ ion of piperidine to Ames test mutagenicities.

Electrophiles	m/z of P^+	Gas-Phase[f] Reactivity	Ames Test[g] Mutagenicity	Mutagenicity References
Allyl isothiocyanate	126	1.0	+	Eder et al., 1982
Allyl chloride	126	1.2	+	Eder et al., 1982
2,3-dichloropropene	160,162	2.0	+	Eder et al., 1982
Epichlorohydrin	142,98[a]	5.0	+	Eder et al., 1982
Allyl bromide	126	3.3	+	Eder et al., 1982
Allyl iodide	126	5.4	+	Eder et al., 1982
Acrolein	142[b]	0.4	+	Eder et al., 1982
Benzyl chloride	176	4.4	+	Eder et al., 1982
Benzyl bromide	176	10.1	NR[h]	
Propyl chloride	128	0.3	-	Eder et al., 1982
Propyl bromide	128	1.8	-	Eder et al., 1982
t-Butyl bromide	142	0.4	NR	
sec-Butyl bromide	142	2.5	NR	
n-Butyl bromide	142	2.8	NR	
t-Butyl iodide	142	0.4	NR	
sec-Butyl iodide	142	2.0	NR	
n-Butyl iodide	142	1.0	NR	
Nonane	128,142	0.4	NR	
Decane	128,142	0.3	NR	
Cyclohexane	154	0.3	NR	
Benzene	----[c]	---	-	Dean, 1985
Ethyl benzene	176	6.6	-	Dean, 1985
Chlorobenzene	162	<0.1	-	Shimizu et al., 1983
Bromobenzene	162	0.2	-	Shimizu et al., 1983
m-Difluorobenzene	95	<0.1	-	Shimizu et al., 1983
m-Dichlorobenzene	196,198	<0.1	-	Shimizu et al., 1983
o-Xylene	176	2.8	-	Dean, 1985
Styrene	189[d]	6.9	-	Busk, 1979
Benzoyl chloride	275[e]	4.2	-	Yasuo et al., 1978

[a] m/z 98 is $[P-C_2H_4O]^+$.
[b] m/z 142 is $[N+H+E]^+$.
[c] no product ion detected above 0.01 million counts.
[d] m/z 189 is $[N+E]^+$.
[e] m/z 275 is $[N_2+(E-X)]^+$.
[f] gas-phase reactivity is the P^+ ion area normalized to P^+ ion area of allyl isothiocyanate.
[g] without metabolic activation.
[h] no literature references found.

hydrolysis of benzoyl chloride in the aqueous medium of the bacteriological test (Yasuo et al., 1978). No literature on the mutagenicity of the straight chain alkanes and cyclohexane has been discovered; however, one can postulate that these compounds would exhibit weak or no electrophilicity due to lack of a suitable leaving group and the lack of formation of an electrophilic carbocation. The gas-phase reactions of nonane, decane and cyclohexane in the gas-phase exhibit little if any reactivity with the piperidine $N^{+\cdot}$ ion. The butyl halides have been shown to be weak electrophiles (or weak carcinogens) in animal tests (Poirier et al., 1975). In general, the carcinogenicity of the butyl halides in the animal tests increased with increased branching of the carbon chain. The gas-phase reactivities of the butyl halides with piperidine are relatively weak; however, no correlation to the branching of the butyl halides can be made. In fact, the t-butyl halides are the least reactive of the butyl halides, which may be due to steric hindrance of the piperidine $N^{+\cdot}$ ion reactive site with these tertiary groups. No attempt to find a mathematical relationship between gas-phase reactivity and mutagenicity is attempted at this point for several reasons. The types of gas-phase reactions occurring are not well understood for some of these analytes. Also, no consistent set of mutagenicity values by the Ames test has been discovered for these analytes; mutagenicity values in the literature tend to vary significantly between laboratories.

Reactions with the $N^{+\cdot}$ Ion of Aniline

The chromatograms shown in Figure 5-4 are obtained by alternately mass-selecting the radical molecular ion of aniline ($93^{+\cdot}$) and the radical molecular ion of methane ($16^{+\cdot}$) with Q1 to react with the components of mixture 1 eluting from the gas chromatograph into the collision cell. Thus, chromatograms are obtained that either depict only reactive compounds (reaction with $93^{+\cdot}$ of aniline) or depict all the compounds in the mixture (charge exchange reaction with $16^{+\cdot}$ of methane). Mixtures 2 and 3 were not analyzed for reactivity with the $N^{+\cdot}$ ion of aniline.

Chromatogram (b) in Figure 5-4 displays the reconstructed ion current (RIC) resulting from the mass-selection of the $16^{+\cdot}$ ion of methane and subsequent reaction with the equimolar GC eluates of mixture 1. This chromatogram includes peaks for all compounds in the mixture. The only major ion detected in the background mass spectrum is the $N^{+\cdot}$ ion (m/z 93) of aniline due to neutral aniline which makes it into the collision cell from the ion source. Aniline exhibits no significant reaction to form the $[N_2+H]^+$ ion at m/z 187. The significant difference in the proton affinities (Aue and Bowers, 1979) of aniline (PA = 9.17 eV) and piperidine (PA = 9.77 eV) may contribute to the mass spectral differences observed with these two nucleophiles.

The chromatograms of Figures 5-1b and 5-4b, in which the $16^{+\cdot}$ ion of methane is mass-selected to react with the electrophiles, are quite similar, as one
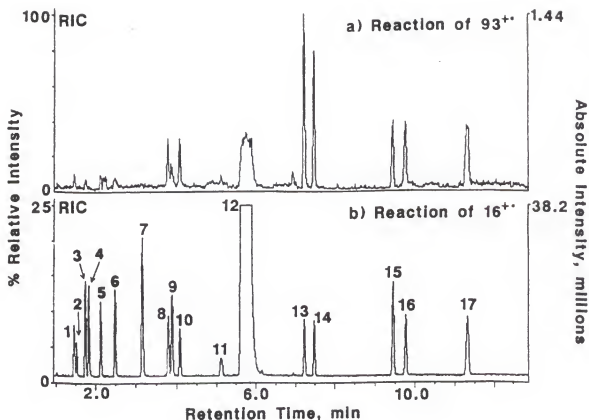
Figure 5-4: Chromatograms obtained by mass-selected reactions of (a) the N$^{+\cdot}$ ion (93$^{+\cdot}$) of aniline and (b) the 16$^{+\cdot}$ ion of methane with the following neutral analytes introduced into the collision cell via a GC column: (1) acrolein, (2) pentane, (3) allyl chloride, (4) propyl chloride, (5) propyl bromide, (6) allyl bromide, (7) co-elution of benzene and cylcohexane, (8) 2,3-dichloropropene, (9) allyl iodide, (10) epichlorohydrin, (11) 7-methyl heptane, (12) octane (solvent), (13) allyl isothiocyanate, (14) o-xylene, (15) decane, (16) benzyl chloride, and (17) benzyl bromide.

would expect. The greater absolute intensities ($\approx$10 times) in Figure 5-4b can be attributed to the higher intensity of the mass-selected $16^{+\cdot}$ ion of methane in that experiment. The pressure, IE and PA of the nucleophile will affect the intensity of the $CH_4^{+\cdot}$ ion in the ion source.

Chromatogram (a) in Figure 5-4 illustrates the RIC resulting from the mass-selection of the $93^{+\cdot}$ ion of aniline with Q1 and subsequent reaction with the GC eluates of mixture 1. During mass-selection of the $93^{+\cdot}$ ion of aniline, Q3 is scanned from 96 to 350 amu in order to avoid scanning over the saturated reactant ion. This chromatogram illustrates the capability to monitor eluates that react in any way with the aniline reactant ion. Many of the chromatographic peaks indicating reactivity with the aniline $N^{+\cdot}$ ion in Figure 5-4a are less intense than the chromatographic peaks produced upon reaction of these electrophiles with the piperidine $N^{+\cdot}$ in Figure 5-1a, even though the mass-selected aniline ion is approximately 7 times more abundant than the piperidine mass-selected ion. The absolute intensities of the mass-selected nucleophile ions are determined by lowering the electron multiplier voltage during the first 30 scans of the chromatogram. The electrophiles may be more reactive with the piperidine $N^{+\cdot}$ ion due to the greater gas-phase basicity (GB) of piperidine (GB = 9.42 eV) compared to aniline (GB = 8.81 eV) (Aue and Bowers, 1979).

Similar to the reactions with the piperidine $N^{+\cdot}$ ion, benzene and cyclohexane (co-elute in peak 7) do not react with the $N^{+\cdot}$ ion of aniline, nor does pentane (peak 2) or propyl chloride (peak 4). In contrast to the reactions with the

piperidine $N^{+\cdot}$ ion, the reactions of allyl isothiocyanate (peak 13) and decane (peak 15) with the aniline $N^{+\cdot}$ ion produce abundant chromatographic peaks, as described below.

The mass spectral data obtained by the reaction of the $93^{+\cdot}$ ion of aniline with the GC eluates in the collision cell are presented in Table 5-4, including the major ions (≥ 0.01 million counts), their structures and their peak areas (in millions). Similar product ions are observed for the reactions with the aniline $N^{+\cdot}$ ion as with the piperidine $N^{+\cdot}$ ion for most of the analytes. Allyl isothiocyanate was observed to be the most reactive analyte with the aniline $N^{+\cdot}$ ion in the chromatogram of Figure 5-4a; however, the most abundant ions in the mass spectrum are the radical molecular ion ($E^{+\cdot}$) and the protonated molecule ($[E+H]^+$) of the electrophile. Two possible mechanisms can be suggested for the production of these electrophile ions. Proton transfer could occur between the allyl isothiocyanate (proton affinity not known) and aniline to form $[E+H]^+$, while the higher proton affinity of piperidine may prevent the formation of this ion. Alternatively, the $[N+H+E]^+$ ion, which is observed to a small extent in the mass spectrum, may undergo unimolecular decomposition or CAD to form the $[E+H]^+$ and $E^{+\cdot}$ ions. Reaction of decane with aniline also produces $E^{+\cdot}$ and $[E+H]^+$ ions, in addition to the $[E-C_2H_5]^+$ and $[E-C_3H_7]^+$ fragment ions, which accounts for the large chromatographic peak in Figure 5-4a.

Table 5-5 compares the gas-phase reactivity of the various equimolar analytes with the radical molecular ion of aniline to mutagenicities (+/-) determined

Table 5-4: The major ions observed in the mass spectra obtained by reaction with the $N^{+\bullet}$ ion of aniline.

Electrophile	MW^a	P^{+b}	E$^{+\bullet}$	[E+H]$^+$	[E-X]$^+$	Others
Allyl isothiocyanate	99	134 (0.02)	99 (1.83)	100 (1.42)	ND	193 (0.05) [N+H+E]$^+$ / 191 (0.05) [N+(E-H)]$^+$
Allyl chloride	76	134 (0.05)	ND^e	ND	ND	106 (0.08)
2,3-dichloropropene	110	168,170 (0.10)	---	---	ND	113 (0.43); 115 (0.14)
Epichlorohydrin	92	150 (----)^c	ND	ND	ND	106 (0.75) [P-C$_2$H$_4$O]$^+$
Allyl bromide	120	134 (0.07)	---	---	ND	106 (0.10)
Allyl iodide	168	134 (0.29)	---	---	ND	106 (0.08)
Acrolein	56	NL^d	ND	ND	ND	113 (0.09) [E$_2$+H]$^+$ / 150 (0.04) [N+H+E]$^+$
Benzyl chloride	126	184 (1.09)	126 (0.35)	127 (0.03)	ND	106 (0.07)
Benzyl bromide	170	184 (0.99)	---	---	ND	106 (0.12)
Propyl chloride	78	136 (----)	ND	---	ND	ND
Propyl bromide	122	136 (0.07)	---	---	ND	ND
Pentane	72	136 (----)	ND	ND	ND	ND
Decane	142	136,150 (----)	142 (0.07)	143 (0.06)	ND	99 (0.74) [E-C$_3$H$_7$$^+$]$^+$ / 113 (0.16) [E-C$_2$H$_5$$^+$]$^+$
Cyclohexane	84	162 (----)	ND	ND	ND	ND
Benzene	78	NL	ND	ND	ND	ND
o-Xylene	106	184 (0.03)	106 (1.83)	107 (0.30)	ND	119 (0.64) [E+CH]$^+$ / 212 (0.22) [N+(E+CH)]$^+$

^{a}molecular weights of most abundant isotope.
^{b}m/z of P$^+$ ion defined as [N+(E-X)]$^+$; peak areas (in millions) in parenthesis.
^{c}ion areas <0.01 million.
^{d}no suitable leaving group.
^{e}m/z is below the first mass scanned (95 amu).

Table 5-5: Comparison of gas-phase reactivities of various analytes with the $N^{+\cdot}$ ion of aniline to Ames test mutagenicities.

Electrophiles	m/z of P^+	Gas-Phase[d] Reactivity	Ames Test[e] Mutagenicity	Mutagenicity References
Allyl isothiocyanate	134	1.0	+	Eder et al., 1982
Allyl chloride	134	2.5	+	Eder et al., 1982
2,3-dichloropropene	168,170	5.0	+	Eder et al., 1982
Epichlorohydrin	150,106[a]	37.5	+	Eder et al., 1982
Allyl bromide	134	3.5	+	Eder et al., 1982
Allyl iodide	134	14.5	+	Eder et al., 1982
Acrolein	150[b]	2.0	+	Eder et al., 1982
Benzyl chloride	184	54.5	+	Eder et al., 1982
Benzyl bromide	184	49.5	NR[f]	
Propyl chloride	136	<0.1	-	Eder et al., 1982
Propyl bromide	136	3.5	-	Eder et al., 1982
Pentane	136	<0.1	NR	
Decane	136,150	<0.1	NR	
Cyclohexane	162	<0.1	NR	
Benzene	---[c]	---	-	Dean, 1985
o-Xylene	184	1.5	-	Dean, 1985

[a] m/z 106 is $[P-C_2H_4O]^+$.
[b] m/z 150 is $[N+H+E]^+$.
[c] no product ion detected above 0.01 million counts.
[d] gas-phase reactivity is the P^+ ion area normalized to P^+ ion area of allyl isothiocyanate.
[e] without metabolic activation.
[f] no literature references found.

by the Ames test (without metabolic activation). The gas-phase reactivity is defined as the product ion areas of the electrophiles normalized to the weakly mutagenic allyl isothiocyanate for ease of comparison. Note that even though allyl isothiocyanate and decane produce unexpectedly large peaks in the chromatogram of Figure 5-4a, the gas-phase reactivities in Table 5-5 are reasonable. Considering the compounds for which references to mutagenicity were found, all of the eight mutagens reacted with the aniline $N^{+\cdot}$ ion in the gas-phase. Acrolein appears to be slightly more reactive with the $N^{+\cdot}$ ion of aniline than with that of piperidine in the gas-phase; however acrolein is more mutagenic than allyl iodide in the Ames test. Also, benzyl chloride and benzyl bromide are significantly more reactive with the $N^{+\cdot}$ ion of aniline than with the $N^{+\cdot}$ ion of piperidine. If the gas-phase reactivity threshold is assigned a value of 1, then two of the four non-mutagens would be classified as non-reactive or weakly reactive with the $N^{+\cdot}$ ion of aniline. The gas-phase reactivities of propyl bromide and o-xylene with aniline appear as false positives in this method. Postulating that cyclohexane and the alkanes compounds would exhibit little or no electrophilicity is in agreement with the observation that pentane, decane and cyclohexane exhibit little if any reactivity in the gas-phase with the $N^{+\cdot}$ ion of aniline.

Reactions with the $[N+H]^+$ Ion of Piperidine

In Chapter 3, the gas-phase reactivity of allyl isothiocyanate, allyl chloride, allyl bromide and allyl iodide with various nucleophile ions of pyridine was

investigated. It was discovered that the mass-selected $[N+H]^+$ ion of pyridine did not react with these electrophiles. However, Figure 5-5 illustrates that the mass-selected $[N+H]^+$ ion (m/z 86) of piperidine does react with the analytes in mixture 1, resulting in qualitatively similar results as reactions with the $N^{+\cdot}$ ion of piperidine. It is not known at the present time why the $[N+H]^+$ ion of piperidine reacts, while the $[N+H]^+$ ion of pyridine does not. It is conceivable that piperidine could have several reactive sites (ring and nitrogen) while pyridine may only have one reactive site. For instance, aniline has been demonstrated to have competitive protonation on the ring and the nitrogen; however, methylation and ethylation occurred predominantly at the nitrogen (Wood et al., 1983). It is also possible that some or all of the protonated piperidine ring opens to form an ion very different in reactivity from protonated pyridine. Studies of structurally similar saturated and unsaturated nucleophiles may aid in understanding the effect of protonation on the gas-phase reactivity of these nucleophiles.

The mass spectra obtained by the reaction of the 86^+ ion of piperidine with the GC eluates in the collision cell are presented in Table 5-6, including the major ions (≥ 0.01 million counts), their structures and their peak areas (in millions). The same product ions are observed as in the reactions with the $N^{+\cdot}$ ion of piperidine, except for $[P+H]^{+\cdot}$ ions which are greater than the ^{13}C contribution of the electrophile. These $[P+H]^{+\cdot}$ ions are formed by reaction of the $[N+H]^+$ ion of piperidine with the neutral electrophile (E) followed by loss of a neutral X radical (equation d). The P^+ ion can occur by the two mechanisms depicted in equations
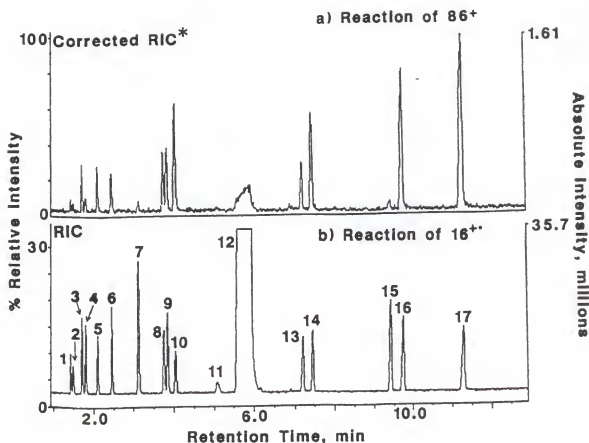
Figure 5-5: Chromatograms obtained by mass-selected reactions of (a) the $[N+H]^+$ ion (86^+) of piperidine and (b) the $16^{+\cdot}$ ion of methane with the following neutral analytes introduced into the collision cell via a GC column: (1) acrolein, (2) pentane, (3) allyl chloride, (4) propyl chloride, (5) propyl bromide, (6) allyl bromide, (7) co-elution of benzene and cylcohexane, (8) 2,3-dichloropropene, (9) allyl iodide, (10) epichlorohydrin, (11) 7-methyl heptane, (12) octane (solvent), (13) allyl isothiocyanate, (14) o-xylene, (15) decane, (16) benzyl chloride, and (17) benzyl bromide. (* RIC minus m/z 169 to 172)

Table 5-6: The major ions observed in the mass spectra obtained by reaction with the [N+H]$^+$ ion of piperidine.

Electrophile	MW	P^{+a}	[P+H]$^+$	[E-X]$^+$	Others
Allyl isothiocyanate	99	126 (0.26)	127 (0.04)	ND^d	99 (0.07) E$^{+\cdot}$, 100 (0.12) [E+H]$^+$
Allyl chloride	76,78	126 (0.38)	127 (0.07)	ND	166 (0.12)
2,3-dichloropropene	110,112	160,162 (0.59)	161,163 (0.05)	ND	124 (0.25) [P-HCl]$^+$
Epichlorohydrin	92	142 (0.11)	143 (---)^b	ND	98 (1.83) [P-C$_2$H$_4$O]$^+$
Allyl bromide	120,122	126 (0.56)	127 (0.09)	ND	166 (0.15)
Allyl iodide	168	126 (1.24)	127 (0.19)	ND	166 (0.13)
Acrolein	56	NL^c	NL	ND	142 (0.11) [P+H+E]$^+$
Benzyl chloride	126,128	176 (2.98)	177 (0.52)	91 (1.15)	
Benzyl bromide	170,172	176 (4.70)	177 (0.64)	91 (1.63)	
Propyl chloride	78,80	128 (0.22)	129 (0.01)	ND	
Propyl bromide	122,124	128 (0.80)	129 (0.08)	ND	
Pentane	72	128 (0.07), 142 (0.02)	129 (---)	ND	
Decane	142	128 (0.01), 142 (0.06)	129 (---), 143 (---)	ND	99 (0.08)
Cyclohexane	84	154 (0.12)	155 (0.01)	ND	
Benzene	78	NL	NL	ND	
o-Xylene	106	176 (0.75)	177 (0.11)	91 (0.87)	190 (0.13), 240 (0.83)

^{a} m/z of P$^+$ ion defined as [N+(E-X)]$^+$; peak areas (in millions) in parenthesis.
^{b} ion area <0.01 million.
^{c} no suitable leaving group.
^{d} m/z is below the first mass scanned (90 amu).

(e). The $[N+H]^+$ can react with the neutral electrophile to produce the P^+ ion with loss of HX or the P^+ ion can occur by unimolecular decomposition or CAD of the $[P+H]^+$ ion.

(d) $[N+H]^+$ + E $\longrightarrow$ $[P+H]^{+\cdot}$ + $X^\cdot$

(e) $[N+H]^+$ + E $\longrightarrow$ P^+ + HX

or $[P+H]^{+\cdot}$ $\longrightarrow$ P^+ + $H^\cdot$

Table 5-7 compares the gas-phase reactivity of the various equimolar analytes with the radical molecular ion of piperidine to mutagenicity determined by the Ames test (without metabolic activation). The gas-phase reactivity is defined as the product ion areas of the electrophiles normalized to the weakly mutagenic allyl isothiocyanate for ease of comparison. Considering the compounds for which references to mutagenicity were found, seven of the eight mutagens were observed to react appreciably (≥ 1.0) in the gas-phase with the $[N+H]^+$ ion of piperidine. Reaction of acrolein with the $[N+H]^+$ ion of piperidine appears a false negative in these reactions as well as in the reactions with the $N^{+\cdot}$ ion piperidine. If the gas-phase reactivity threshold is assigned a value of 1.0, then two of the four non-mutagens would be classified as non-reactive or weakly reactive with the $[N+H]^+$ ion of piperidine. The gas-phase reactivities of o-xylene and propyl bromide are false positives in the reactions with the $[N+H]^+$ and the $N^{+\cdot}$ of

Table 5-7: Comparison of gas-phase reactivities of various analytes with the $[N+H]^+$ ion of piperidine to Ames test mutagenicities.

Electrophiles	m/z of P^+ and $[P+H]^{+\cdot}$	Gas-Phase[d] Reactivity	Ames Test[e] Mutagenicity	Mutagenicity References
Allyl isothiocyanate	126,127	1.0	+	Eder et al., 1982
Allyl chloride	126,127	2.1	+	Eder et al., 1982
2,3-dichloropropene	160,162 161,163	2.3	+	Eder et al., 1982
Epichlorohydrin	142,98[a]	6.5	+	Eder et al., 1982
Allyl bromide	126,127	2.2	+	Eder et al., 1982
Allyl iodide	126,127	4.8	+	Eder et al., 1982
Acrolein	142[b]	0.4	+	Eder et al., 1982
Benzyl chloride	176,177	11.7	+	Eder et al., 1982
Benzyl bromide	176,177	17.8	NR[f]	
Propyl chloride	128,129	0.8	-	Eder et al., 1982
Propyl bromide	128,129	2.9	-	Eder et al., 1982
Pentane	128,142	0.3	NR	
Decane	128,142	0.2	NR	
Cyclohexane	154,155	0.4	NR	
Benzene	---[c]	<0.1	-	Shimizu et al., 1983 Dean, 1985
o-Xylene	176,177	2.9	-	Busk, 1979

[a]m/z 98 is $[P-C_2H_4O]^+$.
[b]m/z 142 is $[N+H+E]^+$.
[c]no product ion detected above 0.01 million counts.
[d]gas-phase reactivity is the P^+ ion area normalized to P^+ ion area of allyl isothiocyanate.
[e]without metabolic activation.
[f]no literature references found.

piperidine. Overall, the gas-phase reactions with the $[N+H]^+$ ion of piperidine result in the same +/- classification of chemicals as the gas-phase reactions of the $N^{+\cdot}$ ion.

<div align="center">
Electrophile Ion/Nucleophile Neutral Reactions
in the Collision Cell
</div>

Experimental

All experiments were performed on a Finnigan MAT TSQ 70 equipped with a Varian 3400 gas chromatograph. The electrophiles were introduced into the ion source via a GC column and ionized under electron ionization (EI) conditions. All experiments were performed at an emission current of 200 μA, electron energy of 70 eV, a manifold temperature of 100°C, and ion source temperatures of 170°C.

Gas chromatography was carried out on a J & W Scientific DB-5 (20 m long, 0.178 mm i.d., 0.4 μm film thickness) capillary column in the split mode (SR=100:1) with helium carrier gas at an inlet pressure of 5 psig. The GC oven was temperature programmed from 35°C to 150°C at 10°C/min after an initial hold time of 1.5 minutes. The injection port and TSQ 70 transfer line were held at a temperature of 200°C. One μL injections were made of three equimolar mixtures (59.6 nmoles) prepared in octane. The contents of the three mixtures are listed in Table 5-1, along with the ionization energy (IE) of each analyte.

As the complexity of the mixtures increases, it becomes increasingly difficult to mass-select one m/z of the analytes (e.g., $E^{+\cdot}$) as a function of retention time. Instead, as each analyte elutes into the ion source, all ions of the analyte were passed simultaneously into the collision cell by setting Q1 to pass all ions above 30 amu (rf only). The analyte ions were reacted with the neutral nucleophile in the collision cell at a nucleophile pressure of approximately 2.5 mtorr, as measured by a Granville Phillips convectron gauge. The product ions (P^+) were mass analyzed with Q3 scanned from 30 to 350 amu in 0.25 seconds at an electron multiplier voltage of -1200 V.

The mass spectrometer was mass-calibrated with FC43, then tuned for ion-molecule reactions in the collision cell. Allyl chloride was constantly introduced into the ion source with a Negretti fine-metering valve (Hampshire, England). The collision energy, collision cell rf potential, and potential on the lenses immediately before and following the collision cell were optimized for maximum transmission of the reactant ion ($E^{+\cdot}$) and the product ion (120^+).

Reactions with Piperidine

Electrophile ion reactions as implemented here are not as useful for screening complex environmental mixtures for potential carcinogens because all the analytes will produce a chromatographic peak whether or not reaction with the nucleophile occurs. The analytes elute by GC into the ion source and all ions of m/z >30 (i.e., molecular and fragment ions) produced in the ion source are passed

simultaneously into the collision cell to react with the neutral piperidine. Thus, the chromatogram depicted in Figure 5-6 is relatively uninformative in comparison to that obtained for nucleophile ion reactions (Figure 5-1a). The chromatographic peaks observed in Figure 5-6 consist of analyte ions from the ion source, as well as any ions produced by reaction with piperidine. Due to the limited information attainable from the chromatograms of electrophile ion reactions, those for mixtures 2 and 3 are not shown.

The mass spectral data obtained by the reaction of the analyte ions with piperidine in the collision cell are presented in Table 5-8, including the major ions (≥ 0.01 million counts, electrophile ions not included), their structures and their peak areas (in millions). Similar ions are observed as with the nucleophile ion reactions, except for a few notable differences. Most of the mass spectra are dominated by the $[N+H]^+$ (m/z 86) and $[N_2+H]^+$ (m/z 171) ions of piperidine produced by proton transfer from the analyte ions. Due to the large concentration of piperidine neutrals present in the collision cell, the $[N_2+H]^+$ ion undergoes further reaction to form the $[N_3+H]^+$ ion (m/z 256, not shown in table). Also, a 261^+ ion is observed in the mass spectra of the analytes which fragment to form the $C_7H_7^+$ ion, such as benzyl chloride, benzyl bromide, ethyl benzene, and o-xylene. It is postulated that the 261^+ ion produced upon reaction with neutral piperidine corresponds to the $[N_2+(E-X)]^+$ ion. This ion is not observed in the piperidine $N^{+\cdot}$ ion reactions for these analytes mentioned above; however the $[N_2+(E-X)]^+$ ion (m/z 275) is observed in both piperidine $N^{+\cdot}$ ion and electrophile ion reactions for benzoyl chloride. The reactions of benzoyl chloride ions would involve the $[C_7H_5O]^+$
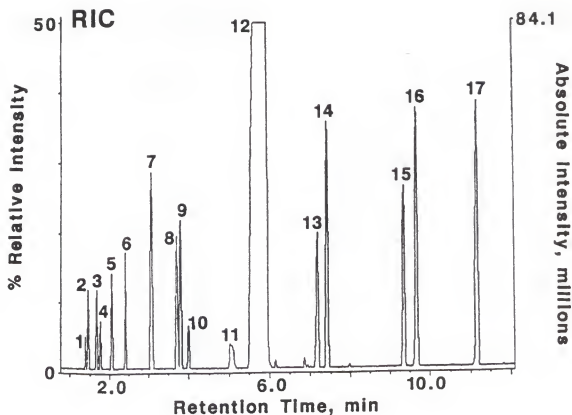
Figure 5-6: Chromatogram obtained by reactions of the analyte ions introduced into the ion source via a GC column with neutral piperidine in the collision cell. The analytes (mix 1) are: (1) acrolein, (2) pentane, (3) allyl chloride, (4) propyl chloride, (5) propyl bromide, (6) allyl bromide, (7) co-elution of benzene and cylcohexane, (8) 2,3-dichloropropene, (9) allyl iodide, (10) epichlorohydrin, (11) 7-methyl heptane, (12) octane (solvent), (13) allyl isothiocyanate, (14) o-xylene, (15) decane, (16) benzyl chloride, and (17) benzyl bromide.

Table 5-8: The major ions observed in the mass spectra obtained by reaction with the analyte ions with neutral piperidine.

Electrophiles	MW[a]	P[+b]	[N+H][+]	[N2+H][+]	Others
Allyl isothiocyanate	99	126 (0.16)	(26.2)	(66.0)	
Allyl chloride	76	126 (0.35)	(5.13)	(46.0)	
2,3-dichloropropene	110	160, 162 (1.63)	(17.2)	(44.8)	124 (1.46) [P-HCl]+
Epichlorohydrin	92	142 (----)[c]	(2.25)	(13.6)	98 (3.96) [P-C2H4O]+
Allyl bromide	120	126 (0.77)	(11.5)	(34.1)	
Allyl iodide	168	126 (1.11)	(21.4)	(47.0)	
Acrolein	56	NL[d]	(6.60)	(5.16)	
Benzyl chloride	126	176 (46.9)	(39.2)	(76.9)	261 (0.65) [N+(E-X)]+
Benzyl bromide	170	176 (52.6)	(39.0)	(80.2)	261 (0.60) [N+(E-X)]+
Propyl chloride	78	128 (----)	(1.81)	(11.9)	
Propyl bromide	122	128 (1.08)	(7.50)	(26.3)	
t-Butyl bromide	136	142 (0.04)	(7.75)	(30.6)	
sec-Butyl bromide	136	142 (1.54)	(8.07)	(35.5)	
n-Butyl bromide	136	142 (1.19)	(8.39)	(40.9)	
t-Butyl iodide	184	142 (0.23)	(30.5)	(53.8)	
sec-Butyl iodide	184	142 (2.86)	(31.3)	(89.3)	
n-Butyl iodide	184	142 (1.22)	(12.1)	(70.6)	
Nonane	128	128 NA[e]	(19.4)	(53.1)	
	142	142 NA			

Table 5-8: continued

Electrophiles	MW[a]	P[+b]	[N+H]$^+$	[N$_2$+H]$^+$	Others
Decane	142	128 NA 142 NA	(49.2)	(70.0)	
Cyclohexane	84	154 (0.65)	(40.8)	(58.9)	
Benzene	78	NL	(40.8)	(58.9)	
Ethyl benzene	106	176 (25.2)	(14.0)	(52.3)	190 (0.33) 261 (1.66) [N$_2$+(E-X)]$^+$
Chlorobenzene	116	162 (0.16)	(12.0)	(54.2)	
Bromobenzene	156	162 (0.25)	(16.0)	(59.7)	
m-Difluorobenzene	114	95 (0.06)	(23.9)	(48.3)	
m-Dichlorobenzene	146	196,198 (0.20)	(51.3)	(86.1)	
o-Xylene	106	176 (28.7)	(31.2)	(58.9)	190 (2.35) 261 (0.51)
Styrene	104	NL	(12.9)	(55.8)	189 (0.24) [N+E]$^+$ 274 (0.06) [N$_2$+E]$^+$
Benzoyl chloride	140	190 (1.39)	(15.0)	(61.4)	275 (0.08) [N$_2$+(E-X)]$^+$

[a] molecular weight of most abundant isotope.
[b] m/z of P$^+$ ion defined as [N+(E-X)]$^+$; peak area (in millions) in parenthesis.
[c] ion area <0.01 million.
[d] no suitable leaving group.
[e] product ions coincide with the electrophile ions.

species ($[E-X]^+$) rather than the $[C_7H_7]^+$ species. In addition to the $[N_2+(E-X)]^+$ ion, the reaction of the benzoyl chloride ions with neutral piperidine produces the $[N+(E-X)]^+$ (m/z 190) which was not observed in the piperidine $N^{+\cdot}$ ion reactions.

The expected product ions (128^+ and 142^+) of the nonane and decane reactions with neutral piperidine coincide with the radical molecular ions of nonane (128^+) and decane (142^+) and a fragment ion of decane (128^+, $[E-CH_2]^+$). Thus, no determination of product ion formation can be determined for these compounds.

Table 5-9 compares the gas-phase reactivity of the various analyte ions with neutral piperidine in the collision cell to mutagenicity (+/-) determined by the Ames test (without metabolic activation). The gas-phase reactivity is defined as the product ion area of the electrophiles normalized to the weakly mutagenic allyl isothiocyanate for ease of comparison. Considering the compounds for which references to mutagenicity were found, seven of the eight mutagens were observed to react in the gas-phase with the neutral piperidine in the collision cell. Reaction of acrolein with neutral piperidine appears as a false negative in these electrophile ion reactions, as well as in the nucleophile ion reactions with piperidine. Benzyl chloride and benzyl bromide reactions are much more reactive in these electrophile ion reactions than the nucleophile ion reactions. The transmission into the collision cell of the $C_7H_7^+$ ion produced in the ion source, could be the reason for the increased reactivity in the electrophile ion reactions of benzyl chloride and benzyl bromide.

Table 5-9: Comparison of gas-phase reactivities of various analyte ions with neutral piperidine to Ames test mutagenicities.

Electrophiles	m/z of P$^+$	Gas-Phase[g] Reactivity	Ames Test[h] Mutagenicity	Mutagenicity References
Allyl isothiocyanate	126	1.0	+	Eder et al., 1982
Allyl chloride	126	2.2	+	Eder et al., 1982
2,3-dichloropropene	160,162	10.2	+	Eder et al., 1982
Epichlorohydrin	142,98[a]	24.8	+	Eder et al., 1982
Allyl bromide	126	4.8	+	Eder et al., 1982
Allyl iodide	126	6.9	+	Eder et al., 1982
Acrolein	142[b]	<0.1	+	Eder et al., 1982
Benzyl chloride	176	293.2	+	Eder et al., 1982
Benzyl bromide	176	329.6	NR[i]	
Propyl chloride	128	<0.1	-	Eder et al., 1982
Propyl bromide	128	6.8	-	
t-Butyl bromide	142	0.3	NR	
sec-Butyl bromide	142	9.6	NR	
n-Butyl bromide	142	7.4	NR	
t-Butyl iodide	142	1.4	NR	
sec-Butyl iodide	142	17.9	NR	
n-Butyl iodide	142	7.6	NR	
Pentane	128,142	1.9	NR	
Nonane	142	4.1	NR	
Decane	NA[c]	NA	NR	
Cyclohexane	154	4.1	NR	
Benzene	---[d]	<0.1	-	Dean, 1985
Ethyl benzene	176	157.8	-	Dean et al., 1985
Chlorobenzene	162	1.0	-	Shimizu et al., 1983
Bromobenzene	162	1.6	-	Shimizu et al., 1983
m-Difluorobenzene	95	0.4	-	Shimizu et al., 1983
m-Dichlorobenzene	196,198	1.3	-	Shimizu et al., 1983
o-Xylene	176	179.4	-	Dean, 1985
Styrene	189[e]	1.5	-	Busk, 1979
Benzoyl chloride	190,275[f]	9.2	-	Yasuo et al., 1978

[a] m/z 98 is [P-C$_2$H$_4$O]$^+$.
[b] m/z 142 is [N+H+E]$^+$.
[c] product ions coincide with the electrophile ions.
[d] no product ion detected above 0.01 million counts.
[e] m/z 189 is [N$_2$+E]$^+$.
[f] m/z 275 is [N$_2$+(E-X)]$^+$.
[g] gas-phase reactivity is the P$^+$ ion area normalized to P$^+$ ion area of allyl isothiocyanate.
[h] without metabolic activation.
[i] no literature references found.

If the gas-phase reactivity threshold is assigned a value of 1.0, then only three of the eleven non-mutagens would be classified as non-reactive or weakly reactive with neutral piperidine. As in the nucleophile ion reactions, the gas-phase reactivities of ethyl benzene, o-xylene, and benzoyl chloride with piperidine are definite false positives in this method. Many of the non-mutagens (e.g., chlorobenzene, bromobenzene, and m-dichlorobenzene) are weakly reactive as electrophile ions with the neutral piperidine in the collision cell. In the case of ethyl benzene, o-xylene, and styrene, the formation of the $C_7H_7^+$ fragment ion in the ion source may be the cause of the high gas-phase reactivity. The non-mutagens, chlorobenzene, bromobenzene, m-difluorobenzene, m-dichlorobenzene, and styrene are slightly more reactive in the gas-phase electrophile ion reactions than the weak mutagen allyl isothiocyanate.

Conclusions

The ability of mass-selected nucleophile ion reactions to produce chromatograms which predict mutagenicity or non-mutagenicity has been demonstrated. In the same experiment, alternate mass-selection of the $16^{+\cdot}$ ion of methane yields quantitative information on all the analytes in the GC mixtures. In contrast, the chromatograms produced during electrophile ion reactions as implemented here are not as informative as nucleophile ion reactions, because chromatographic peaks will be observed for all analytes whether or not reaction

with the neutral nucleophile occurs. Furthermore, the transmission of all ions greater than m/z 30 into the collision cell means that the observed ions reflect the reactivity of not only the electrophile molecular ion ($E^{+\cdot}$), but also that of the EI-produced fragment ions, which may be of greater abundance than the molecular ion.

Acrolein is consistently found to be the only false negative of the analytes studied in these gas-phase nucleophile ion and electrophile ion reactions. Significantly more false positives are observed in the gas-phase reactions, especially reactions of ethyl benzene and o-xylene. The electrophile ion reactions appear to result in more false positives, presumably due to the variety of ions other than the molecular ion (produced by EI in the ion source) which are allowed to interact in the collision cell with the neutral nucleophile. False positives are more tolerable in terms of screening for risk assessment than are false negatives, since positives are investigated further. Studies involving more chemicals, especially classes of compounds, will aid in the understanding of the types of reactions occurring as well as the false positive and negatives obtained.

In addition, understanding the types of reactions occurring may aid in choosing the appropriate nucleophile. Of the limited nucleophiles studied so far (pyridine, piperidine and aniline), piperidine appears to be the most appropriate choice of nucleophile based on limited competitive reactions and reasonable sensitivity. Preliminary data suggest that the gas-phase basicity of the nucleophile will affect the extent of product ion formation. Reactions with pyridine have been

demonstrated to be adversely affected by charge exchange reactions in cases where the IE of the analyte is lower than the IE of pyridine. Reactions with aniline are characterized by low sensitivity, thus weak mutagens may not be detected.

Conceptually, it should be possible to identify the molecular ion early in an analyte's GC peak via a Q1 mass spectrum, and then mass select this ion with Q1 for the balance of the GC peak and monitor its reactivity with the neutral nucleophile in Q2. In practice, this would require development of a rapid and efficient algorithm to identify the radical molecular ion of the eluate in the Q1 mass spectrum, as well as the software to permit rapidly switching to mass selection of that ion with Q1 and scanning Q3 to detect the product ions. As noted in Chapter 3, the presence of a collision gas in Q2 will have little effect on the Q1 spectrum. However, identification of the molecular ion of compounds which fragment extensively under EI conditions (i.e., little or no $M^{+\cdot}$ remains) or compounds which co-elute may present difficulties. Note that current software on the TSQ 45 and TSQ 70 would not support such rapid decision making on the capillary GC time scale.

A more practical (but labor-intensive) approach would be to inject the sample and acquire normal EI mass spectra. Inspection of each EI mass spectrum would permit assignment of the molecular ions. A second injection of the sample would permit determination of the reactivity of each radical molecular ion with the nucleophile by switching Q1 to pass the appropriate m/z in each retention time window. Clearly the requirement for two injections of each sample

combined with manual inspection of the first chromatogram to establish conditions for the reactivity experiment makes this approach unattractive for screening complex environmental samples. The strategy employed here, while less informative than either of the two approaches described above, offers the advantage of being possible with current software.

In-depth studies of the reaction mechanisms and structural information on the ions formed in these collision cell reactions may aid in the understanding of the false positives and negatives. Further confirmation of the ions formed in these reactions via their collisionally activated decomposition (i.e., MS/MS/MS) is not possible on the triple quadrupole mass spectrometer used. The use of quadrupole ion trap mass spectrometers (QITMS) or Fourier transform mass spectrometers (FTMS) with MS^n capabilities may aid in structure elucidation of the ions produced during these mass-selected ion-molecule reactions.

CHAPTER 6
CONCLUSIONS AND FUTURE WORK

Conclusions

The ability to detect product ions of ion-molecule reactions between nucleophiles and electrophiles has been demonstrated in the ion source and the collision cell of a triple quadrupole mass spectrometer (TQMS). The ability to screen mixtures for gas-phase reactivity between nucleophiles and potential carcinogens has been demonstrated.

Ion-molecule reactions between adenine and benzoyl chloride performed in the ion source of a TQMS produce complicated mass spectra. The mass spectra obtained by ion source reactions are difficult to interpret since it is not known which form of which species (e.g. $N^{+\cdot}$, $[N+H]^+$, $E^{+\cdot}$, $[E+H]^+$, $[E-X]^+$ or neutral) is reacting. However, the product ions of ion-molecule reactions in the ion source can be further characterized by tandem mass spectrometry (MS/MS). The analysis of complex environmental mixtures would be complicated in the ion source since every analyte produces a chromatographic peak which must be evaluated. If the mixture components are unknown, identifying a possible product ion in the complicated mass spectra would not be an easy task.

Ion-molecule reactions in the collision cell are characterized by simpler mass spectra and ease of interpretation since only one ion is mass-selected to react with the neutral species in the collision cell. Studies have shown that qualitatively similar mass spectra are obtained by mass-selected electrophile ion reactions and mass-selected nucleophile ion reactions. In both electrophile ion and nucleophile ion reactions, the product ions obtained by the reaction of allyl halides with pyridine optimize at low collision energies of 2 to 3 eV. Detection limits in the low picogram (femtomole) range are obtained for the reaction of allyl chloride and allyl iodide with pyridine in the selected reaction monitoring mode (SRM). Full scan limits of detection for the product ions of these reactions are observed at quantities approximately five times higher than in the SRM mode.

Pressure optimization studies revealed that competitive reactions, especially charge exchange, can have a significant effect on product ion formation in nucleophile ion reactions. Thus, the choice of nucleophile is an important factor in these ion-molecule reactions. Typical requirements are that the nucleophile be reasonably volatile (for ease of introduction) and possess an ionization energy lower than the electrophiles to be analyzed to reduce the occurrence of competitive reactions. The gas-phase basicity of the nucleophile will also affect the extent of interaction between the nucleophile and electrophile. Preliminary studies suggest that nucleophiles with higher gas-phase basicities may react with the electrophiles to a larger extent with the electrophiles.

On-line chromatographic introduction of the electrophiles allows for the rapid analysis of complex environmental mixtures; thus, this technique offers

enhanced speed and sensitivity over current methods (e.g., Ames test) for detecting potential carcinogens. Mass-selected nucleophile ion reactions are particularly attractive for use as an environmental screening technique because only those GC eluates which react with the nucleophile ion will give rise to chromatographic peaks. Thus, the number of chromatographic peaks in a complex mixture which need further evaluation for potential carcinogenicity is significantly reduced compared to GC/MS.

Electrophile ion reactions are not as adaptable for environmental screening because all the GC eluates give rise to chromatographic peaks whether or not reaction with the neutral nucleophile occurs. Also, these reactions are limited by the necessity of knowing the sample components in order to mass-select the appropriate ion. However, these electrophile ion reactions can be utilized to further understand the gas-phase interactions between nucleophile and electrophiles. Rather than mass-selecting only one ion of the electrophile, all of the electrophile ions produced in the ion source can be passed into the collision cell to react with the neutral nucleophile. However, passing all of the electrophile ions into the collision cell adds ambiguity to the source of the product ions formed.

Future Work

Currently, the mass-selected nucleophile ion reactions are limited to electrophiles with boiling points below ≈200°C for two reasons. First, the last 7 to 8 cm of the GC column from the edge of the vacuum manifold to the collision

cell is heated only by the manifold heaters; its temperature is not independently controlled. This problem could be alleviated by resistively heating the portion of the GC column inside the vacuum chamber separately from that outside of the vacuum chamber. The whole column cannot be heated to a uniform temperature with one circuit due to the differences in the rate of thermal loss at atmosphere and at vacuum. Also, the nucleophile ion reactions are limited to volatile electrophiles because the mass spectrometer cannot be operated above a manifold temperature (i.e., collision cell temperature) of 100°C due to temperature limits of the electron multiplier and the glass-mounted quadrupole mass filters. The collision cell could be heated independently of the manifold temperature; however, care must be taken to thermally isolate the quadrupole mass analyzers on either side of the collision cell.

Mass-selected electrophile ion reactions are not limited by the volatility of the electrophile since the entire column length is heated and the ion source is heated to 170°C. Electrophile mixtures not amenable to GC introduction could be separated by liquid chromatography (LC) and introduced into the ion source by traditional LC/MS interfaces such as particle beam. Note that the introduction of the nucleophile into the collision cell requires that it be reasonably volatile.

In Chapter 4, brief mention was made of the interactive effect of lens voltage and collision energy on the formation of the product ions in the collision cell. Future studies using computer simulations to model the potential fields in and around the collision cell could increase our understanding of what is occurring. The effect of helium carrier gas introduced via the GC column into the collision cell

is another important factor which warrants further investigation. Helium may buffer the ions in the collision cell causing increased sensitivity; however, high helium pressures may cause collisionally activated decomposition (CAD) of the product ions. The extent of CAD may depend on the stability of the product ion; thus excess helium in the collision cell could alter the relative gas-phase reactivities of the electrophiles.

Development of these ion-molecule reactions as an environmental screening technique requires analysis of an extensive set of electrophiles with appropriate nucleophiles. Currently, work is underway in our laboratory to develop methods to react electrophiles with actual DNA bases, nucleosides, nucleotides or even oligonucleotides. The false positives and false negatives need to be characterized over a wide range of carcinogens and non-carcinogens. However, presently the technique is limited to direct-acting carcinogens which are a small portion of the total number of carcinogens. Off-line metabolic activation of the electrophiles with the S9 mix (rat liver) traditionally used in the Ames test could be investigated. Another alternative is on-line activation by use of electrochemical oxidation or immobilized enzymatic reactors. Previous work has demonstrated the capability to assess the metabolic reaction pathways of pyrimidines and purines by electrochemical and enzymatic oxidation on-line with thermospray (TSP) MS/MS (Volk et al., 1988).

Future work in our group includes development of LC techniques using a particle beam interface on a quadrupole ion trap mass spectrometer (QITMS). Once the LC/QITMS is developed, metabolic activation of the pro-carcinogen could

be investigated on-line by the previously mentioned electrochemical or enzymatic oxidation. Transport of the potential carcinogen into the cell membrane could be estimated by octanol/water partition coefficients (K_{ow}) obtained with the LC/QITMS system.

Performing ion-molecule reactions in the QITMS offers several advantages over triple quadrupole mass spectrometers (TQMS). The most obvious advantage is the capability to perform MS^n on the reaction products with the QITMS to obtain additional structure information. In the TQMS, switching between $N^{+\cdot}$ ion and $E^{+\cdot}$ ion reactions requires relocation of the GC column - into the GC for nucleophile ion reactions and into the ion source for electrophile ion reactions. This problem could be circumvented on the TQMS by using two GC columns and two injection ports. Switching between $N^{+\cdot}$ ion and $E^{+\cdot}$ ion reactions on the QITMS is simply a matter of altering the scan function to mass-select either the $N^{+\cdot}$ or $E^{+\cdot}$ ion. Finally, the ability to mass select and then store the ion of interest for a variable reaction time with the QITMS could provide kinetics data (profiles of changes in the reactant ion and product ion intensities as a function of reaction time) on these gas-phase ion molecule reactions. The kinetics data obtained with the QITMS may aid in understanding results obtained with the TQMS.

The major disadvantage of performing these reactions in the QITMS is the inability to spatially separate the neutrals from the ions. Both the electrophile and nucleophile neutrals will be present in the trap to react with the mass-selected reactant ion which could increase the occurrence of competitive or side reactions. The incorporation of off-axis ion injection into the quadrupole ion trap could help

overcome this limitation (Pedder and Yost, 1989; Nourse and Cooks, 1990). Off-axis ion injection (with a differentially pumped system) of the electrophile ions into the ion trap permits spatial separation of the nucleophile and electrophile neutrals.

LITERATURE CITED

Aberth, W.; Straub, K.W.; Burlingame, A.L. Anal. Chem., 1982, **54**, 2029-2034.

Agarwal, S.C.; Van Duren, B.L.; Solomon, J.J.; Kline, S.A. Environ. Sci. Technol., 1980, **14**, 1249-1253.

Ames, B.N. Cancer, 1984, **53**, 2034-2040.

Ames, B.N., McCann, J.; Yamasaki, E. Mutat. Res., 1975, **31**, 347-364.

Ashby, J. and Tennant, R.W. Mutat Res., 1988, **204**, 17-115.

Aue, D.H. and Bowers, M.T. In: ed. Bowers, M.T. Gas Phase Ion Chemistry, Vol. 2, Academic Press, New York, 1979, 2-51.

Bannasch, P.; Griesemer, R.A.; Anders, F.; Becker, R.; Cabral, J.R.; Della Porta, G.; Feron, V.J.; Henschler, D.; Ito, N.; Kroes, R.; Magee, P.N.; McKnight, B.; Mohr, W.; Montesano, R.; Napalkov, N.P.; Nesnow, S.; Pegg, A.E; Rao, G.N.; Turusov, V.S.; Wahrendorf, S.; Wilbourn, J. In: eds., Montesano, R.; Bartsch, H.; Vainio, H.; Wilbourn, J.; Yamasaki, H. Long Term and Short Term Assays for Carcinogenesis: A Critical Appraisal, IARC Scientific Publication, Lyons, France, 1986, 10-83.

Barrett, J.C. In: ed. Barrett, J.C. Mechanisms of Environmental Carcinogenesis, Vol. 1, CRC Press, Boca Raton, Florida, 1987a, 1-16.

Barrett, J.C. In: ed. Barrett, J.C. Mechanisms of Environmental Carcinogenesis, Vol. 1, CRC Press, Boca Raton, Florida, 1987b, 135.

Barrett, J.C. and Elmore, E. In: eds., Flamm, W.G. and Lorentzen, R.J. Advances in Modern Environmental Toxicology, Vol. 12, Princeton, New Jersey, 1985, 171-206.

Bartsch, H. Mutat. Res., 1976, **38**, 177-190.

Bone, L.I. and Futrell, J.H. J. Chem. Phys., 1967, **46**, 4084.

Borman, S. C & E News, 1990, **70**, 20-23.

Boutwell, R.K. Models, Mechanisms and Etiology of Tumor Promotion, IARC, Lyons, France, 1984, 3-12.

Budzikiewicz, H. and Busker, E. Tetrahedron, 1980, **36**, 255-266.

Budzikiewicz, H.; Laufenberg, G.; Brauner, A. Org. Mass Spectrom., 1985, **20**, 65-67.

Burinsky, D.J. and Campana, J.E. Org. Mass Spectrom., 1988, **23**, 613-619.

Burinsky, D.J.; Campana, J.E.; Cooks, R.G. Int. J. Mass Spectrom. Ion Proc., 1984, **62**, 303-315.

Busk, L. Mutat. Res., 1979, **67**, 201-208.

Buzzi, R. and Würgler, E.E. Mutat. Res., 1990, **234**, 269-288.

Chen, A.M. and Carlson, R.E. Anal. Chem., 1981, **53**, 1001-1006.

Clayson, D.B. Chemical Carcinogenesis, Little, Brown and Company, Boston, 1962, 5.

Clayson, D.B. Mutat. Res., 1980, **75**, 205-213.

Colburn, N.H; Vorder Bruegge, W.F.; Bates, J.; Yuspa, S.H. In: eds., Slaga, T.J.; Sivak, A.; Boutwell, R.K. Carcinogenesis, Raven Press, New York, 1978, 257-271.

Crain, P.F. and McCloskey, J.A. Anal. Biochem., 1983, **132**, 124-131.

Crow, F.W.; Tomer, K.B.; Gross, M.L.; McCloskey, J.A.; Bergstrom, D.E. Anal Biochem., 1984, **139**, 243-262.

Davoli, E; Cerny, R.L.; Gross, M.L. Adv. Mass Spectrom., 1989, **11A**, 268.

Dean, B.J. Mutat. Res., 1985, **154**, 153-181.

Dizdaroglu, M. Anal. Biochem., 1985, **144**, 593-603.

Eder, E.; Henschler, D.; Neudecker, T. Xenobiotica, 1982a, **12**, 831-848.

Eder, E.; Neudecker, T.; Lutz, D.; Henschler, D. Chem. Biol. Interactions, 1982b, **38**, 303-315.

Everson, R.B.; Randerath, E.; Santella, R.M.; Cefalo, R.C.; Avitts, T.A.; Randerath, K. Science, 1986, **231**, 54-57.

Fetterolf, D.D. Ph.D. Dissertation, University of Florida, April, 1983.

Fetterolf, D.D.; Yost, R.A.; Eyler, J.R. Org. Mass Spectrom., 1984, **19**, 104-150.

Field, F.H. Acc. Chem. Res., 1968, **1**, 42-49.

Munson, M.S.B. and Field, F.H. J. Am. Chem. Soc., 1966, **88**, 2621.

Foltz, R.L. Proceedings of the 31st ASMS Conference on Mass Spectrometry and Allied Topics, 1983, 454-455.

Gothe, R.; Calleman, C.J.; Ehrenberg, L.; Wachtmeister, C. A. Ambio, 1974, **3**, 234-236.

Gupta, R.C.; Reddy, M.V.; Randerath, K. Carcinogenesis, 1982, **3**, 1081-1092.

Hail, M.E. Ph.D. Dissertation, University of Florida, May 1989.

Hail, M.E.; Berberich, D.W.; Yost. R.A. Anal. Chem, 1989, **61**, 1874-1879.

Hansch, C. and Fujita, T. J. Am. Chem. Soc., 1964, **86**, 1616-1626.

Hardin, E.D.; Fan, T.P.; Blakely, C.R.; Vestal, M.L. Anal. Chem., 1984, **56**, 2-7.

Harrison, A.G. Chemical Ionization Mass Spectrometry, CRC Press, Boca Raton, Florida, 1983, 12-22.

Hattox, S.E.; and McCloskey, J.A. Anal. Chem., 1974, **46**, 1378-1383.

Hermens, J.; Busser, F.; Leeuwanch, P.; Musch, A. Toxicol. Environ. Chem., 1985, **9**, 219-236.

IARC. Monographs on the Evalution of the Carcinogenic Risk of Chemicals to Humans, vol. 29, 1982, 49.

ICPEMC. (International Commission for Protection Against Environmental Mutagens and Carcinogens), Mutat. Res., 1982, **99**, 73-91.

Isern-Flecha, I.M. Ph.D. Dissertation, Purdue Univeristy, 1986.

Isern-Flecha, I; Cooks R.G.; Wood, K.V. Int. J. Mass Spectrom. Ion Proc., 1984, **62**,

73-87.

Johnson, J.V. and Yost, R.A. Anal. Chem., 1985, **57**, 758A-768A.

Johnson, J.V. and Yost, R.A. Proceedings of the 34th ASMS Conference on Mass Spectrometry and Allied Topics, 1986, 521-522.

Kier, L.D.; Yamasaki, E.; Ames, B.N. Proc. Nat. Acad. Sci. USA, 1974, **71**, 4195-4163.

Klopman, G. and Raychaudhury, C. J. Computat. Chem., 1988, **9**, 232-243.

Könemann, H. Toxicology, 1981, **19**, 209-221.

Lambert, B.; Chu, E.H.Y.; DeCarli, L.; Ehling, U.H.; Evans, H.J.; Hayashi, M.; Thilly, W.G.; Vainio, H.; In: eds., Montesano, R.; Bartsch, H.; Vainio, H.; Wilbourn, J.; Yamasaki, H. Long Term and Short Term Assays for Carcinogenesis: A Critical Appraisal, IARC Scientific Publication, Lyons, France, 1986, 167-243.

Laurier, C.; Tatematsu, M.; Rao, P.M.; Rajalakshm, S.; Sarma, D.S.R. Cancer Res., 1984, **44**, 2186-2191.

Lawson, A. M.; Stillwell, R.N.; Tacker, M.M.; Tsuboyama, K.; McCloskey, J.A. J. Am. Chem. Soc., 1971, **93**, 1014-1023.

Lias, S.G.; Bartmess, J.E.; Liebman, J.F.; Holmes, J.L.; Levin, R.D.; Mallard, W.G. J. of Phys. and Chem. Reference Data, ed. Lide, D.R. Jr., 1988, **17**, Supplement 1.

Lipnick, R.L. Environ. Toxicol. Chem., 1989, **8**, 1-12.

Lohman, P.H.M. In: eds., Bartsch, H.; Hemminki, K.; O'Neill, I.K. Methods for Detecting DNA Damaging Agents in Humans: Application in Cancer Epidemiology and Prevention, IARC Scientific Publications, Lyons, France, 1988, 13-20.

Lu, F.C. Regul. Toxic. Pharm., 1983, **3**, 121-132.

Malling H.V. Mutat. Res., 1971, **13**, 425-429.

McCann, J.; Choi, E.; Yamasaki, E.; Ames, B.N. Proc. Nat. Acad. Sci. USA, 1975, **72**, 5135-5139.

McCloskey, J.A. In: eds., Gaskell, S.J. Mass Spectrometry in Biomedical Research, John Wiley & Sons, New York, 1986, 75-95.

McLafferty, F.W. Science, 1981, **214**, 280-287.

Miller, D.L. and Gross, M.L. J. Am. Chem. Soc., 1983, **105**, 3783-3788.

Miller, J.A. Cancer Res., 1970, **30**, 559-576.

Miller, J.A. and Miller, E.C. In: eds., Hiatt H.H.; Watson J.D.; Winsten J.A., Origins of Human Cancer, Cold Spring Harbor, New York, 1977, 605-627.

Mondal, S.; Brankow, D.W.; Heidelberger, C. Cancer Res., 1976, **36**, 2254-2260.

Montesano, R. J. Supramol. Structure Cellular Biochem., 1981, **17**, 259-273.

Munson, B. Anal. Chem., 1971, **43**, 28A-40A.

Nourse, B.D. and Cooks, R.G. Anal. Chim. Acta, 1990, **228**, 1-21.

Peake, D.A. and Gross, M.L. Organometallics, 1986, **5**, 1236-1243.

Pedder, R.E. and Yost, R.A. Proceedings of the 37th ASMS Conference on Mass Spectrometry and Allied Topics, 1989, 468.

Peraino, C.; Fry, R.J.M.; Staffeldt, E.E.; Christopher, J.P. Cancer Res., 1975, **35**, 2284-2289.

Pitot, H.C.; Barsness, L.; Goldsworthy, T. Nature, 1978, **271**, 456-457.

Poirier, L.A.; Stoner, G.D.; Shimkin, M.B. Cancer Res., 1975, **35**, 1411-1415.

Randerath, K.; Miller, R.H.; Mittal, D.; Randerath, E. In: eds., Bartsch, H.; Hemminki, K.; O'Neill, I.K. Methods for Detecting DNA Damaging Agents in Humans: Application in Cancer Epidemiology and Prevention, IARC Scientific Publications, Lyons, France, 1988, 361-367.

Randerath, K.; Reddy, M.V.; Gupta, R.C. Proc. Nat. Acad. Sci. USA, 1981, **78**, 6126-6129.

Reddy, M.V.; Gupta, R.C.; Randerath, E.; Randerath, K. Carcinogenesis, 1984, **5**, 231-243.

Reddy, M.V.; Gupta, R.C.; Randerath, K. Anal. Biochem., 1981, **117**, 271-279.

Rogan, E.G.; Cavalieri, E.L.; Tibbels, S.R.; Cremonesi, P.; Warner, C.D.; Nagel, D.L.; Tomer, K.B.; Cerny, R.L.; Gross, M.L. J. Amer. Chem. Soc., 1988, **110**, 4023-

4029.

Rudewicz, P.; Feng, T.; Blom, K.; Munson, B. Anal. Chem., 1984, 56, 2610-2611.

Sakabe, H. and Fukuda, K. Ind. Health, 1977, 15, 173-174.

Sakabe, H.; Matsushita, H.; Koshi, S. Ann. N.Y. Acad. Sci., 1976, 271, 67-70.

Schram, K.H. Trends Anal. Chem., 1988, 7, 28-32.

Shimizu, M; Yasui,Y; Matsumoto, N. Mutat. Res., 1983, 116, 217-238.

Siegel, M.W. and Fite, W.L. J. Phys. Chem., 1976, 80, 2871-2881.

Sims, P. and Grover, P.L. In: eds., Gelboin, H.V. and Ts'o, P.O.P. Polycyclic Hydrocarbons and Cancer, Academic Press, New York, 1981, 117-181.

Sivak, A. Biochim. Biophys. Acta, 1979, 560, 67-89.

Slater, E.E.; Anderson, M.D.; Rosenkranz, H.S. Cancer Res., 1971, 31, 970-973.

Solt, D.B.; Cayama, E.; Tsuda, H.; Enomoto, K.; Lee, G.; Farber, E. Cancer Res., 1983, 43, 188-191.

Solt, D.B. and Farber, E. Nature, 1976, 263, 701-703.

Sontag, J.M. In: eds., Hiatt, H.H.; Watson, J.D.; Winsten, J.A. Origins of Human Cancer, Cold Spring Harbor, New York, 1977, 1327-1338.

Sugimura, T. and Sato, S. Cancer Res., 1983, 43, (Suppl), 2415s-2421s.

Swanstrom, R. and Shank, P.R. Anal. Biochem., 1978, 86, 184-192.

Tondeur, Y.; Moschel, R.C.; Dipple, A.; Koepke, S.R. Anal. Chem., 1988, 58, 1316-1324.

Turner, L.; Choplin, F.; Dugard, P.; Hermens, J.; Jaeckh, R.; Marsmann, M.; Roberts, D. Toxic. in Vitro, 1987, 1, 143-171.

van Sittert, N.J. In: eds., Berlin A.; Draper, M.; Hemminki, K.; Vainio, H. Monitoring Human Exposure to Carcinogenic and Mutagenic Agents, IARC Scientific Publications, Lyons France, 1983, 153-168.

Volk, K.J.; Lee, M.S.; Yost, R.A.; Brajter-Toth, A. Anal. Chem., 1988, 60, 722-724.

White, E.; Krueger, P.M.; McCloskey, J.A. J. Org. Chem., 1972, **37**, 430-438.

Williams, G.M. In: ed., Barrett, J.C. Mechanisms of Environmental Carcinogenesis, Vol. 1, CRC Press, Boca Raton, Florida, 1987, 113-127.

Woo, Y.-T.; Arcos, J.C.; Lai, D.Y. In: eds., Milman, H.A.; Weisburger, E.K. Handbook of Carcinogen Testing, Noyes Publications, Park Ridge, New Jersey, 1985, 2-26.

Wood, K.V.; Burinsky, D.J.; Cameron, D.; Cooks, R.G. J. Org. Chem., 1983, **48**, 5236-5242.

Yamasaki, E. and Ames, B.N. Proc. Nat. Acad. Sci. USA, 1977, **74**, 3555-3559.

Yasuo, K.; Fujimoto, S.; Katoh, M.; Kikuchi, Y.; Kada, T. Mutat. Res., 1978, **58**, 143-150.

Yost, R.A. and Enke, C.G. Anal. Chem., 1979, **51**, 1251A-1264A.

Zeiger, E. In: eds., Milman, H.A.; Weisburger, E.K. Handbook of Carcinogen Testing, Noyes Publications, Park Ridge, New Jersey, 1985, 83-84.
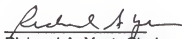
BIOGRAPHICAL SKETCH

Jody Anne Freeman was born on February 4, 1964 in Columbus, Ohio. Growing up in Bloomingdale, Ohio, she graduated from Steubenville Catholic Central High School in 1982.
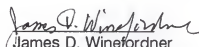
From 1982 to 1986, Jody attended Notre Dame College of Ohio in Cleveland, Ohio with a four year academic scholarship. During the summer of 1985, Jody participated in the Summer Undergraduate Research Program at the University of Alabama in Tuscaloosa, Alabama. She graduated Cum Laude in May 1986 with a B.S. degree in chemistry and received the American Institute of Chemists Award.

During the summer of 1986, Jody participated in the Summer Analytical Research Program at Procter & Gamble in Cincinnati, Ohio. In August of 1986, she began her graduate studies towards a doctorate in analytical chemistry at the University of Florida in Gainesville, Florida, under the direction of Richard A. Yost. Presentation of her research resulted in her being a finalist in the National Graduate Student Competition at the 1990 ACS Analytical Summer Symposium on Mass Spectrometry in Oak Ridge, Tennessee. Upon completion of her graduate studies, Jody will begin work at the Environmental Protection Agency in Cincinnati, Ohio.
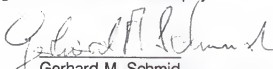
I certify that I have read this study and that in my opinion it conforms to acceptable standards of scholarly presentation and is fully adequate, in scope and quality, as a dissertation for the degree of Doctor of Philosophy.

Richard A. Yost, Chair
Professor of Chemistry

I certify that I have read this study and that in my opinion it conforms to acceptable standards of scholarly presentation and is fully adequate, in scope and quality, as a dissertation for the degree of Doctor of Philosophy.

James D. Winefordner
Graduate Research Professor of Chemistry

I certify that I have read this study and that in my opinion it conforms to acceptable standards of scholarly presentation and is fully adequate, in scope and quality, as a dissertation for the degree of Doctor of Philosophy.

David H. Powell
Assistant Scientist of Chemistry

I certify that I have read this study and that in my opinion it conforms to acceptable standards of scholarly presentation and is fully adequate, in scope and quality, as a dissertation for the degree of Doctor of Philosophy.

Gerhard M. Schmid
Associate Professor of Chemistry

I certify that I have read this study and that in my opinion it conforms to acceptable standards of scholarly presentation and is fully adequate, in scope and quality, as a dissertation for the degree of Doctor of Philosophy.

Kathleen T. Shiverick
Professor of Pharmacology
and Therapeutics

This dissertation was submitted to the Graduate Faculty of the Department of Chemistry, to the College of Liberal Arts and Sciences, and to the Graduate School and was accepted as partial fulfillment of the requirements for the degree of Doctor of Philosophy.

August 1991

_____
Dean, Graduate School